**UNIVERSIDADE ESTADUAL PAULISTA**
**"JÚLIO DE MESQUITA FILHO"**
**Instituto de Biociências**
**Câmpus do Litoral Paulista**

ÁLISON LUÍS CARA

# Perfil floral de representantes do clado hylocereoide (Cactaceae: Hylocereeae)

SÃO VICENTE-SP
2026

**UNIVERSIDADE ESTADUAL PAULISTA**

**"JÚLIO DE MESQUITA FILHO"**

**Instituto de Biociências**

**Câmpus do Litoral Paulista**

ÁLISON LUÍS CARA

# Perfil floral de representantes do clado hylocereoide (Cactaceae: Hylocereeae)

Tese apresentada à Universidade Estadual Paulista (UNESP), Instituto de Biociências, Campus do Litoral Paulista, para obtenção do título de Doutor(a) em Ciências no Programa de Pós-Graduação em Biodiversidade de Ambientes Costeiros.

Orientador(a): Prof. Dr. Odair José Garcia de Almeida

SÃO VICENTE-SP

2026

C257p

Cara, Álison Luís

Perfil floral de representantes do clado hylocereoide (Cactaceae: Hylocereeae) / Álison Luís Cara. -- São Vicente, 2026

88 p.

Tese (doutorado) - Universidade Estadual Paulista (UNESP), Instituto de Biociências, São Vicente

Orientador: Odair José Garcia de Almeida

1. Botanica. 2. Plantas suculentas. 3. Celulas e tecidos vegetais. 4. Flores Anatomia. 5. Flores Morfologia. I. Título.

Sistema de geração automática de fichas catalográficas da Unesp. Dados fornecidos pelo autor(a).

UNIVERSIDADE ESTADUAL PAULISTA

**Câmpus do Litoral Paulista**

ATA DA DEFESA PÚBLICA DA TESE DE DOUTORADO DE ÁLISON LUIS CARA, DISCENTE DO PROGRAMA DE PÓS-GRADUAÇÃO EM BIODIVERSIDADE DE AMBIENTES COSTEIROS, DO INSTITUTO DE BIOCIÊNCIAS - CÂMPUS DO LITORAL PAULISTA.

Aos 28 de agosto de 2026, às 14h, por meio de Videoconferência, realizou-se a defesa de TESE DE DOUTORADO de ÁLISON LUIS CARA, intitulada "Perfil floral de representantes do clado Hylocereoide (Cactaceae: Hylocereeae)". A Comissão Examinadora foi constituída pelos seguintes membros: Prof. Dr. ODAIR JOSÉ GARCIA DE ALMEIDA (Orientador(a) - Participação Virtual) do(a) Diretoria / UNESP / Câmpus do Litoral Paulista - IBCLP, Profa. Dra. MARA ANGELINA GALVÃO MAGENTA (Participação Virtual) do(a) UNISANTA / Universidade Santa Cecília, Prof. Dr. YOANNIS DOMÍNGUEZ RODRÍGUEZ (Participação Virtual) do(a) Departamento de Ciências Biológicas e Ambientais / UNESP / Câmpus do Litoral Paulista - IBCLP, Profa. Dra. ANA BEATRIZ SICCHIERI ZIOTTI (Participação Virtual) do(a) UNIP / Universidade Paulista, Prof. Dr. PAULO DE SALLES PENTEADO SAMPAIO (Participação Virtual) do(a) UNISANTA / Universidade Santa Cecília, Após a exposição pelo doutorando e arguição pelos membros da Comissão Examinadora que participaram do ato, de forma presencial e/ou virtual, o discente recebeu o conceito final: APROVADO . Nada mais havendo, foi lavrada a presente ata, que após lida e aprovada, foi assinada pelo(a) Presidente(a) da Comissão Examinadora.

gov.br Documento assinado digitalmente
ODAIR JOSE GARCIA DE ALMEIDA
Data: 28/08/2026 18:00:01-0300
Verifique em https://validar.iti.gov.br

Prof. Dr. ODAIR JOSÉ GARCIA DE ALMEIDA

*Gratidão ao Universo por estar aqui, neste planeta,*
*realizando a minha missão.*

*“Feel the thorns embrace”*

Zyra (League of Legends).

## AGRADECIMENTOS

*“O presente trabalho foi realizado com apoio da Coordenação de Aperfeiçoamento de Pessoal de Nível Superior – Brasil (CAPES) – Código de Financiamento 001”.*

Agradeço, primeiramente, ao Professor Dr. Odair José Garcia de Almeida, meu orientador, pelos ensinamentos, pela orientação segura e pela dedicação em cada etapa deste trabalho.

Ao professor Dr. Yoannis Dominguez, pela amizade e pelos valiosos ensinamentos durante as disciplinas de monitoria em Morfologia e Sistemática Vegetal, que contribuíram de forma significativa para a minha formação acadêmica e pessoal.

À professora Dra. Amanda Aparecida Carminatto, minha referência de vida, por inspirar-me a seguir adiante com determinação e resiliência.

Agradecimento especial ao meu amigo André Escudeiro, que, ao disponibilizar seu ChatGPT, contribuiu indiretamente para o desenvolvimento da minha pesquisa e da minha tese. Muito obrigado pela parceria, pela amizade e pelo "investimento científico" mais inusitado de todos. Sua colaboração também faz parte dessa jornada científica!

À professora Dra. Helen Sadauskas-Henrique, pelo apoio incondicional, pela amizade verdadeira e pela indicação ao Professor Odair, nada disso teria sido possível sem você.

À professora Dra. Mara Angelina Galvão Magenta, eterna professora, pela honra de tê-la em minha banca e pelo exemplo de profissionalismo e dedicação.

Ao Matheus e à Fazenda Brasil Pitayas, pela amizade, pelas inúmeras ajudas e por acreditar em meu trabalho, tornando-se parte fundamental desta trajetória

À professora Dra. Renata Mari, pelos auxílios sempre que possível no laboratório, contribuindo para o avanço deste estudo.

Aos meus familiares, pelo apoio e total incentivo em todas as minhas escolhas.

Às queridas Luciana e Márcia, pelo apoio, dedicação, disponibilidade e pela ajuda fundamental em todas as etapas das análises laboratoriais. Minha sincera gratidão por todo o cuidado e contribuição ao longo deste trabalho.

Ao meu amigo Alifer, pelo conhecimento compartilhado em campo, pelo auxílio na identificação e coleta dos botões florais de *Selenicereus validus*.

À Marina Achkar, pelos congressos, pelas risadas e pelo apoio constante, afinal, o Rio de Janeiro ficou pequeno para a gente.

À Laura Barros, por estar ao meu lado desde o Mestrado, acompanhando toda essa trajetória desde o início.

Ao meu aluno de iniciação científica, Vinicius, pelo interesse genuíno em aprender Botânica e por compartilhar comigo o entusiasmo pelo melhor gênero botânico, *Selenicereus*.

Ao Edenilson, que chegou ao ponto de aprender sobre cactos só para me ajudar, o que diz muito sobre parceria e amizade.

À Lays, Isabelly, Gabriela, Letícia e Alexandre, bem como a todos do laboratório, pela convivência, apoio e por fazerem desse ambiente um espaço de aprendizado e colaboração.

Por fim, agradeço à Luísa Sonza, cuja voz atravessou inúmeras madrugadas desta tese. Entre o *Brutal* e o *Paraíso*, suas músicas acompanharam esse processo em todas as suas nuances, do íntimo ao expansivo, do doce ao intenso, sempre em constante reinvenção, tornando evidente que nenhuma pesquisa se sustenta apenas em método, mas também em movimento, intensidade e na liberdade de se transformar ao longo do caminho.

Gratidão!

# SUMÁRIO

**1. INTRODUÇÃO À HYLOCEREEAE** ..... 16

1.1 Nomenclatura dos gêneros que compõem o clado hylocereoide ..... 18

1.2 Interesse comercial ..... 18

1.3 Morfologia floral ..... 19

**2. OBJETIVO GERAL** ..... 21

**3. REFERÊNCIAS BIBLIOGRÁFICAS** ..... 21

**CAPÍTULO 1: Floral morphoanatomy of representatives of the hylocereoid clade (Cactaceae: Hylocereeae)** ..... 25

**1.INTRODUCTION** ..... 25

**2. MATERIALS AND METHODS** ..... 27

2.1 Selected species ..... 27

2.2 Study area ..... 28

2.3 Sampling and morphological assessment of floral specimens ..... 28

2.4 Statistical analysis ..... 29

**3. RESULTS** ..... 29

3.1 Floral morphology of selected species of the hylocereoid clade ..... 29

3.2 Floral anatomy of selected species of the hylocereoid clade ..... 31

3.2.1 *Aporocactus flagelliformis* ..... 31

3.2.2 *Epiphyllum phyllanthus* ..... 32

3.2.3 *Selenicereus anthonyanus* ..... 33

3.2.4 *Selenicereus megalanthus* ..... 35

3.2.5 *Selenicereus purpusii* ..... 36

3.2.6 *Selenicereus vagans* ..... 38

3.2.7 *Selenicereus validus* ..... 40

3.2.8 *Weberocereus bradei* ..... 41

3.2.9 Statistical analysis ..... 43

**4. DISCUSSION** ..... 44

**5. CONCLUSION** ..... 47

**6. REFERENCES** ..... 48

**FIGURE LEGENDS** ..... 51
**SUPPLEMENTARY MATERIAL** ..... 66
**CAPÍTULO 2: Palinologia de Hylocereeae, com foco em espécies do clado hylocereoide (Hylocereeae: Cactaceae)** ..... 72
**1. INTRODUÇÃO** ..... 72
**2. MATERIAL E MÉTODOS** ..... 74
2.1. Análise palinológica ..... 74
2.2. Análise estatística ..... 75
**3. RESULTADOS** ..... 75
3.1. Palinologia do clado hylocereoide ..... 75
3.1.1. *Aporocactus flagelliformis* ..... 76
3.1.2. *Selenicereus anthonyanus* ..... 76
3.1.3. *Selenicereus megalanthus* ..... 76
3.1.4. *Selenicereus purpusii* ..... 78
3.1.5. *Selenicereus vagans* ..... 78
3.1.6. *Selenicereus validus* ..... 78
3.1.7. *Weberocereus bradei* ..... 78
3.2. Análises estatísticas ..... 80
**4. DISCUSSÃO** ..... 83
**5. CONCLUSÃO** ..... 85
**6. REFERÊNCIAS** ..... 85
**CONSIDERAÇÕES FINAIS** ..... 88

# LISTA DE TABELAS

## CAPÍTULO 1

Table 1. Studied species of the hylocereoid clade and outgroup. Information on the origin and sampling number of each taxa. BC: biological collection, cactus garden of IB/CLP UNESP; C: cultivated at Fazenda Brasil Pitaya; N: natural population. ..... 27

## SUPPLEMENTARY MATERIAL

Table S 1. Floral morphoanatomy characters in selected hylocereoid clade representatives. ..... 68
Table S 2. Qualitative and quantitative floral morphoanatomical characters in selected representatives of the hylocereoid clade, with corresponding $R^2$ (goodness-of-fit) and p -values..... 70

## CAPÍTULO 2

Tabela 1. Caracterização morfológica de grãos de pólen de espécies selecionadas do clado hylocereoide. ..... 80

## LISTA DE FIGURAS

Figura 1.Distribuição de espécies de Hylocereeae, coloração verde representa distribuição natural, coloração em roxo representa locais com espécies introduzidas. Fonte: POWO (2022). .....**Erro! Indicador não definido.7**

## CAPÍTULO 1

Figure 1. Floral morphology (photos) in selected hylocereoid clade representatives. A, B. Flower in lateral and frontal view. C. Flower in longitudinal section. D. Detail of the external pericarpel structure. Bars = 1cm (D); 2 cm (A); 2cm (B); 3cm (C). ..... 51
Figure 2. Floral morphology (photos) in selected hylocereoid clade representatives. A, B. Flower in lateral and frontal view. C. Flower in longitudinal section. D. Detail of the external pericarpel structure. Bars = 1cm (D); 2 cm (C); 3cm (B); 5cm (A). ..... 52
Figure 3. Perigone in transversal sections. A-C. *Selenicereus validus*, A. scale; B. outer tepal; C. internal tepal; D-F. *Selenicereus megalanthus*, D. scale; E. outer tepal; F. internal tepal; G-I. *Selenicereus anthonyanus*, G. scale. H. outer tepal; I. internal tepal; J-L. *Selenicereus vagans*, J. scale. K. outer tepal; L. internal tepal. Bars: 50µm = B; C 100µm =A; D; E; I-L; 200µm=F-H. Legends: be= adaxial apidermis; co= collenchimatous cells; de= abaxial epidermis; pa= papillae; id= idioblasts; vb= vascular bundles; cs= secretory canal. ..... 53
Figure 4. Perigone in transversal sections. A-C. *Selenicereus purpusii*, A. scale; B. outer tepal; C. internal tepal; D-F. *Aporocactus flagelliformis*, D. scale; E. outer tepal; F. internal tepal; G-I. *Weberocereus bradei*, G. scale. H. outer tepal; I. internal tepal; J-L. *Epiphyllum phyllanthus*, J. scale. K. outer tepal; L. internal tepal. Bars: 50µm = A; B; 100µm =D; F; H; J-L; 200µm=C; E; G; I. Legends: be= adaxial apidermis; co= collenchimatous cells; de= abaxial epidermis; pa= papillae; id= idioblasts; vb= vascular bundles; cs= secretory canal; ms= mesophyl. ..... 54
Figure 5. Androecium in transversal and longitudinal section. A-C. *S. validus*, A. anthers; B. filament in longitudinal section; C. filament in transversal section; D-E. *S. megalanthus*, D. anthers; E. filament in longitudinal section; F-G. *S. anthonyanus*, F. dehiscent anther. G. filament in transversal section; H-I. S. vagans, H. dehiscent anther. I. filament in transversal section. Bars = 50µm= C; G-I; 100µm= B;D;E 200µm= A Legends: (pa= papillae; vb= vascular bundles; gp= polen grain; end= endoecium; id= idioblast; st= stomata. ..... 55
Figure 6. Androecium in transversal and longitudinal section. A-B. *S. purpusi*i, A. anthers; B. filament in longitudinal and transversal sections; C-E. *A. flagelliformis*, C. anthers; D-E. filament in longitudinal and transversal sections; F-G. *W. bradei*, F. anther in transversal section. G. filament in transversal section; H-I. *E. phyllanthus*, H. anther in transversal section. I. filament in transversal section. Bars = 25µm= C;H-I; 50µm= D; F; G; 100µm= A-B; E. Legends: (pa= papillae; vb= vascular bundles; gp= polen grain; end= endoecium; id= idioblast; st= stomata. ..... 56

Figure 7. Gynoecium in transversal and longitudinal section. A-B. *S. validus*, A. lobe of style in longitudinal section; B. lobe of style in transversal section; C-D. *S. megalanthus*, C-D. lobe of style in transversal section; E-F. *S. anthonyanus*, E-F. lobe of style in transversal section; G-H. *S. vagans*, G-H. lobe of style in transversal section. Bars= 50 µm= (A; B; D; H); 100 µm = (C; F; G); 200µm= (E). Legends: cf= phenolic compound; vb= vascular bundle; id= idioblast. ..... 57
Figure 8. Gynoecium in transversal and longitudinal section. A-B. *S. purpusii*, A-B. lobe of style in transversal section; C-D. *A. flagelliformis*, C-D. lobe of style in transversal section; E-F. *W. bradei.* E-F. lobe of style in transversal and longitudinal section; G-H. E. phyllanthus. G-H. lobe of style in transversal section. Bars= 50 µm= (D); 100 µm =(C; G;H); 200µm= (A; B;E). Legends: cf= phenolic compound; vb= vascular bundle; id= idioblast. ..... 58
Figure 9. Style in transversal sections. A-B. *S. validus*, A. Apex of style; B. base of style; C-D. *S. megalanthus*, C. Apex of style; D. base of style; E-F. *S. anthonyanus*, E. Apex of style; F. base of style. G-H. *S. vagans*. G. apex of style. H. base of style. Bars=50µm (); 100µm (A; B; D -H). Legends: cf= phenolic compounds; vb= vascular bundles; id=idioblasts; st= stomata; tt= transmitting tissue; cst= stylar canal. ..... 59
Figure 10. Style in transversal sections. A-B. *S. purpusii*, A. Apex of style; B. base of style; C-D. *A. flagelliformis*, C. Apex of style; D. base of style; E-F. *W. bradei*. E. Apex of style; F. base of style. G-H. *E. phyllanthus*. G. apex of style. H. base of style. Bars=50µm (C; D); 100µm (E;F); 200 µm = (A; B; G; H). Legends: cf= phenolic compounds; vb= vascular bundles; id= idioblasts; st= stomata; tt= transmitting tissue; cst= stylar canal. ..... 59
Figure 11. Pericarpel and ovary. A-B. *S. validus*, A. pericarpel; B. ovules; C-E. *S. megalanthus*, C; D. pericarpel and ovary; E. ovule; F-H. *S. anthonyanus*, F; G. pericarpel and ovary; H. ovule. I-J. *S. vagans*. I. pericarpel and ovary; J. ovule. Bars=25 µm (H) 100µm (G); 200µm (A-F). Legends: ch= chalaza; et= external tegument; vb= vascular bundle; fu= funicle; id= idioblast; it= internal tegument; pe= pericarpel; ov= ovary. ... 60
Figure 12. Pericarpel and ovary. A-C. *S. purpusii*, A. pericarpel; B. ovary; C. ovules. D; E. *A. flagelliformis*, D. pericarpel and ovary; E. ovule; F; G. *W. bradei*, F. pericarpel and ovary; G. ovule. H; I. *E. phyllanthus*. H. pericarpel and ovary; I. ovule. Bars=50 µm (A; E; G) 100µm (B; C; D; F; H); 200µm (I). Legends: ch= chalaza; et= external tegument; vb= vascular bundle; fu= funicle; id= idioblast; it= internal tegument; pe= pericarpel; ov= ovary. tr= trichomes; cf= phenolic compounds. ..... 61
Figure 13. Floral tube. A-F. *S. validus*, A. base of the tube; B. median region; C. apex. D.base of the tube epidermis. E. median region epidermis. F. apex epidermis. G-L. *S. megalanthus*, G. base of the tube; H. median region; I. apex. J. base of the tube epidermis. K. median region epidermis. L. apex epidermis. Bars=50 µm (A; D) 100µm (B; E; F-L); 200µm (C). Legends: vb= vascular bundle; fi= filament; id= idioblast; tr= trichome; tn= nectar tissue. ..... 62
Figure 14. Floral tube. A-F. *S. anthonyanus*, A. base of the tube; B. median region; C. apex. D.base of the tube epidermis. E. median region epidermis. F. apex epidermis. G-L. *S. vagans*, G. base of the tube; H. median region; I. apex. J. base of the tube epidermis.

K. median region epidermis. L. apex epidermis. Bars=100 µm (A-L). Legends: vb= vascular bundle; fi= filament; id= idioblast; tr= trichome; tn= nectar tissue. ..... 63
Figure 15. Floral tube. A-F. *S. purpusii*, A. base of the tube; B. median region; C. apex. D.base of the tube epidermis. E. median region epidermis. F. apex epidermis. G-I. *A. flagelliformis*, G. base of the tube; H. median region; I. apex. Bars=50µm (B); 100 µm (A; C-G; I), 200µm= (H). Legends: vb= vascular bundle; fi= filament; id= idioblast; tn= nectar tissue. ..... 64
Figure 16. Floral tube. A-F. *W. bradei*, A. base of the tube; B. median region; C. apex. D.base of the tube epidermis. E. median region epidermis. F. apex epidermis. G-L. *E. phyllanthus*, G. base of the tube; H. median region; I. apex. J. base of the tube epidermis. K. median region epidermis. L. apex epidermis. I. apex. Bars=50µm (B); 100 µm (A; C-G; I), 200µm= (H). Legends: vb= vascular bundle; fi= filament; id= idioblast; tn= nectar tissue. ..... 65
Figure 17. Morphological relationships among selected species of Hylocereeae based on qualitative floral characters. (**A**) UPGMA dendrogram generated from Gower dissimilarity. (**B**) Principal Coordinates Analysis (PCoA) based on the same similarity matrix. Legends: V1 (nocturnal anthesis), V2 (diurnal anthesis), V3 (normal scale epidermis), V4 (irregular external tepal epidermis), V5 (normal external tepal epidermis), V6 (number of stamens). ..... 66

## SUPPLEMENTARY MATERIAL

Figure S 1. Native geographic distribution of the species analyzed in the present study: *Aporocactus flagelliformis*, *Selenicereus anthonyanus*, *Selenicereus megalanthus*, *Selenicereus purpusii*, *Selenicereus vagans*, *Selenicereus validus*, *Weberocereus bradei*, and *Epiphyllum phyllanthus.* Colored points represent native occurrence records for each species across the Americas, as indicated in the legend. The inset map shows the location of the represented area within the American continent. ..... 67

## CAPÍTULO 2

Figura 1. Fotomicrografias obtidas por microscopia óptica de grãos de pólen de espécies selecionadas do clado hylocereoide. A. Vista equatorial; B. Vista polar; C. Ornamentação da exina; D. Espessura da exina e espínulas. Barras = 10 µm..... 77
Figura 2. Média e intervalo de confiança (95%) dos diâmetros polar e equatorial dos grãos de pólen das espécies selecionadas do clado hylocereoide. A. Diâmetro polar; B. Diâmetro equatorial. ..... 81
Figura 3. Dendrograma de similaridade morfológica entre os táxons de Hylocereeae, obtidos pelo método UPGMA e coeficiente de Gower. Dados complementares obtidos de Ruiz-Domínguez et al. (2019). ..... 82

Figura 4. Análise de Coordenadas Principais (PCoA) dos táxons de Hylocereeae, baseada na matriz de dissimilaridade de Gower calculada a partir dos caracteres polínicos quantitativos. ..... 83

## 1. INTRODUÇÃO À HYLOCEREEAE

Pertencente a ordem Caryophyllales, Cactaceae Juss. possui cerca de 1855 espécies e 151 gêneros (Anderon, 2001; Korotkova *et al*., 2021; Cole, 2024), com distribuição quase que exclusiva das Américas, exceto *Rhipsalis baccifera* (J.S.Muell.) Stearn, com representantes, relatados para a África, Madagascar, Sri Lanka e sul da Índia (Stevens, 2001; Cota-Sánchez e Bomfim-Patrício, 2010). A família está dividida em cinco subfamílias: Leuenbergioideae, Pereskioideae (Engelm.), Opuntioideae (Burnett), Maihuenioideae (Fearn) e Cactoideae (Eaton), destas, somente Maihuenioideae não possui ocorrência em território brasileiro (Stevens, 2001).

Na família são encontradas desde espécies com tecidos mucilaginosos e cutícula espessa, que ocorrem em regiões áridas e semi-áridas (*Melocactus* (Link and Otto.), *Coleocephalocereus* (Backeb.), *Pilosocereus* (Byles & Rowley.), *Micranthocereus* (Backeb.) e *Cereus* (Mill.), até cactos que crescem em florestas tropicais e subtropicais úmidas. Estas últimas, como epífitas, tradicionalmente são incluídas em duas tribos: Rhipsalideaee e Hylocereeae (Barthlott & Hunt 1993; Nyffeler 2002).

Atualmente autores reconhecem a tribo como um grupo monofilético (Cruz *et al*., 2016; Korotkova *et al*., 2017; Cruz 2018; Martínez-Quezada *et al*., 2020), em que, oito gêneros estão suportados com base em análises de DNA cloroplastidial, proposto por Korotkova *et al*. (2017), sendo eles: *Acanthocereus* (Engelm. Ex A. Berger) Britton & Rose, *Aporocactus* Lemaire., *Disocactus* Lindley, *Epiphyllum* Haworth., *Kimnachia* S. Arias & N. Korotkova, *Pseudorhipsalis* (Britton & Rose), *Selenicereus* (incl. *Hylocereus* e *Weberocereus* p.p.) (A.Berger) Britton & Rose e *Weberocereus* (Britton & Rose), entretanto, as relações filogenéticas entre eles, ainda necessitam de resoluções como em *Acanthocereus* e *Kimnachia* (Korotkova et al., 2017; Martínez-Quezada *et al*., 2020). Sem contar, que algumas espécies, foram classificadas como insuficientemente conhecidas devido a essas mudanças como *Selenicereus ocamponis* (Salm-Dyck) D.R. Hunt, *S. purpusii* (Weing.) S. Arias & N. Korotkova, *S. triangularis* (L.) D.R. Hunt, *S. trigonus* (Haw.) S. Arias & N. Korotkova, *S. vagans* (K. Brandegee) Britton & Rose, *S. murrillii* Britton & Rose, e *S. costaricensis* (F.A.C. Weber) S. Arias & N. Korotkova, *S. monacanthus* (hort. ex Lem.) D.R. Hunt, e necessitam de mais estudos (Korotkova *et al*., 2017).

Hylocereeae (Buxb.) é uma tribo com centros de diversidade concentrados na América Central e do Sul e possui espécies introduzidas e cultivadas como pitayas na África, Ásia e Europa, (Figura 1).

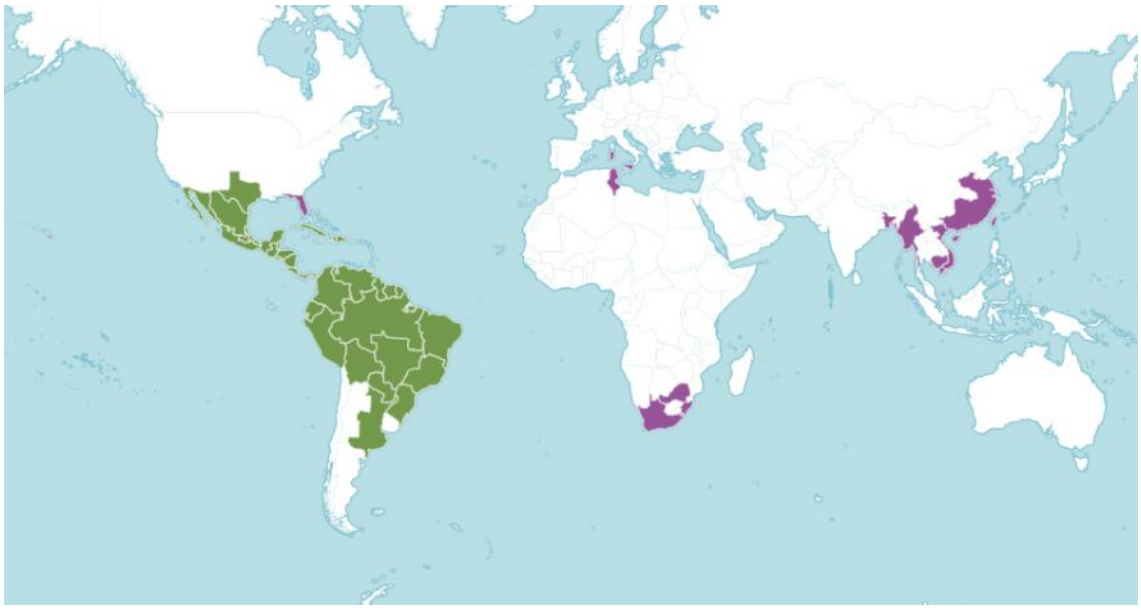


Figura 1 Distribuição de espécies de Hylocereeae, Coloração verde representa distribuição natural, coloração em roxo representa locais com espécies introduzidas. Fonte: POWO (2022).

Hylocereeae tem dois clados distinguíveis morfologicamente. Sendo Phyllocactóide representado principalmente por espécies epífitas, de caules achatados (filocládios), sem espinhos, tornando a tribo bastante heterogênea (Almeida, 2013; Cruz *et al*. 2016; Korotkova *et al*., 2017); muitos de seus representantes são utilizados como ornamentais especialmente *Disocactus* e *Epiphyllum*. Em contraste, o clado Hylocereoide, em especial, é atualmente representado por 3 gêneros, *Aporocactus*, *Selenicereus* e *Weberocereus* (Korotkova *et al*. 2017; Martínez-Quezada *et al*., 2020) devido sinapomorfias descritas em que os gêneros compartilham de hábitos hemiepifíticos e possuem cladódios espinhosos com raízes adventícias. Hylocereoide ainda possui espécies de valor comercial, amplamente cultivadas por seus vistosos frutos, que popularmente são conhecidos como, pitaya ou fruto do dragão, como espécies de *Selenicereus* (A.Berger) Britton & Rose [=*Hylocereus* (A.Berger) Britton & Rose] (Korotkova *et al*. 2017, Martínez-Quezada *et al*. 2020). O entendimento sobre a classificação de Hylocereeae tem mudado, principalmente, após recentes análises moleculares. Outra mudança significativa, proposta por Korotkova *et al*. (2017) foi que duas espécies do gênero (*Deamia* Britton & Rose e três de *Strophocactus* Britton & Rose)

foram transferidas para a tribo Echinocereaae, uma tribo até então reconhecida por abrigar apenas espécies terrestres.

## 1.1 Nomenclatura dos gêneros que compõem o clado hylocereoide

O nome *Aporocactus* apresenta origem greco-latina. O termo grego áporos (ἄποροϛ), que significa "sem passagem", "sem caminho" ou "sem saída", pode ser associado ao hábito de crescimento característico das espécies do gênero, que apresentam caules longos, pendentes e de crescimento contínuo. Já o termo cactus, incorporado ao latim a partir do grego káktos, é tradicionalmente utilizado para designar plantas espinhosas e, posteriormente, passou a integrar a nomenclatura de representantes da família Cactaceae.

O gênero *Selenicereus*, cujas espécies são popularmente conhecidas como "dama-da-noite" ou "rainha-da-noite", também possui um nome de origem greco-latina. Segundo Anderson (2001), Selene (Σελήνη) corresponde à deusa grega da Lua, fazendo alusão à característica floração noturna observada em diversas espécies do gênero. O termo *Cereus*, de origem latina, significa "ceroso" ou "vela de cera", em referência ao aspecto alongado e semelhante a uma vela apresentado pelos caules de muitos cactos. Dessa forma, *Selenicereus* pode ser interpretado como "cacto da Lua", denominação que remete principalmente à abertura de suas flores durante o período noturno.

Por sua vez, o nome *Weberocereus* foi estabelecido em homenagem ao botânico Frédéric Albert Constantin Weber, que realizou importantes contribuições para o estudo e a classificação das cactáceas no final do século XIX. *Cereus*, derivado do latim, está relacionado ao significado de "vela de cera" ou "semelhante a uma vela", em referência à morfologia dos caules (Anderson, 2001). Assim, *Weberocereus* pode ser compreendido, de maneira simplificada, como "cacto de Weber", perpetuando na nomenclatura botânica a contribuição desse pesquisador para o conhecimento da família Cactaceae.

## 1.2 Interesse comercial

Os cactos possuem considerável interesse comercial, devido à sua diversidade, facilidade de manutenção e beleza, eles estiveram entre as primeiras plantas exportadas da América por exploradores europeus no século XV (Howard & Touw, 1981); Anderson (2001) menciona diversos gêneros com potencial econômico, *Opuntia* (Mill.) por exemplo, utilizado tanto na culinária como para fins farmacêuticos; espécies do gênero

*Selenicereus* que produzem frutos comestíves, conhecidos como pitayas, pytahaya e dragon fruit, dentre outros.

Os frutos da pitaya possuem atributos físicos, sensoriais e nutricionais atraentes para o consumo humano, como diferentes colorações no pericarpo, uma grande quantidade de polpa de sabor adocicado, ricos em carboidratos, além apresentarem variados tipos de vitaminas e minerais de potencial antioxidante (Abreu *et al*., 2012; Sato *et al*., 2014). Embora apresente pouca expressão econômica, quando comparada a outras frutas, a pitaya tornou-se uma promissora fruta no mercado nacional e internacional (De Paula Queiroga *et al*., 2021).

Apesar de ser originária das regiões tropicais e subtropicais, as pitayas estão sendo cultivadas em várias partes do mundo. Entre as vantagens econômicas do plantio dessas plantas, está a capacidade de serem cultivadas em solo com baixa matéria orgânica e déficit de nutrientes, além de serem muito tolerantes a períodos de seca (Cálix *et al*., 2014). Existem diversas espécies cultivadas como pitayas, entretanto algumas se destacam no cultivo e na distribuição: *Selenicereus undatus* (Haworth) D.R.Hunt., *Selenicereus costaricensis* (F.A.C.Weber) Arias & Korotkova, e *Selenicereus megalanthus* (Schumann ex Vaupel) Moran. (Ortiz-Hernández & Salazar, 2012; Korotkova *et al*. 2017).

## 1.3 Morfologia floral

Os botões florais dos cactos desenvolvem-se a partir de aréolas apicais e laterais, sendo predominantemente solitários e sésseis. No entanto, algumas espécies mais basais apresentam inflorescências, como ocorre em *Pereskiodideae*, por exemplo, (Barthlott & Hunt, 1993; Anderson, 2001).

Existe uma diversidade morfológica notável nas flores das cactáceas, com tamanhos que variam desde pequenas flores de *Rhipsalis*, com aproximadamente 0.4 cm de diâmetro, flores médias de *Aporocactus*, entre 5 e 10 cm de diâmetro, até as grandes flores de *Selenicereus*, que chegam a atingir 40 cm quando totalmente abertas (Barthlott & Hunt, 1993; Anderson, 2001; Almeida, 2013; Korotkova *et al*., 2017). Em sua grande maioria são actinomorfas, embora algumas espécies apresentem flores zigomorfas, como em *Aporocactus flagelliformis,* Rosas-Reinhold *et al*., (2022). A coloração das tépalas é variada, pois abrange flores brancas (*Selenicereus validus*, por exemplo), amarelas (*Opuntia ficus-indica* (L.) Mill. por exemplo), com tons de vermelho brilhante a magenta

(*Disocactus ackermannii* (Haw.). Ralf Bauer, por exemplo, até tépalas de coloração azul, presente em *Pseudorhipsalis amazônica* (K.Schum.). Ralf Bauer (Korotkova *et al*., 2017).

As cactáceas destacam-se pela elevada diversidade morfológica floral, apresentando flores campanuladas (bell-shaped), afuniladas (infundibuliformes), salverformes (hipocrateriformes), tubulares (tubular) e rotadas (Anderson, 2001). As flores geralmente possuem numerosos estames, com anteras pequenas e predominantemente basifixas, além de um gineceu composto por estilete e estigma multilobado. O tubo floral pode ser conspícuo, como observado em espécies de Selenicereus, ou reduzido a ausente (inconspícuo), condição comum em espécies do gênero Rhipsalis.

O nectário floral localiza-se internamente ao tubo, enquanto externamente as flores apresentam um pericarpelo de origem receptacular (hipanto), recoberto por escamas e aréolas, geralmente portando espinhos, gloquídeos ou tricomas. O ovário é, em geral, ínfero em relação às peças do perigônio, unilocular, com numerosos óvulos inseridos em placenta, conectados por um longo funículo (Almeida *et al*., 2013). O pólen é abundante, apresenta variação morfológica significativa entre os táxons e caracteriza-se por uma exina rígida (Ruiz-Domínguez *et al*., 2019).

Estudos envolvendo a morfoanatomia floral possuem grande valor na taxonomia vegetal (Stuessy, 2009; Almeida *et al*., 2013), devido ao caráter conservado deste órgão. Poucos trabalhos que contemplem aspectos da biologia reprodutiva e da morfologia floral em Cactaceae são encontrados, entre os quais se destacam Fuentes-Pérez *et al*., (2009); Almeida *et al*. (2010, 2012, 2013); Cota-Sánchez *et al*., (2007, 2013); Gutiérrez-Flores *et al*., (2017); Muniz *et al*., (2019;) Cardoso *et al*., (2019); Silva (2020); Sampaio (2022). Em adição, existe pouca literatura sobre biologia floral e requisitos de polinização das espécies de pitaya, o que pode limitar a produtividade de seus frutos (Muniz *et al*. 2019).

Os estudos palinológicos também constituem uma importante fonte de caracteres para melhor compreensão de Cactaceae, uma vez que variações no tamanho e na forma dos grãos, no número e tipo de aberturas e ornamentação da exina, podem contribuir para a identificação e delimitação dos táxons. Embora diversos grupos da família sejam considerados estenopolínicos, apresentando um padrão morfológico geral relativamente conservado, a análise integrada de caracteres qualitativos e quantitativos tem demonstrado grande valor na diferenciação de espécies e gêneros, inclusive entre cactáceas epífitas e representantes da tribo Hylocereeae (Cancelli *et al*., 2017; Gonzaga *et al*., 2019; Ruiz-Domínguez *et al*., 2019).

A presente tese está organizada em dois capítulos complementares, que abordam diferentes aspectos da diversidade floral e palinológica da tribo Hylocereeae, com ênfase no clado hylocereoide. O **Capítulo 1**, intitulado **Floral morphoanatomy of representatives of the hylocereoid clade (Cactaceae: Hylocereeae),** apresenta uma análise comparativa da morfologia e anatomia floral de espécies selecionadas do clado, contemplando principalmente caracteres do perigônio, androceu, gineceu e pericarpelo, com o objetivo de identificar padrões estruturais e atributos potencialmente informativos para a compreensão da diversidade floral e da circunscrição taxonômica do grupo. O **Capítulo 2**, intitulado **Palinologia de Hylocereeae, com foco em espécies do clado hylocereoide (Cactaceae: Hylocereeae***)*, aborda a morfologia dos grãos de pólen por meio de caracteres qualitativos e quantitativos, incluindo tamanho, forma, área polar, número de aberturas e ornamentação da exina, além de análises multivariadas de similaridade morfológica. Em conjunto, os dois capítulos integram evidências florais e palinológicas, contribuindo para ampliar o conhecimento sobre a diversidade morfológica, os padrões estruturais e o potencial taxonômico desses caracteres em Hylocereeae.

## 2. OBJETIVO GERAL

O objetivo geral deste estudo foi caracterizar comparativamente a morfoanatomia floral de espécies do clado hylocereoide, com ênfase no perigônio, androceu, gineceu e pólen, a fim de identificar caracteres estruturais potencialmente informativos e avaliar sua contribuição para a na atual classificação dos táxons do clado.

## 3. REFERÊNCIAS BIBLIOGRÁFICAS

Almeida, O.J.G., 2013. Órgãos reprodutivos em Hylocereeae e Rhipsalideae (Cactaceae): morfologia floral e desenvolvimento estrutural do fruto e da semente. Tese (Doutorado em Biologia Vegetal) – Universidade Estadual Paulista, Rio Claro, São Paulo.

Almeida, O.J.G., Cota-Sánchez, J. H., Paoli, A.A. S., 2013. The systematic significance of floral morphology, nectaries, and nectar concentration in epiphytic cacti of tribes Hylocereeae and Rhipsalideae (Cactaceae). Perspectives in Plant Ecology,

Evolution and Systematics, 15(5), 255–268. https://doi.org/10.1016/j.ppees.2013.08.001

Almeida, O.J.G., Paoli, A.A.S., Cota-Sánchez, J.H., 2012. A macro- and micromorphological survey of floral and extrafloral nectaries in the epiphytic cactus *Rhipsalis teres* (Cactoideae: Rhipsalideae). Flora 207(2), 119–125. https://doi.org/10.1016/j.flora.2011.11.004

Almeida, O.J.G., Paoli, A.A.S., Souza, L.A., 2010. Flower morpho-anatomy in *Epiphyllum phyllanthus* (Cactaceae). Revista Mexicana de Biodiversidade 81, 65-80.

Anderson, E.F., 2001. The cactus family. Timber Press, Inc. Oregon.

Abreu, W.C., de Oliveira Lopes, C., Pinto, K.M., Oliveira, L.A., de Carvalho, G.B.M., Barcelo, M.D.F.P., 2012. Características físico-químicas e atividade antioxidante total de pitaias vermelha e branca. Revista do Instituto Adolfo Lutz, 71(4), 656-661.

Barthlott, W., Hunt, D.R., 1993. Cactaceae. In: Kubitzki, K., Rohwer, J.G., Bittrich, V. (eds) Flowering Plants: Dicotyledons. The Families and Genera of Vascular Plants, vol 2. Springer, Berlin, Heidelberg. https://doi.org/10.1007/978-3-662-02899-5_17

Cancelli, R. R., Menezes, I. C., & Souza, P. A. (2017). Morfologia polínica de espécies epífitas de Cactaceae Juss. do Rio Grande do Sul, Brasil. *Iheringia, Série Botânica.*, *72*(2), 181-189. https://doi.org/10.21826/2446-8231201772205

Cálix De Dios, H., Castillo Martínez, R., Caamal Canché, H.J., 2014. Caracterización de la producción de Pitahaya (*Hylocereus* spp.) en la Zona Maya de Quintana Roo, México. Agroecología, 9, 123-132.

Cardoso, C.W., Versieux, A.C.M., Almeida, O.J.G., Sakuragui, C.M., 2019. Floral Biology of Cacti and Ecological Implications. In book: Cacti: Ecology, Conservation, Uses and Significance (57–78) Publisher: Nova Science Publishers

Cole, Theodor. (2024). CACTACEAE Phylogeny Poster (CactusPP).

Cota-Sánchez, H., Bomfim-Patrício, C., 2010. Seed morphlogy, polyploidy and the evolutionary history of the epiphitic cactus *Rhipsalis baccifera* (Cactaceae). Polibotánica 29:107-129

Cota-Sánchez, J. H., Croutch, D.S., 2007. Notes on the floral biology of *Praecereus euchlorus* subsp. *euchlorus* (Cactaceae). Schumannia 5, 1–5.

Cota-Sánchez, J.H., Almeida, O.J.G., Falconer, D.J., Choi, H.J., Bevan, L., 2013. Intriguing thigmonastic (sensitive) stamens in the Plains Prickly Pear *Opuntia*

*polyacantha* (Cactaceae). Flora - Morphology, Distribution, Functional Ecology of Plants, 208(5-6), 381–389. https://doi.org/10.1016/j.flora.2013.04.009

Cruz M.A., 2018. Sistemática flogenética del género Disocactus (Cactaceae). PhD Thesis, Universidad Nacional Autónoma de México, México.

Cruz, M.A., Arias, S. and Terrazas, T., 2016. Molecular phylogeny and taxonomy of the genus Disocactus (Cactaceae), based on the DNA sequences of six chloroplast markers. Willdenowia 46: 145–164. https://doi.org/10.3372/wi.46.46112

De Paula Queiroga, V., Girão, Ê.G., Gomes, J.P., de Melo Queiroz, A.J., de Figueirêdo, R.M. F., de Albuquerque, E.M.B., 2021. Pitahaya (*Hylocereus* spp.) sistema produtivo de cactos trepadeiras. Associação Da Revista Eletrônica A Barriguda – Arepb, 1, 221.

Fuentes-Pérez, M., Terrazas, T., Arias, S., 2009. Anatomía floral de cinco especies de *Opuntia* (Opuntioideae, Cactaceae) de México. Polibotánica, (27), 89-102.

Gonzaga, D. R., de Souza, M. A., Neto, L. M., Peixoto, A. L., Mendonça, C. B. F., & Goncalves-Esteves, V. (2019). The systematic value of pollen morphology in Arthrocereus A. Berger (Cactaceae, Cactoideae). *Review of Palaeobotany and Palynology*, *269*, 33-41. https://doi.org/10.1016/j.revpalbo.2019.06.009

Gutiérrez-Rodríguez, B.E., Guevara, R., Angulo, D.F. *et al*., 2022. Ecological niches, endemism and conservation of the species in *Selenicereus* (Hylocereeae, Cactaceae). Braz. J. Bot 45, 1149–1160. https://doi.org/10.1007/s40415-022-00818-z

Howard, R.A., Touw, M., 1981. The cacti of the Lesser Antilles and the typification of the genus *Opuntia Miller*. Cactus and Succulent Journal (U.S.A.) 53:233-237.

Korotkova, N., Borsch, T., and Arias, S. (2017). A phylogenetic framework for the Hylocereeae (Cactaceae) and implications for the circumscription of the genera. Phytotaxa, 327(1), 1. https://doi.org/10.11646/phytotaxa.327.1.1

Korotkova, N., Aquino, D., Arias, S., Eggli, U., Franck, A., Gómez-Hinostrosa, C., Guerrero, P., Hernández, H., Kohlbecker, A., Köhler, M., Luther, K., Majure, L., Müller, A., Metzing, D., Nyffeler, R., Sánchez, D., Schlumpberger, B., Berendsohn, W., 2021. Cactaceae at Caryophyllales.org - a dynamic online species-level taxonomic backbone for the family. Willdenowia. 51. 251-270. https://doi.org/10.3372/wi.51.51208.

Martínez-Quezada, D.M., Arias, S., Korotkova, N., Terrazas, T. (2020). The phylogenetic significance of the stem morpho-anatomy in the Hylocereeae (Cactoideae,

Cactaceae). Plant Systematics and Evolution, 306(1). https://doi.org/10.1007/s00606-020-01639-x

Muniz, J.P.D.O., Bomfim, I.G.A., Corrêa, M. C.D.M., Freitas, B.M., 2019. Floral biology, pollination requirements and behavior of floral visitors in two species of pitaya. Revista Ciência Agronômica, 50(4), 640-649. https://doi.org/10.5935/1806-6690.20190076.

Ortiz-Hernández, Y.D., Salazar, J.A.C., 2012. Pitahaya (*Hylocereus* spp.): a short review. Comunicata Scientiae, 3, 4, 220-237.

Nyffeler, R., 2002. Phylogenetic relationships in the cactus family (Cactaceae) based on evidence from trnK/ matK and trnL-trnF sequences. American Journal of Botany, 89(2), 312–326. https://doi.org/10.3732/ajb.89.2.312.

Rosas-Reinhold, I., Sánchez, D., Arias, S., 2022. Systematic study and niche differentiation of the genus *Aporocactus* (Hylocereeae, Cactoideae, Cactaceae). Botanical Sciences, 100(2), 423-445.

Ruiz-Domínguez C, Vovides A.P., Sosa V. Systematic relevance of pollen morphology in tribe Hylocereeae (Cactaceae). PhytoKeys. 2019 Aug 19;128:121-140. doi: 10.3897/phytokeys.128.35842. PMID: 31523156; PMCID: PMC6711936.

Sampaio, P. D. S. P., 2022. Morfo-anatomia floral e biologia reprodutiva de *Selenicereus setaceu*s (Salm-Dyck) Berger (Cactaceae) em São Thomé das Letras, Minas Gerais, Brasil. Tese (Doutorado em Biodiversidade de Ambientes Costeiros) – Universidade Estadual Paulista, São Vicente, São Paulo.

Silva, M.J.D. Anatomia comparada dos órgãos florais de *Cereus fernambucensis* Lem. e *Cereus hildmannianus* K. Schum. (Cactaceae)., 2020. Dissertação (Mestrado em Biodiversidade de Ambientes Continentais) Universidade Estadual Paulista, São Vicente, São Paulo.

Sato, S.T.A., Ribeiro, S.D.C.A., Sato, M. K., Souza, J.N.S., 2014. Caracterização física e físico-química de pitayas vermelhas (*Hylocereus costaricensis*) produzidas em três municípios paraenses. Journal of Bioenergy and Food Science, 1(2).

Stevens, P.F., 2001. Angiosperm Phylogeny Website. Version 14, July 2017 [and continuously updated since].” http://www.mobot.org/MOBOT/research/APweb/”.

Stuessy, T.F., 2009. Plant taxonomy – the systematic evaluation of comparative data. New York: Columbia University Press, 2.ed., 539.

**CAPÍTULO 1: Floral morphoanatomy of representatives of the hylocereoid clade (Cactaceae: Hylocereeae)**

ABSTRACT

Floral morphoanatomy in Cactaceae remains underexplored despite its taxonomic and ecological relevance. This study aimed to characterize the floral morphology and anatomy of representative species of the hylocereoid clade (*Aporocactus*, *Selenicereus*, and *Weberocereus*), integrating structural data from the perianth, androecium, and gynoecium to improve the understanding of floral diversification within Hylocereeae. Floral buds at pre-anthesis and anthesis stages were analyzed using morphological measurements and histological techniques. The analyzed species exhibit considerable variation in floral traits, including size, symmetry, anthesis period, and structural organization. Flowers range from small, diurnal and zygomorphic forms in *Aporocactus* to large, nocturnal and actinomorphic forms in *Selenicereus* and *Weberocereus*, reflecting distinct pollination syndromes. Anatomically, all taxa share a general pattern of secretory-rich tissues, with abundant idioblasts, mucilage cells, and amphicribal vascular bundles. However, differences were observed in epidermal features, cuticle thickness, and the organization of the style and pericarpel, including the presence or absence of papillae and variation in appendages such as scales, spines, bristles, and wool. These results indicate that the hylocereoid clade exhibits a mixed floral pattern, combining conserved structural traits with marked morphological plasticity. This variability is associated with ecological adaptations and diverse pollination strategies. The integration of morphological and anatomical data highlights important characters for taxonomic interpretation and supports a more comprehensive understanding of floral evolution within Hylocereeae.

Keywords: Epiphytic cacti, perigone, inferior ovary, pericarpel, *Selenicereus*
[1]

## 1.INTRODUCTION

Among all the angiosperm families, Cactaceae stands out for its high morphological diversity, comprising approximately 1,855 species distributed across 151 genera (Anderson, 2001; Korotkova *et al*., 2021; Cole, 2024). The family has a wide geographic distribution, with native representatives mainly from the Americas, in addition to occurrences of *Rhipsalis baccifera* (Sol.) Stearn recorded in Africa, Madagascar, Sri Lanka, and southern India (Stevens, 2001; Cota-Sánchez and Bomfim-Patrício, 2010). The group includes species typical of arid and semi-arid environments, as well as taxa adapted to humid forests, mostly epiphytes and nomadic vines, traditionally included in the tribes Rhipsalideae and Hylocereeae (Barthlott and Hunt, 1993; Nyffeler, 2002; Nava-Bernabé *et al*., 2025).

Hylocereeae is one of the most diverse tribes within Cactaceae, with a native distribution extending from Mexico to northern Brazil (Barthlott *et al*., 2015). Beyond its Neotropical range, several species (particularly those cultivated as pitayas) have been widely introduced into Africa, Asia, and Europe. The tribe is consistently recognized as monophyletic based on molecular phylogenetic evidence (Cruz *et al*., 2016; Korotkova *et al*., 2017; Cruz, 2018; Martínez-Quezada *et al*., 2020). Based on chloroplast DNA analyses, Korotkova *et al*., (2017) circumscribed eight genera within Hylocereeae:

[1] *Artigo submetido na revista Flora. Referências bibliográficas de acordo com as normas da revista.

*Acanthocereus* (Engelm. ex A. Berger) Britton and Rose, *Aporocactus* Lem., *Disocactus* Lindl., *Epiphyllum* Haw., *Kimnachia* S. Arias and N. Korotkova, *Pseudorhipsalis* (Britton and Rose), *Selenicereus* (A. Berger) Britton and Rose (including *Hylocereus* and part of *Weberocereus*), and *Weberocereus* (Britton and Rose), (Figure 17). Moreover, several species have been classified as insufficiently known, because of recent taxonomic rearrangements, including *Selenicereus ocamponis* (Salm-Dyck) D.R. Hunt, *S. purpusii* (Weing.) S. Arias and N. Korotkova, *S. triangularis* (L.) D.R. Hunt, *S. trigonus* (Haw.) S. Arias and N. Korotkova, *S. vagans* (K. Brandegee) Britton and Rose, *S. murrillii* Britton and Rose, *S. costaricensis* (F.A.C. Weber) S. Arias and N. Korotkova, and *S. monacanthus* (hort. ex Lem.) D.R. Hunt, all of which require further investigation (Korotkova *et al*., 2017).

Morphologically, Hylocereeae comprises two well-supported clades. The phyllocactoid clade is predominantly composed of epiphytic species characterized by flattened, leaf-like stems (phylloclades) and the absence of spines, resulting in pronounced morphological heterogeneity within the tribe (Almeida, 2013; Cruz *et al*., 2016; Korotkova *et al*., 2017). In contrast, the hylocereoid clade is mainly composed of hemiepiphytic species or nomadic vines (Nava-Bernabé *et al*., 2025; Martínez-Quezada, 2025) and is currently represented by three genera, *Aporocactus*, *Selenicereus*, and *Weberocereus*. These genera share the presence of spiny cladodes bearing adventitious roots, a set of traits interpreted as synapomorphic for the clade (Korotkova *et al*., 2017; Martínez-Quezada *et al*., 2020).

Although hylocereoid's genera share a similar vegetative architecture, they differ clearly in floral morphology. *Aporocactus* comprises species with predominantly diurnal, brightly colored funnelform flowers, which may be actinomorphic or zygomorphic and generally do not exceed 10 cm in length. *Weberocereus* is characterized by mostly nocturnal, fragrant, funnelform flowers, typically pale white to yellow, consistently actinomorphic, and likewise shorter than 10 cm. *Selenicereus*, exhibits predominantly nocturnal, actinomorphic, and strongly scented salverform and funnelform flowers, with a wide size range from approximately 3.5 cm in *Selenicereus minutiflorus* (Britton and Rose) D.R.Hunt to nearly 40 cm in *Selenicereus megalanthus* (K. Schumann ex Vaupel) Moran. Flower coloration in *Selenicereus* is mainly white to greenish-yellow, although some species display reddish to purplish tepals, as observed in *Selenicereus anthonyanus* (Alexander) D.R. Hunt.

In the floral context, species of the hylocereoid clade share a common structure typical of most Cactaceae, characterized by a well-developed hypanthium known as pericarpel. According to Almeida *et al*., (2018), the ovary is of carpellary origin and is surrounded by the pericarpel, a receptacular tissue of cauline origin. These two tissues are merged, forming a single wall at the base of the flower. Consequently, the outer layers, including the external epidermis, are referred to as the pericarpel, whereas the inner layers correspond to the true ovary (carpels). Notably, in the ovary region, there is no clear anatomical boundary indicating the junction between these tissues. For the purposes of this study, the band of large collateral vascular bundles located in the central portion of the floral base was considered the morphoanatomical boundary between the ovary and the pericarpel.

The variation in floral morphology provides an additional set of comparative characters that, when analyzed together with anatomical characteristics, contribute to the interpretation of evolutionary and ecological patterns within the hylocereoid clade. In addition, secretory regions along the floral tube that give rise to a nectar chamber nectary, positioned above the ovary, are also observed in species of this clade. Those nectaries produce and accumulate nectar throughout the floral tube is commonly associated with

specialized pollination systems (Almeida *et al*., 2013). In parallel, variation in external floral morphology provides an additional set of comparative characters that, when analyzed in conjunction with anatomical traits, contributes to the interpretation of evolutionary and ecological patterns within the hylocereoid clade.

Studies addressing floral morphoanatomy have long been recognized as highly informative for plant taxonomy, largely due to the relatively conserved nature of floral structures (Stuessy, 2009; Almeida *et al*., 2013). However, investigations focusing on floral morphology and reproductive biology remain relatively scarce. Available studies include those by Fuentes-Pérez *et al*., (2009), Almeida *et al*., (2010, 2012, 2013), Cota-Sánchez *et al*., (2007, 2013), Gutiérrez-Flores *et al*., (2017), Muniz *et al*., (2019), Cardoso *et al*., (2019), Silva (2020), and Sampaio and Almeida (in press). In addition, information on floral biology and pollination requirements of pitaya species is still limited, these data may be relevant to improve the fruit set and productivity under both natural and cultivated conditions (Muniz *et al*., 2019).

We aimed to analyze the floral structure of species from to the hylocereoid clade, through an integrated assessment of morphological and anatomical characters of the perigone, androecium, and gynoecium, to improve the understanding of the clade, increase the visibility of still poorly studied species.

## 2. MATERIALS AND METHODS

### 2.1 Selected species

The species selected for analysis represent a sampling of seven taxa of the hylocereoid clade within the tribe Hylocereeae (Table 1, Figure 17), and included *Epiphyllum phyllanthus*, from the phyllocactoid clade, used as outgroup for comparative purposes.

Table 1. Studied species of the hylocereoid clade and outgroup. Information on the origin and sampling number of each taxa. BC: biological collection, cactus garden of IB/CLP UNESP; C: cultivated at Fazenda Brasil Pitaya; N: natural population.

| SPECIES | POPULAR NAME | SOURCE | | | n | Voucher |
|---|---|---|---|---|---|---|
| | | BC | C | N | | |
| *Aporocactus flagelliformis* (L.) Lemaire | Rat tail cactus | x | | | 5 | HUSC1 5885 |
| *Epiphyllum phyllanthus* (L.) Haw. | Orchid cactus, pitainha | x | x | x | 5 | HUEM0 0000278 4 |
| *Selenicereus anthonyanus* (Alexander) D.R. Hunt | Fishbone cactus, zig-zag cactus | x | | | 4 | HUSC1 5886 |
| *Selenicereus megalanthus* (K. Schumann ex Vaupel) Moran | Yellow dragon fruit | x | x | | 5 | HUSC1 6196 |
| *Selenicereus purpusii* (Weingart) S. | Pink dragon fruit | x | x | | 4 | HUSC1 |

| | | | | | | |
|---|---|---|---|---|---|---|
| Arias and N. Korotkova | | | | | | 6197 |
| *Selenicereus vagans* (K. Brandegee) Britton and Rose | Moonlight cactus | x | | | 3 | HUSC1 6198 |
| *Selenicereus validus* S. Arias and U. Guzmán | Fern cactus | x | | | 3 | HUSC1 6211 |
| *Weberocereus bradei* (Britton and Rose) G.D.Rowley | Short-flower peacock | | x | | 1 | HUSC1 6212 |

2.2 Study area

The species analyzed in this study are predominantly cultivated and ornamental specimens, many of which also have commercial relevance. For this reason, part of the botanical material was collected at Fazenda Brasil Pitaia, Sítio Jatobá, located in the municipality of Votuporanga, São Paulo State, southeastern Brazil (20°17′04.58″ S, 49°54′55.96″ W). This site was selected because it hosts an extensive cultivation area comprising multiple species of *Selenicereus*.

2.3 Sampling and morphological assessment of floral specimens

Data was obtained from the random selection of floral buds at pre-anthesis and anthesis stages, which were subsequently analyzed under laboratory conditions. The number of buds sampled varied according to the availability of each species (Table 1). Buds were classified as being in pre-anthesis when the scales covering the tepals began to detach. Fresh flowers were examined during anthesis to record the number, arrangement, dimensions, and coloration of floral organs.

In the laboratory, floral buds were fixed in FAA 50 (formaldehyde, acetic acid, and 50% ethanol) for five days and subsequently stored in 70% ethanol (Johansen, 1940). Measurements of floral structures were obtained using a digital caliper graduated in millimeters (precision 0.1 mm) and with the aid of a Leica® stereomicroscope. Flowers were sectioned longitudinally from the apex of the perigone to the base of the pericarpel to obtain the following measurements: (1) total flower length (from the floral apex to the base of the pericarpel at its insertion on the cladode); (2) flower diameter (distance between the most distant opposing apices of the external perigone segments; (3) nectar chamber length (from the apex of the ovary to the first free filament arising from the floral tube wall); (4) stamens (mean); (5) gynoecium (ovary, style, and stigma lobes).

Sugar concentration of the nectar solution (°Brix) was measured in flowers at anthesis using a manual refractometer (Bellingham and Stanley). It was not possible to obtain °Brix values for all species.

All collected material was fixed and preserved at the Laboratory of Plant Morphology, Campus do Litoral Paulista, UNESP, São Vicente, São Paulo State, Brazil. Voucher specimens (Table 1) were deposited in the HUSC Herbarium of the Universidade Santa Cecília (UNISANTA) and the HRCB (Herbairum Rio Clarense of the São Paulo State University – UNESP). The licenses for sample collecting were authorized by the Biodiversity Information and Authorization System/Chico Mendes Institute for Biodiversity Conservation/Federal Environment Ministry (MMA) - (SISBIO number 105633-1/ SISGEN number ADC0714.

2.4 Statistical analysis

Morphological similarity among species was assessed using a multivariate statistical approach integrating dissimilarity, hierarchical clustering, and ordination methods. Forty-two quantitative (6) and qualitative (36) characters (Table A2) were used to calculate a dissimilarity matrix using Gower's coefficient (Gower, 1971), which is suitable for mixed data types, allowing the integration of variables measured on different scales.

Hierarchical cluster analysis was conducted using the UPGMA method (Unweighted Pair-Group Method with Arithmetic Mean; Sokal and Michener, 1958), which represents relationships among species based on average distances between groups. The results were visualized as a dendrogram. To explore morphological variation in a continuous space, a Principal Coordinates Analysis (PCoA) was performed based on the dissimilarity matrix. The contribution of morphological variables to the ordination structure was evaluated through vector fitting and statistical significance was assessed using permutation tests (n = 999), adopting a threshold of $p < 0.05$.

To assess whether the morphological groups identified in the PCoA differed significantly, a PERMANOVA (*Permutational Multivariate Analysis of Variance*) was performed using the Gower distance matrix. In addition, a multivariate dispersion analysis (BETADISPER) was conducted to determine whether any differences detected by the PERMANOVA could be associated with heterogeneity in within-group data dispersion. All analyses were conducted in R version 4.5.3 (R Core Team, 2026), using the *vegan* (Oksanen *et al*., 2022) and *cluster* (Maechler *et al*., 2026) packages.

## 3. RESULTS

3.1 Floral morphology of selected species of the hylocereoid clade

*Aporocactus flagelliformis*. The flowers are diurnal, lateral, conspicuous, and ascending, displaying zygomorphic symmetry. They are infundibuliform, measuring 4.26–6.75 cm in length (occasionally up to 10 cm) and 2.4–4 cm in diameter. The tepals are shades of pink to magenta. The flowers are polystemonous, with approximately 75 stamens, each up to 4 cm in length. The anthers are papillose, basifixed, and the style and stigma are relatively small, measuring 0.54 cm and 6 lobes, respectively. Externally, the pericarpal and ovary is covered by bristle and spines, and measure 0.13–0.43 cm in length. The nectary, located at the internal base of the floral tube, forms a diffuse nectar chamber measuring 0.25–0.45 cm, with nectar concentration around 25%, (Figure 2, Table A1).

*Epiphyllum phyllanthus*. The flower occurring solitarily, are nocturnal, actinomorphic, with white tepals, scent, with anthesis lasting one night; they are hypocrateriform, with buds measuring 22-27cm in length. The flowers are polystemonous, with 36 anthers, measuring 0,7-1cm in length, they are light brown with complete longitudinal dehiscence. The style measuring 10,5 in length, is light yellow, and the stigma is white with 9-10 lobes. Externally, the pericarpel and ovary is covered by scales in the areolar regions and measuring 1.3 cm in length and 0.2 cm in width. The nectary, located at the internal base of the floral tube, forms an open nectar chamber measuring 14.1 cm, with nectar concentration around 16.6%, (Figure 2, Table A1).

*Selenicereus anthonyanus.* The flowers are conspicuous, nocturnal, and actinomorphic, pink and white tepals, scent and a salverform corolla, measuring 15cm in length and 8cm in diameter. The flowers are polystemonous, with 246 stamens, and basifixed anthers measuring 5 mm. The style measures 7 cm, and the stigma is plurilobate,

comprising 15–16 lobes. The pericarpal and ovary are covered by scales, spines, bristle and gray wool, 1.5cm in length and diameter. The nectary is a diffuse nectar chamber type, with papillae and stomata measuring 0.3-0.4mm, (Figure 1, Table A1).

*Selenicereus megalanthus*. The flowers are initially odorless, becoming strongly fragrant at anthesis. They are nocturnal, conspicuous, and actinomorphic, with a funnelform corolla. The flowers measure approximately 39 cm in length and 21 cm in diameter, with white tepals. The androecium is polystemonous, comprising approximately 317 stamens with basifixed anthers measuring 1 mm in length. The style is 15–17 cm long, and the stigma is plurilobate, with 23 lobes. The pericarpal and ovary are covered by scales, spines and wool, measuring 5.5cm in length and 1.5 cm in diameter. The nectary, located at the base of the floral tube, measures 6-10 cm in length and forms a diffuse nectar chamber, with a nectar concentration around 20%, (Figure 1, Table A1).

*Selenicereus purpusii.* The flowers are large, showy, nocturnal, and strongly scented, with radial symmetry and a funnel-shaped (infundibuliform) corolla. They reach up to 25 cm in length and diameter. The perigone is composed of numerous tepals differing in color and shape: the innermost tepals are broad and white, the median tepals golden, and the outer tepals narrow and purplish, forming scale-like structures. The flowers are polystemonous, with approximately 335 stamens inserted at different levels along the floral tube. The anthers are basifixed, measuring 0.6–0.8 cm. The style measures approximately 13 cm in length and 0.8 cm in width, and the stigma is plurilobate, bearing 26–27 lobes, which may be bifid or entire, ranging 0.6–1.8 cm in length. Externally, the pericarpal and ovary are covered by scales, and measuring 2.5cm in length. The nectary, at the base of the floral tube, is diffuse, measuring 1.5–2.0 cm, with a nectar concentration around 30%, (Figure 1, Table A1).

*Selenicereus vagans.* The flowers are nocturnal, conspicuous, and actinomorphic, with a salverform corolla. Flowers measure approximately 23 cm in length and 16 cm in diameter., with white tepals and greenish bracteoles. They are polystemonous, with approximately 336 stamens, and oblong, basifixed anthers. The style measures 18 cm, and the stigma is plurilobate, with 11–13 lobes. Externally, the pericarpel and ovary are covered spines and wool, and measure 1.2–1.6 cm in length and 0.5–1.6 cm in diameter. The nectary is a diffuse, open chamber, measuring 4.1–4.8 cm with a nectar concentration around 35% and possess an extranuptial nectary, (Figure 1, Table A1).

*Selenicereus validus*. The flowers are conspicuous, nocturnal, with a salverform corolla. Tepals white coloration and actinomorphic symmetry, emitting a white chocolate fragrance, measuring 16–22 cm in length and 12–13.5 cm in diameter, the scales are greenish. The flowers are polystemonous, with approximately 116–120 stamens, and basifixed anthers measuring 4 mm. The style is long, and the stigma is plurilobate, comprising 13–15 lobes of 0.7 mm. Externally, the pericarpel and ovary are covered with greenish-reddish scales, spines and bristles, and measure 1cm in length, bearing spines in the areolas. The nectary is located at the base of the floral tube, forming a diffuse nectar chamber measuring 1.5 cm in length (Figure 1, Table A1).

*Weberocereus bradei.* The flowers are nocturnal, located at the apical portion of the cladodes, occurring either solitarily or in small clusters. They are infundibuliform, with buds measuring 5.5–7 cm in length. The tepals are white to yellowish, and the floral scales are greenish red. The flowers are polystemonous, with 116 stamens measuring 1.2–1.5 cm. The anthers are papillose, basifixed, measuring 0.2–0.4 cm. The style is short, measures 3.5 cm in length. Externally the pericarpal and ovary segments are fleshy, sometimes only slightly expanded, covered by scales in the areolar regions, and measure 1.2 cm in length and 0.4 cm in width. The nectary, located at the internal base of the floral tube, forms an open nectar chamber measuring 1.09 cm, (Figure 2, Table A1).

## 3.2 Floral anatomy of selected species of the hylocereoid clade

### 3.2.1 *Aporocactus flagelliformis*

Scale structure. The epidermis is uniseriate, with a thin cuticle and composed of isodiametric cells with some papillose projections. The mesophyll contains 2 layers of collenchyma, followed by cells of variable sizes, containing starch grains, as well as large secretory idioblasts and developing secretory cavities. Small collateral vascular bundles are longitudinally distributed throughout the mesophyll, (Figure 4, D).
Outer tepal structure. The epidermis is uniseriate, with thin cuticle, and variable cell shapes with some papillose projections. The mesophyll contains one layer of angular collenchyma cells, followed by parenchymatous cells of variable sizes, including starch grains, secretory idioblasts, and developing secretory cavities. Small collateral vascular bundles are longitudinally distributed along the central region of the tepal, (Figure 4, E).
Inner tepal structure. The epidermis is uniseriate, with thin cuticle, and variable cell shapes with some papillose projections. The mesophyll includes one layer of collenchyma, followed by parenchymatous cells of variable size, starch grains, secretory idioblasts, and developing secretory cavities. Small collateral vascular bundles are present centrally along the tepal, (Figure 4, F).

Androecium structure. The filament is composed of a uniseriate epidermis with large, elongated, papillose cells, (Figure 6, D-E). The mesophyll consists of 5–6 layers of parenchymatous cells, containing secretory cavities, and a central amphicribal vascular bundle. The dehiscent anther of the flower at anthesis presents a papillose epidermis, followed by a uniseriate endothecium composed of rectangular cells with secondary wall thickenings in bands along the anticlinal walls, and stomial cells along the dehiscence line, facilitating pollen release. Centrally, a concentric amphicribal vascular bundle, derived from the filament, is observed, (Figure 6, C).

Pericarpel structure. The outer epidermis is uniseriate, composed of irregular cells. The mesophyll consists of 1–2 layers of collenchyma cells of variable size, followed by the parenchyma tissue containing several cell layers, and mucilage-secreting idioblasts, extending internally to a large ring of collateral vascular bundles that delimit the pericarpel and ovary, (Figure 12, D). The ovarian parenchyma consists of 23–30 layers of smaller cells (compared to the pericarpel), with variable shapes and abundant starch grains, decreasing in size toward the placenta, where small vascular bundles encircle the ovarian cavity to supply the ovules. The inner epidermis of the ovary is uniseriate, composed of small cells and bearing trichomes in the placental region (Figure 12, E).

Ovule structure. The ovule presents a long funiculus containing a central vascular bundle that extends to the chalazal region. It is circinotropous with two integuments (internal and external), with the micropyle delimited by the inner integument. The outer tegument is composed of 3–5 cell layers, with visible lignin (phenolic compound) accumulation in the outermost layer. The inner tegument, separated by a thin cuticle, consists of 5–12 cell layers, (Figure 12, E).

Floral tube structure. The outer epidermis at the apex is formed by a thick cuticle, small and irregular cells, and just below, the mesophyll begins with 1-2 layers of collenchyma cells, prismatic in shape and with an irregular outline; around it, the presence of medium caliber collateral vascular bundles is observed, which occur through a loose parenchyma, composed of smaller prismatic cells, with varied shapes and wide intercellular spaces, (Figure 15, I); The next inner epidermis presents vascular traces individualizing into free filaments. In median region, it is histologically similar to the

apex, except for having an internal epidermis with a transition zone where nectar tissue is replaced by numerous vascular bundles of filaments, (Figure 15, H). The number of small collateral vascular bundles is greater than in the non-apex. These bundles exhibit vascular traces that individually vascularize each stage. At the base of the floral tube, the epidermis is composed of a layer of small, irregularly formed cells, covered with a thin layer of cuticle. The mesophyll has prismatic cells, larger in relation to the epidermis, and many mucilage-secreting idioblasts; they have small parallel vascular bundles that join to form larger bundles. Inside the tube, there is the nectar tissue, characterized by a unicellular trichomatous epidermis. Below the epidermis, there are 6 to 12 layers of secretory parenchyma cells, which are small, prismatic, with dense cytoplasm, providing intense metabolic activity. In addition, a series of small vascular bundles (traces) are present, performing a possible dual function: vascularizing both the nectar tissue and the filaments and anthers later, (Figure 15, G).

### 3.2.2 *Epiphyllum phyllanthus*

Scale structure. The epidermis is covered by a thick cuticle and is composed of irregular cells with some stomata. Beneath the epidermis, 1 layer of collenchyma is present. The mesophyll consists of cells of variable size, interspersed with large secretory idioblasts distributed throughout the tissue. Small collateral vascular bundles are longitudinally arranged near the center of the organ, (Figure 14, J).

Outer tepal epidermis and organization are like the scale, (Figure 14, K). Inner tepal structure. The epidermis is uniseriate, with thick cuticle and irregular cells. The mesophyll comprises cells with variable shapes, and a lot of idioblasts cells, forming a loose parenchyma, with small collateral vascular bundles organized centrally throughout the tepal, (Figure 14, L).

Androecium structure. The filament is composed of a uniseriate epidermis, formed by irregular cells, (Figure 6, H). The mesophyll is circular, consisting of parenchyma tissue arranged in layers, containing large secretory idioblasts. Centrally, a concentric amphicribal vascular bundle is observed, in which the xylem is surrounded by the phloem. The anther of a flower at anthesis, near pollen release, presents a papillose epidermis and a uniseriate endothecium composed of rectangular cells exhibiting secondary wall thickenings in bands along the anticline walls. Stomial cells are located along the dehiscence line, which rupture during anthesis to release pollen grains. Centrally, a concentric amphicribal vascular bundle occurs, derived from the filament, (Figure 6, I).

Gynoecium structure. The epidermis of each stigma lobe is composed of trichomatous cells containing phenolic compounds, (Figure 8, G, H). The underlying mesophyll comprises six superficial layers of very small cells with few intercellular spaces, followed by layers of larger, rounded cells containing numerous starch grains and idioblasts. Centrally, a concentric amphicribal vascular bundle is present. In the apical portion of the style, the uniseriate epidermis exhibits a thick cuticle over isodiametric cells. The mesophyll shows a circular organization, consisting of one to two layers of collenchymatous cells followed by approximately six layers of circular parenchyma cells, with large mucilage-secreting cells forming a ring around the vascular tissue. The vascular system is composed of approximately 9–10 small amphicribal bundles surrounding the central transmitting tissue, (Figure 10, G). In the basal portion of the style, the epidermis differs from the apical region by the presence of papillary cells, (Figure 10, H).

Pericarpel structure. The pericarpel has a circular shape with indentations forming small ribs on the outside and exhibits a thick cuticle and is composed of small, uniseriate

and irregular cells, (Figure 12, H). The mesophyll consists of 1–2 layers of collenchyma cells, followed by a parenchyma tissue with cells of variable size, containing mucilage-secreting idioblasts internally, which extend toward a large ring of collateral vascular bundles delimiting the pericarpel and ovary. Additionally, large idioblasts, numerous starch grains, and parenchyma cells similar in size to the pericarpel mesophyll are present, gradually decreasing in size toward the funiculi. The inner epidermis of the ovary is uniseriate, composed of small cells of variable shape, and bears trichomes in the placental region. Beneath this layer, there are elongated parenchymatous cells and small vascular bundles that encircle the ovary wall and vascularize the ovules. The ovule presents a long funiculus containing a central vascular bundle that extends to the chalazal region. The ovule is circinotropous with two integuments (external and internal), with the micropyle delineated by the inner integument. The outer integument consists of 1–2 cell layers, with visible lignin accumulation in the outermost layer, while the inner internal tegument, separated by a thin cuticle, is composed of 1–2 layers of cells. In the region near the micropyle, a large intercellular space occurs between the internal integuments, (Figure 12, I).

Floral tube structure. The outer epidermis at the apex of the floral tube has a thick cuticle and is composed of normal cells, (Figure 16, L). The mesophyll contains 1–2 layers of large collenchyma cells of variable shape, interspersed with numerous layers of parenchyma cells, and larger idioblasts. Collateral vascular bundles of medium caliber are distributed up to the median region. Adjacent to the vascular bundles, the parenchymatous cells form a loose parenchyma, composed of smaller cells with variable shapes and wide intercellular spaces. Near the inner epidermis, vascular traces are observed, which later individualize into free bundles, in significantly lower numbers than in the central region of the tube. The outer epidermis of the median portion of the floral tube exhibits a thick cuticle over one layer of cells, (Figure 16, K). The mesophyll begins with one layer of collenchymatous cells, larger than the epidermal cells, containing numerous layers of parenchyma cells, idioblasts and small collateral vascular bundles. Internally, a transition zone can be identified where nectar tissue is replaced by numerous vascular bundles of filaments. At the base of the floral tube, the epidermis and outer mesophyll layers are organized similarly to the middle and apical portions, (Figure 16, J). The nectary tissue is distinguished by a unicellular papillose epidermis, (Figure 16, G). Beneath it, there are secretory parenchyma, composed of small prismatic cells with dense cytoplasm, indicating high metabolic activity. Large vascular bundles are present in the underlying region, likely performing a dual function, supplying both the nectar tissue and the filaments and anthers.

### 3.2.3 *Selenicereus anthonyanus*

Scale structure. The epidermis exhibits a thin cuticle with irregular cells and some stomata. The mesophyll begins with 1–2 layers of collenchyma cells, followed by approximately 10 layers of larger cells with variable shapes, interspersed with large idioblasts, secretory canal in formation, and small collateral vascular bundles arranged longitudinally along the entire scale, (Figure 3, G).

Outer tepal structure. The epidermis has a thin cuticle, small, and irregular cells. The mesophyll is composed of larger cells, with variable shapes, interspersed with large idioblasts and small collateral vascular bundles arranged longitudinally along the central region of the tepal, (Figure 3, H).

Inner tepal structure. The epidermis has a thin cuticle, small and irregular cells. The mesophyll contains larger cells of variable shape and size, with large idioblasts,

secretory cavities in formation, forming a region of loose parenchyma with numerous intercellular spaces, and small collateral vascular bundles longitudinally arranged along the entire tepal, (Figure 3, I).

Androecium structure. The filament exhibits uniseriate epidermis composed of rounded cells with stomata, (Figure 5, G). The mesophyll is circular, begins with 2 layers of collenchyma cells, which are initially rounded and gradually decrease in size toward the central region, with some idioblasts interspersed. Centrally, a concentric amphicribal vascular bundle is present, in which the xylem is surrounded by the phloem. The dehiscent anther presents a papillose epidermis and a uniseriate endothecium composed of rectangular cells exhibiting secondary wall thickenings in bands along the anticlinal walls. Stomium region occurs along the dehiscence line, which rupture during anthesis to release pollen grains. Centrally, a concentric amphicribal vascular bundle, derived from the filament, is present, with the xylem surrounded by the phloem, (Figure 5, F).

Gynoecium structure. The epidermis of each stigma lobe is composed of trichomatous cells, (Figure 7, E-F). The mesophyll contains elongated cells with few intercellular spaces, and secretory idioblasts are observed near a six smalls vascular bundle. Style structure. The epidermis at the apex of the style exhibits a thin cuticle and normal cells containing phenolic compounds. The mesophyll is circular, beginning with 2–4 layers of collenchyma cells, followed by 30 layers of rounded parenchymatous cells, that decrease in size in direction to the center of the stigma lobe. Large idioblasts and secretory cavities form a ring around small amphicribal vascular bundles, which merge to form 15 large bundles. Internal to these bundles, cell size gradually decreases, and idioblasts are smaller near the transmitting tissue, which is associated with small vascular bundles. The central transmitting tissue contains trichomes and 3–4 layers of small tightly packed cells, forming a stylar cleft. The epidermis at the base of the style is composed of normal cells containing phenolic compounds, (Figure 9, E). The mesophyll is circular, beginning with 3–4 layers of collenchyma cells, followed by approximately 30 layers of small, rounded cells containing numerous starch grains. Large idioblasts, smaller than apex mesophyll, form a ring around small amphicribal vascular bundles, which merge to form 15 large bundles. Internal to these bundles, cell size gradually decreases, and idioblasts become smaller near the central transmitting tissue, which is associated with small vascular bundles, (figure 9, F).

Pericarpel structure. The outer epidermis is uniseriate, composed of small and irregular cells, mostly elongated and stomata, (Figure 11, F). The mesophyll begins with 1–4 layers of small collenchyma cells, elongated to rounded and of variable shape, followed by 15 layers of large cells, containing idioblasts and small vascular bundles that extend toward a large ring of collateral vascular bundles, delimiting the pericarpel/ovary. Internally, the tissue becomes looser, composed mostly of irregular small cells, extending toward small vascular bundles near the funiculi, (Figure 11, G).

The inner epidermis of the ovary is uniseriate, composed of small, irregularly shaped cells, with trichomes in the placental region, followed by elongated parenchymatous cell layers and small vascular bundles that encircle the ovary wall and vascularize the ovules. The ovule presents a long funiculus containing a central vascular bundle extending to the chalazal region. It has two integuments (internal and external) with the micropyle delimited by the internal tegument. The outer integument consists of 1–2 cell layers, while the inner integument is separated by a thin cuticle and composed of small cells. Opposite the micropyle, a large intercellular space occurs between the internal and external integuments, (Figure 11, H).

Floral tube structure. At the apex of the floral tube the epidermis exhibits an irregular cell layer with some stomata, (Figure 14, F). The mesophyll consists of 2–6

layers of small, mostly rounded collenchyma cells, followed by larger cells interspersed with numerous idioblasts and collateral vascular bundles small in caliber near the outer epidermis and medium in caliber in the central region. Toward the inner portion of the tube, small vascular traces individualize into free bundles in smaller numbers than in the central region, forming a region of loose parenchyma with numerous intercellular spaces, (Figure 14, C). The outer epidermis of the median portion is unicellular, with irregular cells. The mesophyll begins with 2-3 layers of small, elongated collenchyma cells, which progressively increase in size and become rounded; medium-caliber bundles are found accompanied by numerous idioblasts. In this portion of the tube is possible to identify a transition zone between the nectary tissue and the filament projections with inumerous vascular bundles, (Figure 14, B, E). At the base of the floral tube, the epidermis and outer mesophyll layers resemble the organization described for the middle and apical portions. The nectar tissue is distinguished by a unicellular, with small papillose internal epidermis with phenolic compounds; below this layer, there are 3–5 layers of small prismatic secretory, parenchymatous cells. The underlying region contains vascular bundles, likely performing a dual function, supplying both the nectar tissue and the filaments and anthers, (Figure 14, D, A).

### 3.2.4 *Selenicereus megalanthus*

Scale structure. The epidermis is covered by a thin cuticle, irregular cells and discreet papillose projections. In the adaxial portion, the cells are mostly small and elongated, while in the abaxial portion, they become larger. The mesophyll consists of one layer of small collenchyma cells, followed by 9 layers of larger cells interspersed with large idioblasts and collateral vascular bundles arranged longitudinally along the entire organ, (Figure 3, D).

Outer tepal structure. The epidermis exhibits thin cuticle, small and irregular cells. The mesophyll begins with one layer of small collenchyma cells, followed by 6–7 layers of larger cells of variable shape, with large idioblasts intercalated with small collateral vascular bundles arranged longitudinally along the central region of the tepal, (Figure 3, E).Inner tepal structure. The epidermis has a thin cuticle, with small cells of variable shape. The mesophyll contains one layer of collenchyma cells, followed by 10–12 layers of cells of variable shape, with large idioblasts distributed throughout the tissue in greater abundance than in previous structures, and small collateral vascular bundles longitudinally arranged along the entire tepal, (Figure 3, F).

Androecium structure. The filament is composed of a uniseriate epidermis, formed by elongated papillose cells, (Figure 5, D). The mesophyll is compact, containing large secretory idioblasts and numerous starch grains. Centrally, a concentric amphicribal vascular bundle is present, in which the xylem is surrounded by phloem. The dehiscent anther presents a papillose epidermis and a uniseriate endothecium, composed of rectangular cells with secondary wall thickenings in bands along the anticlinal walls. In this stage of development, the opening of the anther occurred at stomium region, (Figure 5, E).

Gynoecium structure. The epidermis of each stigma lobe is composed of trichomatous cells, (Figure 7, C). The mesophyll contains elongated cells with few intercellular spaces, and secretory idioblasts are observed near a vascular bundle. Centrally, a concentric amphicribal vascular bundle is present. Style structure: The epidermis at the apex of the style exhibits a thin cuticle and epidermal cells of variable shape, some of which are papillose, (Figure 9, C). The mesophyll is circular, comprising 1–2 layers of collenchyma cells and large mucilage secreting cells forming a ring around

small amphicribal vascular bundles, which merge to form 24 large bundles and some numerous starch grains are present. Internal to the vascular bundles, the cells gradually decrease in size, and idioblasts are smaller near the central transmitting tissue. The central transmitting tissue contains trichomes and layers of small, tightly packed cells, forming a stylar cleft. At the base of the style, the epidermis is composed of small cells of variable shape, some papillose containing phenolic compounds. The mesophyll is circular, with patches of collenchyma, cells of variable size and shape, and small amphicribal vascular bundles that converge to form a single large caliber bundle. Internal to the vascular bundles, cells gradually decrease in size, and smaller vascular traces are present. The central transmitting tissue contains trichomes and layers of small, tightly packed cells, forming a stylar cleft that is more compact than in the apical portion, (Figure 9, D).

Pericarpel structure. The outer epidermis is uniseriate, with small cells of variable shape, some with papillose projections, (Figure 11, C). The mesophyll begins with 1–4 layers of small, elongated, prismatic collenchyma cells, followed by a parenchyma tissue containing idioblasts and small vascular bundles that extend toward a large ring of collateral vascular bundles delimiting the pericarpel and ovary. Internally, the tissue becomes looser, composed mostly of small hexagonal cells, extending toward small vascular bundles near the placental region, (Figure 11, D).

The inner epidermis of the ovary is uniseriate, composed of small cells of variable shape and trichomes in the placental region, followed by elongated parenchymatous cells and small vascular bundles encircle the ovary wall and vascularize the ovules. The ovule presents a long funiculus containing a central vascular bundle that extends to the chalazal region. It has two teguments (internal and external) and the micropyle is delimited by the inner internal tegument. The outer integument consists of 1–2 cell layers, while the inner integument is separated by a thin cuticle and composed of small cells. In the region opposite the micropyle, a large intercellular space occurs between the integuments, (Figure 11, E).

Floral Tube Structure. The outer epidermis at the apex of the floral tube is composed of small papillose cells of variable shape, (Figure 13, L). The mesophyll initially consists of approximately three layers of small prismatic collenchyma cells, followed by 35 layers of larger cells, interspersed with numerous idioblasts and collateral vascular bundles small in caliber near the epidermis and medium in caliber in the central region. Toward the inner portion of the tube, small vascular traces individualize into free bundles, in fewer numbers than in the central region. At the medium region and at the base of the floral tube the epidermal cells and outer mesophyll layers are organized similarly to those at the apex, but in the medium, a transition zone between nectary tissues and parenchyma tissue and the numerous vascular bundles, (Figure 13, H-K). At the base of the tube, the nectary tissue is distinguished by a unicellular trichomatous epidermis and 3–4 layers of small compact secretory parenchymatous cells below the epidermis, (Figure 13, G-J).

### 3.2.5 *Selenicereus purpusii*

Scale structure. The uniseriate epidermis is covered by a thin cuticle, and it consists of small, predominantly isodiametric cells, some stomata and papillae projections. The mesophyll begins with 1-2 collenchyma layers, followed by small parenchymatous cells, progressively increasing in size and exhibiting more variable shapes toward the central region. In the vertical extremities, the mesophyll comprises 5–6 cell layers, whereas in the central portion, it presents 20–24 layers. Collateral vascular bundles of small caliber are distributed throughout the mesophyll, (Figure 4, A).

Outer Tepal Structure. The epidermis exhibits a thin cuticle, small cells, elongated, and papillose, with the presence of a few stomata. The mesophyll consists of 1–2 layers of collenchyma, more concentrated in the abaxial portion. The mesophyll cells are large, and the central region contains secretory channels. Small collateral vascular bundles of reduced size are horizontally distributed along the center of the organ, (Figure 4, B).

Inner Tepal Structure. Exhibits a uniseriate epidermis, covered bythin cuticle, smaller, irregular and more elongated cells than those of the mesophyll. The mesophyll consists of one layer of collenchyma, followed by 5–6 layers of large cells exhibiting diverse morphologies, ranging from rectangular to lenticular shapes, and containing numerous mucilaginous idioblasts. The vascular bundles are collateral and small size, (Figure 4, C).

Androecium structure. The filament is composed of a uniseriate epidermis with large cuboid to slightly prismatic, papillose cells, (Figure 6, B). The mesophyll consists of 5–6 layers of parenchyma cells, containing secretory cavities, and a concentric, amphicribal central vascular bundle, in which the xylem is surrounded by phloem. The anther, at pre-anthesis, is bilocular and longitudinally dehiscent, with a small, papillose epidermis. It is followed by a uniseriate endothecium composed of rectangular cells exhibiting secondary wall thickenings in bands along the anticlinal walls. Internally, the anther contains numerous mature pollen grains, ready for dispersal, (Figure 6, A).

Gynoecium Structure. The stigma epidermis is predominantly composed of trichomes, many of which contain phenolic compounds, (Figure 8, A-B). The mesophyll in the superficial layers exhibits secretory cavities, while the deeper layers are composed of approximately 13 layers of prismatic parenchyma cells. Centrally, a concentric amphicribal vascular bundle is observed, with the phloem surrounding the xylem. The vascular bundle located at the center of each stigma lobe is also amphicribal. Style structure. In the apical portion of the style, the uniseriate epidermis is composed of cells of variable shape, ranging from spherical to cuboid, and some stomata, (Figure 10, A) The mesophyll is circular and begins with 1-2 collenchyma layers organization followed by prismatic cells with 11–16 layers of large parenchyma cells containing abundant idioblasts and secretory mucilage cavities, 27 amphicribal vascular bundles and more than 40 layers of progressively smaller parenchymatous cells toward the center, with a higher concentration of mucilage-secreting cells. The transmitting tissue is composed of small cells with dense cytoplasm and surrounds an internal cavity lined by a trichomatous epidermis, structurally like that of the stigma. Basal portion of the style. The epidermis at the base of the style is covered by a thin cuticle and shows normal cells with phenolic compounds. The mesophyll comprises one to three layers of collenchyma formed by cuboid to slightly elongated cells, with idioblasts distributed throughout the circular mesophyll, forming a ring around the vascular region. Small vascular bundles coalesce into larger bundles, while the parenchymatous cells internal to these bundles are prismatic and arranged in approximately 50 layers, extending toward the transmitting tissue, (Figure 10, B).

Pericarpel structure. The outer epidermis is composed of small cells ranging from prismatic to cuboid, interspersed with larger papillose cells and occasional stomata. The mesophyll begins with 1-2 layers of collenchyma, followed by larger cells varying from rounded to prismatic, which progressively increase in size toward the central portion, and some numerous idioblasts and developing secretory cavities are distributed throughout the tissue. Collateral vascular bundles are present, being smaller near the epidermis and larger toward the median region of the organ, where they delineate the boundaries of the

pericarpal, (Figure 12, A). The inner epidermis of the ovary is uniseriate, composed of isodiametric cells, and trichomes. Beneath the epidermis, approximately 8 layers of small parenchyma cells contain numerous starch grains and small collateral vascular bundles responsible for the ovule vascularization. Internally, an extensive histological region comprises a lot of layers of loose parenchyma, containing small vascular bundles, which extend toward a ring of large collateral vascular bundles, delimiting the ovary externally, (Figure 12, B). Ovule Structure. In the placental region, a projection of the placenta is observed, accompanied by the branching of the funiculi, which are long and possess a bitegmic structure. The chalazal region contains delicate vascular bundles, while an intercellular space is noticeable between the outer integument and the nucellus. The micropyle is delineated exclusively by the inner integument, (Figure 12, C).

Floral Tube Structure. The outer epidermis of the apical portion of the floral tube is composed of small prismatic cells, some exhibiting papillose projections. Beneath the epidermis, the mesophyll begins with 2–3 layers of collenchyma cells, followed by 20–25 layers of large parenchymatous cells with prismatic shapes and irregular contours, containing secretory cells, canals, and secretory cavities, (Figure 15, F, C). Large collateral vascular bundles are present, followed by loose parenchyma, composed of smaller prismatic cells with variable shapes and wide intercellular spaces, totaling over 30 cell layers, (Figure 15). Vascular traces corresponding to the bundles that supply the stamens are also visible. The inner epidermis is composed of small, glabrous, with a thin cuticle. Middle portion of the tube. The outer epidermis consists of small, mostly isodiametric cells, with a few papillae. The mesophyll begins with 4 layers of lamellar collenchyma composed of small cells, followed by approximately 40–50 layers of compact parenchymatous cells of variable shapes and contours, including secretory cavities, (Figure 15, E, B). Collateral vascular bundles of large caliber are present and are followed by loose parenchyma, containing roughly 40 layers of smaller cells and multiple small vascular bundles located near the inner surface of the tube. Internally, this region exhibits alternating zones of nectary tissue and filament insertion projections. Basal portion of the tube. The epidermis at the base of the tube is trichomatous, and some stomata. Beneath the epidermis, 1–4 layers of collenchyma cells are present, with cells of diverse sizes and shapes, numerous collateral vascular bundles, as well as secretory idioblasts and cavities. Internally, the nectar tissue is characterized by a trichomatous epidermis bearing specialized nectar-stomata, which facilitates nectar release. Beneath the epidermis, there are 10–15 layers of secretory parenchyma, composed of small isodiametric cells with dense cytoplasm and large nuclei, indicating high metabolic activity. Additionally, a series of small vascular bundles are present, likely performing a dual function, supplying both the nectary tissues and the filaments and anthers, (Figure 15, D, A).

### 3.2.6 *Selenicereus vagans*

Scale structure**.** The epidermis is uniseriate and covered by a thin cuticle, it is made of small cells predominantly rectangular, with some presenting papillose projections. The mesophyll comprises one to two layers of collenchyma cells adjacent to the adaxial surface, formed by rounded and tightly packed cells. In contrast, the abaxial region exhibits more elongated cells and numerous intercellular spaces. In the central region, large idioblasts associated with small collateral vascular bundles, arranged longitudinally throughout the organ, are evident, (Figure 3, J).

External structure of the tepal. The uniseriate epidermis is characterized and small irregular cells and covered by a thin cuticle. The mesophyll consists of rounded cells, some containing abundant starch grains, whose size increases gradually toward the central region. In this region, small collateral vascular bundles are longitudinally arranged along the entire tepal. Large idioblasts are distributed throughout the mesophyll, (Figure 3, K). The organization, epidermis and mesophyll of the internal structure of the tepal is similar to described for external tepal, (Figure 3, L).

Structure of the androecium. The filament exhibits a uniseriate epidermis composed of elongated cells with papillose projections, (Figure 5, I). The mesophyll is compact and formed by layered parenchymatous tissue containing large secretory idioblasts and numerous starch grains. Centrally, a concentric amphicribal vascular bundle is present, in which the xylem is surrounded by the phloem. The anther is dehiscent and presents a papillose epidermis and a uniseriate endothecium composed of rectangular cells with secondary wall thickenings arranged in bands along the anticlinal walls. Stomial cells are located along the dehiscence line, which rupture during anthesis to release pollen grains, and a central concentric amphicribal vascular bundle, derived from the filament, is also observed, (Figure 5, H).

Gynoecium structure. The epidermis of each stigma lobe is composed of small trichomatous cells containing phenolic compounds, (Figure 7, G-H). The mesophyll consists of elongated cells with few intercellular spaces, and secretory idioblasts occur near a centrally located concentric amphicribal vascular bundle. In the apical portion of the style, the epidermis presents a thick cuticle and predominantly rectangular cells, (Figure 9, G). The mesophyll is circular and composed of one collenchyma layer and approximately ten layers of small cells containing numerous starch grains. Large idioblasts coalesce to form secretory cavities surrounding the vascular tissue, which consists of 13 small amphicribal vascular bundles. The transmitting tissue is composed of small, tightly packed cells containing starch grains and presents a central stylar cleft delimited by a papillose epidermis. At the base of the style, the epidermis also exhibits a thick cuticle and rectangular cells containing phenolic compounds. The mesophyll is compact and composed of up to 20 layers of secretory idioblasts forming a ring around 13 small amphicribal vascular bundles. Internal parenchymatous cells decrease in size toward the transmitting tissue, which is composed of small, juxtaposed cells arranged circularly and presents a more compact stylar cleft compared to the apical region, (Figure 9, H).

Structure of the pericarpel. The outer epidermis is uniseriate, with a thick cuticle and small cells of variable shape, predominantly elongated, (Figure 11, J). The mesophyll begins with one to two layers of collenchyma cells, followed by approximately 18–20 layers of large cells interspersed with idioblasts and small vascular bundles, extending toward a ring of collateral vascular bundles delimiting the pericarp/ovary boundary. Internally to this ring, the tissue becomes looser, with numerous intercellular spaces and composed mainly of small irregular cells extending toward vascular bundles near the funiculi. The inner epidermis of the ovary is uniseriate and composed of small irregular cells with trichomes delimiting the placental region. The ovules are bitegmic, with a long funiculus containing a central vascular bundle extending to the chalazal region. The outer integument consists of one to two cell layers, while the inner integument is separated by a thin cuticle and composed of small cells. A large intercellular space is present in front of the micropyle, (Figure 11, J).

Floral tube structure. In the apical portion, the floral tube exhibits a thick cuticle, covering the uniseriate epidermis, that exhibits papillose cells, and occasional stomata. The mesophyll initially comprises two to three layers of small collenchyma cells,

followed by larger parenchyma cells forming approximately 30 layers interspersed with numerous idioblasts and collateral vascular bundles. These bundles are smaller near the outer epidermis and larger in the median region, (Figure 14, L, I). Toward the inner portion, vascular traces differentiate into free filaments within a loose parenchyma rich in intercellular spaces. The outer epidermis of the median portion is unicellular, with irregular cells. The mesophyll has approximately 40 layers of parenchymatous cells, and starts with elongated cells, which progressively increase in size and become rounded. In this portion of the floral tube is possible to observe a rearrangement of the vascular system, noted by the junction of small vascular bundles that came from the base of the floral tube mesophyll; giving rise, in this median zone, to medium-caliber bundles are found accompanied by numerous idioblasts. Internally, a transition zone can be identified, where nectary tissue is replaced by numerous filament projections, (Figure 14, K, H). At the base of the floral tube, the epidermal and outer mesophyll organization resembles that of the apical region. Internally, nectary tissue is distinguished by a uniseriate trichomatous epidermis. Beneath this layer, approximately 10–14 layers of compact secretory parenchyma indicate high metabolic activity. The underlying region contains large vascular bundles, likely involved in supplying both the nectary tissues and the reproductive structures (stamens), (Figure 14, J, G).

### 3.2.7 *Selenicereus validus*

Scale structure. The epidermis is covered by a thin cuticle, cells with variable shapes and some papillae. The mesophyll contains small collenchyma cells near the epidermis and larger cells toward the center, with large idioblasts observed and small collateral vascular bundles are arranged longitudinally along the scale, (Figure 3, A).
Outer tepal structure. The epidermis has a thin cuticle, small and irregular cells. The mesophyll contains small, rounded cells which increase in size approaching the small collateral vascular bundles arranged longitudinally throughout the tepal, and large idioblasts are distributed throughout the mesophyll in greater abundance than observed in the scales, (Figure 3, B).

Inner tepal structure. The epidermis has a thin cuticle, small and irregular cells. The mesophyll includes one layer of collenchyma cells, followed by small cells with undefined shapes, large idioblasts distributed in the tepal, and small collateral vascular bundles longitudinally arranged, (Figure 3, C).

Androecium structure. The filament is composed of a uniseriate epidermis, formed by elongated cells with papillose projections, (Figure 5, B). The mesophyll is compact, consisting of parenchymatous tissue arranged in layers, containing large secretory idioblasts and numerous starch grains. Centrally, a concentric amphicribal vascular bundle is present, in which the xylem is surrounded by the phloem. The dehiscent anther presents a papillose epidermis and a uniseriate endothecium composed of rectangular cells exhibiting secondary wall thickenings in bands along the anticlinal walls. Stomium region is made for cells located along the dehiscence line, which splits during anthesis to release pollen grains. Centrally, a concentric amphicribal vascular bundle, derived from the filament, is observed, with the xylem surrounded by the phloem, (Figure 5, C).

Gynoecium structure. The epidermis of each stigma lobe is composed of prismatic, trichomatous cells. The mesophyll contains elongated cells with few intercellular spaces, and secretory idioblasts are observed near a vascular bundle, (Figure 7, A, B). Centrally, a concentric amphicribal vascular bundle is present. The epidermis of the apical portion of style exhibits thin cuticle and epidermal cells of variable shape. The mesophyll is circular, with 1–2 layers of collenchyma and large mucilage-secreting cells

forming a ring around the vascular tissue, which consists of 13 small amphicribal vascular bundles and abundant starch grains. The central transmitting tissue shows variation in the number of cell layers, which increases in size toward the inner region of the style. Internally, a cleft is delimited by papillose epidermis, (Figure 9, A). At the base of the style, the epidermis exhibits a thin cuticle with epidermal cells of variable shape. The mesophyll is circular and compact, comprising 2–4 layers of collenchyma, secretory idioblasts, and forming a ring around the vascular region, which consists of amphicribal vascular bundles, parenchymatous cells internal to the vascular bundles extend toward the central transmitting tissue, gradually decreasing in size. The transmitting tissue is composed of cells arranged in a circular pattern, and internally, a cleft is delineated by trichomatous epidermis, (Figure 9, B).

Pericarpel structure. The outer region of the pericarpel exhibits a thin cuticle and is composed of small, uniseriate epidermal cells of variable shape, some with papillose projections, (Figure 11, A). The mesophyll consists of small, elongated cells, interspersed with numerous idioblasts, extending internally to a large ring of collateral vascular bundles that delimit (arbitrarily) the pericarpel and the carpelar tissues, toward the funiculi, the tissue becomes looser, composed of mostly small hexagonal cells, with small idioblasts and minor vascular bundles. The inner epidermis of the ovary is uniseriate, composed of small cells of variable shape, and trichomes in the placental region. The ovule has a long funiculus, containing a central vascular bundle that extends to the chalazal region. It is circinotropous with two integuments, the micropyle delimited by the inner tegument. The outer integument consists of 1–2 cell layers, with visible lignin accumulation in the outermost layer. Opposite the micropyle, a large intercellular space occurs between the integuments, (Figure 11, B).

Floral tube structure. The outer epidermis at the apical of the floral tube is composed of small, rounded, papillose cells, (Figure 13, F). The mesophyll begins with approximately three layers of small prismatic collenchyma cells, followed by more or less 37 layers of larger cells interspersed with numerous idioblasts and collateral vascular bundles, small in caliber near the epidermis and medium in caliber toward the central region. Toward the inner portion of the tube, there are about 20 layers of variable shape cells, forming a loose parenchyma, in which small vascular traces individualize into free bundles, in fewer numbers than in the central region of the tube. The outer epidermis of the median portion is unicellular, with elongated cells, some papillose, (Figure 13, E). The mesophyll begins with one layer of small, elongated collenchyma cells, followed by a parenchyma, which progressively increase in size and become rounded; small vascular bundles are present at the mesophyll, merging to form larger bundles, accompanied by numerous small idioblasts near the epidermis and medium caliber bundles in the median region. At the base of the floral tube, the epidermis and outer mesophyll layers resemble the organization described for the middle and apical portions, (Figure 13, D); while the inner part of the tube, is characterized by the nectary region, (Figure 13, A). Which is distinguished by large vascular bundles, likely performing a dual function, supplying both the nectar tissue and the filaments and anthers, followed by 3–4 layers of small prismatic secretory parenchymatous cells with dense cytoplasm, indicating high metabolic activity, and the internal epidermis of the ovary is papillose.

### 3.2.8 *Weberocereus bradei*

Scale structure. The epidermis is covered by a thick cuticle and is composed of one layer of cuboid to elongated cells. The mesophyll begins with 1–2 layers of collenchyma followed by parenchyma cells with variable size, interspersed with large

secretory idioblasts distributed throughout the tissue. Small collateral vascular bundles are longitudinally arranged near the center of the scale, (Figure 4, G).

Outer tepal structure has an organization is like to described for a scale, (Figure 4, H). Inner tepal structure. The organization is like that described for the scales, but the number of idioblasts is much higher, covering almost the entire tepal, (Figure 4, I).

Androecium structure. The filament is composed of a uniseriate epidermis, formed by elongated cells, some of which are papillose, (Figure 6, G). The mesophyll is compact, consisting of parenchymatous tissue arranged in layers, containing large secretory idioblasts and numerous starch grains. Centrally, a concentric amphicribal vascular bundle is observed, in which the xylem is surrounded by the phloem. The anther of a flower at anthesis, near pollen release, presents a papillose epidermis and a uniseriate endothecium composed of rectangular cells exhibiting secondary wall thickenings in bands along the anticlinal walls. Stomial cells are located along the dehiscence line, which rupture during anthesis to release pollen grains. Centrally, a concentric amphicribal vascular bundle, derived from the filament, is present, with the xylem surrounded by phloem, (Figure 6, F).

Gynoecium structure. The epidermis of each stigma lobe is composed of prismatic, trichomatous cells containing phenomenon (Figure 8, F). The mesophyll in the six superficial layers consists of very small cells with few intercellular spaces, followed by two layers of larger, rounded cells containing numerous starch grains. Secretory idioblasts are observed near the vascular region. Centrally, a concentric amphicribal vascular bundle is present. Apical portion of the style. The epidermal cells of the apical portion of the style are collenchyma with variable shape. The mesophyll has a circular organization, including 1–2 layers of collenchyma and large mucilage-secreting cells forming a ring around the vascular tissue, (Figure 10, E). The vascular system consists of approximately 13 small amphicribal bundles, with abundant starch grains. The transmitting tissue, located centrally, shows variation in the number of cell layers, which increase in size toward the inner region of the style, in contrast to the basal portion, where the arrangement is more uniform and circular. Basal portion of the style. The epidermis at the base of the style is composed of a single layer of prismatic and cuboid parenchymatous cells. The mesophyll has a circular arrangement, with 1–2 layers of collenchyma and secretory cells forming a ring around the amphicribal vascular bundles. Parenchyma cells, internal to the vascular bundles, extend toward the central transmitting tissue, gradually decreasing in size. The transmitting tissue is dense, comprising approximately 12 layers of cells arranged in a circular pattern. Internally, a cleft is present, delineated by trichomes, (Figure 10, F).

Pericarpel structure. The outer epidermis of the pericarpel is uniseriate with smal and irregular cells, covered by a thick cuticle. The mesophyll consists of 1–2 layers of collenchyma cells, followed by a parenchyma tissue of cells of variable size, containing mucilage-secreting idioblasts internally, which extend toward a large ring of collateral vascular bundles delimiting the pericarpel and ovary, (Figure 12, F). Additionally, large idioblasts, numerous starch grains, and parenchymatous cells similar in size to the pericarpel's mesophyll are present, gradually decreasing in size toward the funiculi. The inner epidermis of the ovary is uniseriate, composed of small cells of variable shape, and bears trichomes in the placental region. Beneath this layer, there are elongated parenchymatous cells and small vascular bundles that encircle the ovary wall and vascularize the ovules. The ovule presents a long funiculus containing a central vascular bundle that extends to the chalazal region. The ovule is circinotropous with two integuments (external and internal), with the micropyle delineated by the inner integument. The outer integument consists of 1–2 cell layers, with visible lignin

accumulation in the outermost layer, while the inner internal tegument, separated by a thin cuticle, is composed of 1–2 layers of cells. In the region opposite the micropyle, a large intercellular space occurs between the internal and external integuments, (Figure 12, G).

Floral tube structure. The outer epidermis at the apex of the floral tube is composed of one layer of small prismatic to cuboid cells. The mesophyll contains 1–2 layers of large collenchyma cells of variable shape, interspersed with numerous idioblasts. Collateral vascular bundles of medium caliber are distributed up to the median region. Adjacent to the vascular bundles, the parenchymatous cells form a loose parenchyma, composed of smaller cells with variable shapes and wide intercellular spaces, (Figure 16, F, C). Near the inner epidermis, vascular traces are observed, which later individualize into free bundles, in lower numbers than in the central region of the tube. The outer epidermis of the median portion of the floral tube exhibits a thick cuticle and small prismatic cells. The mesophyll begins with one layer of prismatic collenchyma cells, larger than the epidermal cells, the parenchyma containing numerous cell layers with idioblasts and small collateral vascular bundles. Internally, a transition zone can be identified where nectary tissue is replaced by numerous vascular bundles of filaments, (Figure 16, E, B). At the base of the floral tube, the epidermis and outer mesophyll layers are organized similarly to the middle and apical portions. The nectary tissue is distinguished by a unicellular papillose epidermis. Beneath it, there are 7–12 layers of secretory parenchyma, composed of small prismatic cells with dense cytoplasm, indicating high metabolic activity. Large vascular bundles are present in the underlying region, likely performing a dual function, supplying both the nectar tissue and the filaments and anthers, (Figure 16, A, D).

### 3.2.9 Statistical analysis

The results obtained from the similarity matrix revealed consistent clustering patterns among the species analyzed. In the dendrogram generated using the UPGMA method (Figure 17, A), *A. flagelliformis* was the most distinct taxon, forming an isolated branch distant from the other representatives of the tribe.

The *Selenicereus* species clustered into a group comprising two subgroups. The first included *S. megalanthus*, *S. validus*, and *S. purpusii*, whereas the second comprised *S. anthonyanus* and *S. vagans*. This pattern supports the recognition of the genus as a morphoanatomically coherent unit, despite the broad structural diversity described among its representatives, (Figure 17).

In contrast, *W. bradei* clustered with *E. phyllanthus*, the species used as the outgroup. Although this result does not necessarily reflect phylogenetic relationships, it may be related to similarities in the set of characters used in the analysis. Because only quantitative and qualitative characteristics of floral organs were included, potentially informative vegetative features, such as the presence, distribution, and morphology of stem spines, were not considered. Thus, the observed similarity between *W. bradei* and *E. phyllanthus* likely reflects convergence in floral traits. In addition, *E. phyllanthus* belongs to the Phyllocactoide clade, which is characterized by several floral modifications shared with other groups of epiphytic cacti, (Figure 17).

In the Principal Coordinates Analysis the first two axes jointly explained 72.5% of the data variation, with 37.99% represented by PCo1 and 34.6% by PCo2.) (Figure 17, B) revealed a pattern similar to that observed in the dendrogram, reinforcing the identified

groupings. The first two axes clearly showed the separation of *A. flagelliformis* from the other species, particularly along the PCo1 axis, confirming its distinctiveness associated with its diurnal anthesis. The *Selenicereus* species occupied a central region of the ordination, forming a cluster, although with some degree of internal dispersion, reflecting the morphological diversity already recognized for the genus.

*Weberocereus bradei* and *E. phyllanthus* also remained close to each other in the ordination, corroborating the pattern observed in the dendrogram. Among the *Selenicereus* species, *S. anthonyanus* and *S. vagans* occupied relatively close positions, whereas *S. validus* and *S. purpusii* also showed high similarity, a pattern likewise supported by the dendrogram, (Figure 17).

The correlation analysis between the characters and the PCoA axes indicated that variables V1 (nocturnal anthesis), V3 (scale epidermis), V4 (irregular outer tepal epidermis), and V5 (normal outer tepal epidermis) contributed positively to species distribution along the first axis, whereas V6 (number of stamens) showed a strong negative correlation and was the main vector associated with the observed separation among groups. Variable V2 (diurnal anthesis) showed a stronger association with the second axis, contributing particularly to the distinction of *A. flagelliformis* from the other taxa (Table A2).

PERMANOVA revealed significant differences among the morphological groups ($F = 3.380$; $R^2 = 0.575$; $p = 0.009$), indicating that group membership accounted for approximately 57.5% of the observed morphological variation. The multivariate dispersion analysis (BETADISPER) detected no significant differences in within-group dispersion ($F = 2.565$; $p = 0.188$), suggesting that the significant PERMANOVA result was not attributable to differences in the dispersion of the groups, but rather reflects differences in their multivariate morphological composition.

## 4. DISCUSSION

The floral traits observed in the analyzed species of *Selenicereus* and *Weberocereus*, including an elongated floral tube, actinomorphic flowers, pale tepals (whitish to yellowish), a strong fragrance, and nocturnal anthesis, are consistent with a pollination syndrome associated with sphingophily. These features are typical of nocturnal pollinators, particularly hawkmoths, which predominantly on olfactory cues rather than visual signals to locate floral resources, as discussed by Sampaio (2022) for *Selenicereus setaceus*.

This association has been widely documented in cacti with similar floral morphology, including species of *Cereus* (Silva and Sazima, 1995; Locatelli and Machado, 1999; Albuquerque-Lima *et al*., 2023), *Epiphyllum* (Almeida *et al*., 2010), *Xiquexique* (Pontes *et al*., 2024), *S. grandiflorus* (Stefano *et al*., 2001), *S. undatus* (Kishore, 2016), and *S. setaceus* (Sampaio and Almeida, in press). However, bats (Rocha *et al*., 2019) and bees (Muniz *et al*., 2019; Sampaio and Almeida, in press; Ador and Benedick, 2024) have also been reported as floral visitors and may act as primary or secondary pollinators in cacti exhibiting nocturnal anthesis. In the case of bees, pollination is restricted to species whose flowers remain open during the early morning, when these insects are active (Sampaio and Sampaio, in press).

In contrast, *A. flagelliformis* exhits diurnal anthesis and exhibits a shorter and slightly tapered floral tube (tubular to infundibuliform), zygomorphic flowers with pink to magenta tepals and no fragrance. Diurnal anthesis contributed most strongly to the separation of this species when compared to other evaluated species. (Figure 2). This floral pattern is consistent with that reported by Rosas-Reinhold *et al*., (2022) for wild

populations of the species in Mexico, further supporting the apparent conservatism of its pollination system. These characteristics are typical of ornithophily, with pollination primarily mediated by hummingbirds, as widely documented for cacti with similar corolla morphology (Rowley, 1980; Anderson, 2001; Almeida *et al*., 2013; Apolonio, 2022).

Floral length measurements were generally consistent with the pattern described for Hylocereeae, in which variation occurs among even between species within a genus. *S. megalanthus* had the longest flowers, reaching up to 39 cm, followed by *S. purpusii* (25 cm), *S. vagans* (23 cm), *S. validus* (17 cm), and S. *anthonyanus* (15 cm); *E. phyllanthus* shows flowers with (22-29cm), whereas *W. bradei* and *A. flagelliformis* had considerably shorter flowers (5.8 and 6.75 cm, respectively). Such variation has also been reported by Almeida *et al*., (2013) within the tribe. However, the occurrence of smaller flowers within the same genus, as observed in *Selenicereus minutiflorus* (3.5 cm), highlights the large variation in floral size within the clade.

Cactaceae generally exhibit numerous stamens, although substantial variation occurs among species and genera (Anderson, 2001). Species of *Selenicereus* typically possess a high number of stamens, for example *S. vagans* (336), *S. purpusii* (335), *S. megalanthus* (317), and *S. setaceus* (317–393; Sampaio and Almeida, in press), whereas *S. anthonyanus* has approximately 246 stamens. In contrast, the species analyzed here have lower stamen numbers, with *S. validus* presenting 116–120, *W. bradei* 116, and *A. flagelliformis* 75 stamens. More extreme variation is observed in other genera, such as *E. phyllanthus* (36), *Rhipsalis teres* (15), Santos *et al*., 2019) and *Pilosocereus tuberculatus* (1.000). This wide variation in stamen number highlights the morphological diversity of Cactaceae flowers and may reflect diferences in evolutionary history, ecological factors, and pollination strategies (Anderson, 2001). The importance of stamen number was also supported by multivariate analysis, in which this trait showed the strongest negative correlation with the first PCoA axis and contributed substantially to the separation of the morphological groups.

From a histological perspective, the perigone structures of the analyzed *Selenicereus* species showed considerable similarity, with most epidermal characters contributing to the observed grouping pattern (Figure 3-4). A higher density of stomata was observed on the abaxial surface, often associated with more developed papillae in this region. The mesophyll is composed of an initial layer of collenchymatous cells, followed by larger cells, secretory idioblasts, and medium to large collateral vascular bundles arranged longitudinally. The scales exhibit a more compact mesophyll, with closely packed cells and reduced intercellular spaces, whereas the tepals show larger idioblasts that coalesce to form more evident secretory cavities. A similar pattern was observed in *A. flagelliformis* and has also been reported for *E. phyllanthus* (Almeida *et al*., 2010), in which the tepals present a mesophyll richer in secretory cavities than the scales, with numerous stomata but lacking papillae.

When analyzing the floral bud of *W. bradei*, the absence of papillae on both scales and tepals is evident, with the epidermis characterized by a markedly thick cuticle and relatively uniform cells; as well as the higher abundance of idioblasts and secretory cavities across all floral structures compared with the other species analyzed. This pattern suggests a structural strategy in which protective and functional roles are primarily associated with internal secretory tissues rather than with epidermal specializations. Despite its occurrence in humid tropical environments, the presence of a thick cuticle indicates that cuticular development in epiphytic cacti is not exclusively related to water limitation, but also to protection against pathogens, mechanical stress, and the regulation of water exchange (Kerstiens, 1996; Shepherd and Griffiths, 2006; Reynoud *et al*., 2021). Furthermore, traits traditionally associated with xeromorphic conditions, such as thick

cuticles, do not necessarily indicate adaptation to arid environments and may instead result from multiple ecological pressures (Haworth and McElwain, 2008), reinforcing potential adaptive significance of the observed anatomical features in *W. bradei*.

The gynoecium of the analyzed species shows considerable structural similarity, with all taxa presenting stigma lobes densely covered with trichomatous cells containing phenolic compounds, styles reinforced by collenchyma, and mesophyll tissues rich in starch grains and secretory idioblasts associated with large vascular bundles. However, variation is observed in the characteristics of the stigma lobes. Species of *Selenicereus* exhibit free lobes, ranging from 11–13 in *S. vagans* to 26 in *S. purpusii*, whereas *W. bradei* and *A. flagelliformis* have fewer, partially fused lobes. Similar variation has been reported in other taxa, such as *S. setaceus*, *S. undatus*, and *E. Phyllanthus* (Almeida *et al*., 2018; Sampaio, 2022) highlighting the diversity of gynoecial organization within the group. Notably, *S. anthonyanus* is the only species among those studied to exhibit small, individualized vascular bundles within the stigma lobes.

Differences in style organization were observed among the analyzed taxa. In *Selenicereus*, the basal portion of the style generally exhibits a greater number of cell layers than the apical region, a pattern also observed in *Weberocereus bradei*, in which the apical portion is predominantly composed of secretory idioblasts. In contrast, *Aporocactus* displays a more homogeneous distribution of cell layers along the entire length of the style. This differentiation in *Selenicereus* might be related to structural reinforcement requirements in specific regions of the floral organ. In addition, some species of *Selenicereus* show phenolic compounds in the epidermis, occasionally associated with discrete papillose projections, with *S. anthonyanus* representing the only species studied in which phenolic compounds occur throughout the entire stylar epidermis.

In all studied species (*Aporocactus*, *Selenicereus*, and *Weberocereus*), the interior of the style is hollow, forming a stylar canal lined by transmitting tissue, which is more compact in the basal region than in the apical portion. This organization is similar to that described for *S. setaceus* (Sampaio, 2022), but differs from *E. phyllanthus*, which lacks a stylar canal and presents conspicuous papillae on the outer epidermis of the style (Almeida *et al*., 2010). The presence of a stylar canal may therefore represent a potentially important anatomical characteristic of the hylocereoid clade.In Cactaceae, the ovary is surrounded by receptacular tissue derived from the floral axis, known as the pericarpel, with exceptions in flowers of some basal lineages, such as Pereskioideae and Leuenbergerioideae (Anderson, 2001; Stevens, 2017). This region exhibits high structural complexity due to the fusion of pericarpel and ovarian tissues, often lacking clear anatomical boundaries between them (Almeida *et al*., 2018). In the studied species, papillose epidermis is generally observed in the pericarpel, except in *W. bradei*, which exhibits a glabrous epidermis in this region. The mesophyll is composed of large cells oriented inward toward prominent ascending collateral vascular bundles, that supply the tepals. The ovarian region, in turn, is characterized by a more compact mesophyll composed of smaller mucilage-rich cells, with abundant vascular bundles extending through the funiculi toward the ovules.

From a morphological perspective, considerable diversity is observed in the pericarpel region among the analyzed species. *S. purpusii* and *W. bradei* bear only scales, a condition also reported for *Epiphyllum phyllanthus* and *S. undatus*. In contrast, other species exhibit combinations of different appendages, including scales, spines, bristles, and wool. *Selenicereus megalanthus* shows scales associated with spines and wool, whereas *S. anthonyanus* presents a more complex combination of scales, spines, bristles, and wool. *Selenicereus validus* exhibits scales, spines, and bristles, while *S. vagans* is

characterized by the presence of spines and wool only. In *A. flagelliformis*, the pericarpel bears bristles and spines, with no scales. This variation highlights the morphological diversity of the pericarpel within Hylocereeae and suggests that the combination and distribution of these appendages may represent informative taxonomic and ecological traits among species. The diversity of pericarpel appendages was also consistent with the differentiation observed in the multivariate analysis, indicating that these characters may contribute to the morphological distinction among the analyzed taxa.

The nectariferous tissue of *S. purpusii* is located within an internal chamber at the base of the floral tube, above the ovary. According to Buxbaum (1953), this corresponds to a diffuse chamber-type nectary, in which the primary stamens become free at different heights along the floral tube. A similar pattern is observed in other species of the tribe, including *A. flagelliformis*, *S. anthonyanus*, *S. megalanthus*, *S. validus*, *S. vagans*, and *S. setaceus*. In contrast, species such as *W. bradei*, *W. tunilla* subsp. *biolleyi* (= *W. panamensis*), and *E. phyllanthus* have primary stamens inserted at approximately the same height, characterizing an open chamber-type nectary. The classification of floral nectaries in Cactaceae proposed by Buxbaum (1953), including chamber, disc, and groove types, remains relevant for understanding structural variation within the family. Almeida *et al.* (2013) further emphasized the importance of nectary type and nectar concentration as diagnostic characters for distinguishing genera and species, noting an inverse relationship between flower size and nectar sugar concentration.

In the present study, nectar sugar concentration (°Brix) was measured for several species, with values of 30% in *S. purpusii* (25 cm flowers), 35% in *S. vagans* (23 cm), 20% in *S. megalanthus* (39 cm), and 25% in *A. flagelliformis*, which has intermediate-sized flowers (7 cm). For comparison, smaller flowers such as those of *Rhipsalis grandiflora* (1.1 cm) exhibit much higher sugar concentrations (70.5%) (Almeida et al., 2013), whereas larger flowers, such as those of *E. phyllanthus* (22-29 cm) and *S. setaceus* (27.3 cm), present lower values (16.6% and 28%, respectively). These results suggest a variable relationship between flower size and nectar sugar concentration among the species analyzed, particularly in species with shorter or intermediate-sized flowers, such as *A. flagelliformis*. Nectar was not detected in the flowers of *S. anthonyanus*, preventing the measurement of sugar concentration. The absence of nectar has also been reported for *S. undatus* (Valiente-Banuet *et al*., 2007) and may be associated with domestication processes. Considering that both species are widely cultivated, *S. anthonyanus* as an ornamental and *S. undatus* for fruit production, it is possible that artificial selection may have influenced reproductive traits, potentially reducing dependence on floral rewards such as nectar. However, further comparative studies of nectar production and breeding systems in wild and cultivated populations would be necessary to confirm this interpretation.

## 5. CONCLUSION

Overall, the results demonstrate that the floral morphology and anatomy of the analyzed Hylocereeae exhibit a combination of conserved and highly variable traits. While several structural features of the perigone, gynoecium, and stylar canal were shared among taxa, characters such as anthesis period, stamen number, epidermal features, pericarpel appendages, and nectary organization contributed to the morphological differentiation observed among species. The multivariate analyses reinforced these patterns, particularly the importance of stamen number and floral traits in distinguishing the morphological groups. The observed floral syndromes are also consistent with different pollination strategies, with predominantly nocturnal, sphingophilous

characteristics in *Selenicereus* and *Weberocereus*, contrasting with the diurnal, ornithophilous pattern of *A. flagelliformis*. Together, these findings highlight the considerable floral diversity within hilocereoid clade while identifying a set of morphological and anatomical features with potential taxonomic and ecological relevance, providing a comparative framework for understanding floral diversification within the group.

## 6. REFERENCES


Ador, K., Gobilik, J., Benedick, S., 2024. Flowering Phenology and Evaluation of Pollination Techniques to Achieve Acceptable Fruit Quality of Red-fleshed Pitaya (*Hylocereus polyrhizus*) in Sabah, East Malaysia. Pertanika Journal of Tropical Agricultural Science, 47(3).

Albuquerque-Lima, S., Domingos-Melo, A., Milet-Pinheiro, P., Navarro, D., MARIA, D. A. F., Taylor, N. P., Machado, I. C., 2023. The iconic cactus of the Caatinga dry forest, *Cereus jamacaru* (Cactaceae) has high sphingophily specialization and pollinator dependence. Anais da Academia Brasileira de Ciências, 95, e20220460. https://doi.org/10.1590/0001-3765202320220460

Almeida, O.J.G., 2013. Órgãos reprodutivos em Hylocereeae e Rhipsalideae (Cactaceae): morfologia floral e desenvolvimento estrutural do fruto e da semente. Tese (Doutorado em Biologia Vegetal) – Universidade Estadual Paulista, Rio Claro, São Paulo.

Almeida, O.J.G., Cota-Sánchez, J.H., Paoli, A.A.S., 2013. The systematic significance of floral morphology, nectaries, and nectar concentration in epiphytic cacti of tribes Hylocereeae and Rhipsalideae (Cactaceae). Perspectives in Plant Ecology, Evolution and Systematics, 15(5), 255–268. https://doi.org/10.1016/j.ppees.2013.08.001

Almeida, O.J.G., de Souza, L. A., Paoli, A.A.S., Davis, A.R., Cota-Sánchez, J.H., 2018. Pericarp development in fruit of epiphytic cacti: implications for fruit classification and macro-morphology in the Cactaceae. Botany, 1–15. https://doi:10.1139/cjb-2018-0074

Almeida, O.J.G., Paoli, A.A.S., Cota-Sánchez, J.H., 2012. A macro- and micromorphological survey of floral and extrafloral nectaries in the epiphytic cactus *Rhipsalis teres* (Cactoideae: Rhipsalideae). Flora 207(2), 119–125. https://doi.org/10.1016/j.flora.2011.11.004

Almeida, O.J.G., Paoli, A.A.S., Souza, L.A., 2010. Flower morpho-anatomy in *Epiphyllum phyllanthus* (Cactaceae). Revista Mexicana de Biodiversidade 81, 65-80.

Anderson, E.F., 2001. The cactus family. Timber Press, Inc. Oregon.

Apolonio, V.R., 2022. Morfo-anatomia da flor do cacto epífito *Schlumbergera truncata* (Haw.) Moran (Rhipsalidae: Cactaceae), com ênfase na ontogenia do nectário floral. Dissertação (Mestrado em Biologia Vegetal) – Universidade Estadual Paulista, Rio Claro, São Paulo.

Appezzato-da-Gloria, B., Carmello-Guerreiro, S.M., 2022. Anatomia Vegetal. 4° edição. Editora UFV, Viçosa.

Barthlott, W., Hunt, D.R., 1993. Cactaceae. In: Kubitzki, K., Rohwer, J.G., Bittrich, V. (eds) Flowering Plants: Dicotyledons. The Families and Genera of Vascular Plants, vol 2. Springer, Berlin, Heidelberg. https://doi.org/10.1007/978-3-662-02899-5_17

Bauer, R., 2003. A synopsis of the tribe Hylocereeae F. Buxb. Cactaceae. Systematics Initiatives 17: 3-63.

Cruz M.A., 2018. Sistemática flogenética del género *Disocactus* (Cactaceae). PhD Thesis, Universidad Nacional Autónoma de México, México.

Cruz, M.A., Arias, S. and Terrazas, T., 2016. Molecular phylogeny and taxonomy of the genus *Disocactus* (Cactaceae), based on the DNA sequences of six chloroplast markers. Willdenowia 46: 145–164. https://doi.org/10.3372/wi.46.46112

Gómez-Hinostrosa, C., Hernández, H.M.,2014. Studies on Mexican Cactaceae. VI. A new species of *Weberocereus* (Cactaceae) from Oaxaca, Mexico. Brittonia, 66(3), 250–255. https://doi:10.1007/s12228-014-9327-3

Gómez-Hinostrosa, C., Hernández, H.M., Terrazas, T., Correa-Cano, M.E., 2013. Studies on Mexican Cactaceae. V. Taxonomic notes on *Selenicereus tricae*. Brittonia, 66(1), 51–59. https://doi:10.1007/s12228-013-9308-y

Hunt, D., Taylor, N., Charles, G., 2006. The new cactus lexicon. DH books, Milbourne Port.

Haworth, M., & McElwain, J. C., 2008. Hot, dry, wet or toxic? Revisiting the ecological significance of leaf. https://doi.org/10.1016/j.palaeo.2008.02.009

Jensen, W.,1962. Botanical histochemistry. São Francisco, W.H.

Johansen, D.A., 1940**.** Plant microtechnique. McGraw Hill Books, New York.

Karnovsky, M.J., 1965. A formaldehyde-glutaraldehyde fixative of high osmolality for use in electron-microscopy. Journal of Cell Biology, 27, 137-138A.

Kerstiens, G., 1996. Cuticular water permeability and its physiological significance. Journal of Experimental Botany, 47, 1813–1832. https://doi.org/10.1093/jxb/47.12.1813

Kishore, K., 2016. Phenological growth stages of dragon fruit (*Hylocereus undatus*) according to the extended BBCH-scale. Scientia Horticulturae, 213, 294-302.

Korotkova, N., Aquino, D., Arias, S., Eggli, U., Franck, A., Gómez-Hinostrosa, C., Guerrero, P., Hernández, H., Kohlbecker, A., Köhler, M., Luther, K., Majure, L., Müller, A., Metzing, D., Nyffeler, R., Sánchez, D., Schlumpberger, B., Berendsohn, W., 2021. Cactaceae at Caryophyllales.org - a dynamic online species-level taxonomic backbone for the family. Willdenowia. 51. 251-270. https://doi.org/10.3372/wi.51.51208.

Korotkova, N., Borsch, T., and Arias, S., 2017. A phylogenetic framework for the Hylocereeae (Cactaceae) and implications for the circumscription of the genera. Phytotaxa, 327(1), 1. https://doi.org/10.11646/phytotaxa.327.1.1

Lim, T.K., 2011. *Hylocereus undatus*. Edible Medicinal and Non-Medicinal Plants, 650–655. doi:10.1007/978-90-481-8661-7_92

Locatelli E., Machado I.C. Biologia floral de *Cereus fernambucensis*: Um cacto esfingófilo da restinga. Bradleya. 1999; 17:86–94. https://doi.org/10.25223/brad.n17.1999.a5.

Martínez-Quezada, D.M., Arias, S., Korotkova, N., Terrazas, T., 2020. The phylogenetic significance of the stem morpho-anatomy in the Hylocereeae (Cactoideae, Cactaceae). Plant Systematics and Evolution, 306(1). https://doi.org/10.1007/s00606-020-01639-x

Muniz, J.P.D.O., Bomfim, I.G.A., Corrêa, M.C.D.M., Freitas, B.M., 2019. Floral biology, pollination requirements and behavior of floral visitors in two species of pitaya. Revista Ciência Agronômica, 50(4), 640-649. https://doi.org/10.5935/1806-6690.20190076.

O'Brien, T.P., Feder, N., McCully, M.E., 1964. Polychromatic staining of plant cell walls by toluidine blue O. Protoplasma, 59(2), 368–373. https://doi.org/10.1007/bf01248568.

Pontes, C.A.D.S., Machado, I.C., Domingos-Melo, A., 2024. Floral morphology and pollen placement strategies of bat-pollinated flowers: a comparative analysis within a guild of chiropterophilous plants in a neotropical dry forest. Revista chilena de historia natural, 97.

POWO, 2022. *Selenicereus* Britton and Rose "Plants of the World Online. Facilitated by the Royal Botanic Gardens, Kew. Published on the Internet; https://powo.science.kew.org/taxon/urn:lsid:ipni.org:names:30011812-2. (Accessed 09 March 2022)."

Rocha, E.A., Domingos-Melo, A., Zappi, D.C., Machado, I.C., 2019. Reproductive biology of columnar cacti: are bats the only protagonists in the pollination of *Pilosocereus*, a typical chiropterophilous genus?. Folia Geobotanica, 54(3), 239-256.

Rosas-Reinhold, I., Sánchez, D., Arias, S., 2022. Systematic study and niche differentiation of the genus *Aporocactus* (Hylocereeae, Cactoideae, Cactaceae). Botanical Sciences, 100(2), 423-445.

Reynoud, N., Petit, J., Bres, C., Lahaye, M., Rothan, C., Marion, D., & Bakan, B., 2021. The complex architecture of plant cuticles and its relation to multiple biological functions. Frontiers in Plant Science, 12, 782773. https://doi.org/10.3389/fpls.2021.782773

Rowley, G., 1980. Pollination Syndromes and Cactus Taxonomy. The Cactus and Succulent Journal of Great Britain, 42(4), 95–98. http://www.jstor.org/stable/42786376

Santos, B.M., Almeida, O. J. G., 2019. Anatomia floral do cacto epífito *Rhipsalis teres* (Vell.) Steud.(Cactaceae). Análise crítica das ciências biológicas e da natureza. 1ed. Ponta Grossa: Atenas, 1, 297-303.

Sampaio, P. D. S. P., 2022. Morfo-anatomia floral e biologia reprodutiva de *Selenicereus setaceu*s (Salm-Dyck) Berger (Cactaceae) em São Thomé das Letras, Minas Gerais, Brasil. Tese (Doutorado em Biodiversidade de Ambientes Costeiros) – Universidade Estadual Paulista, São Vicente, São Paulo.

Sampaio, P.S.P., Almeida, O. J. G., 2021.Without moths or bats, cacti form friendships with bees: reproductive biology of the Queen of Night *Selenicereus setaceus* (Cactaceae) in São Thomé das Letras, Brazil. https://doi.org/10.21203/rs.3.rs-690841/v1

Sampaio Almeida., 2026. publicação Iheringia. In press.

Shepherd, T., and Griffiths, D. W., 2006. The effects of stress no plant cuticular waxes. New Phytologist, 171, 469–499. https://doi.org/10.1111/j.1469-8137.2006.01826.x

Silva W.R., Sazima M., 1995. Polinização da mariposa Falcão em *Cereus peruvianus*, um cacto colunar do sudeste do Brasil. Flora. 190:339–343. https://doi.org/10.1016/S0367-2530(17)30674-6.

Stefano, M., Papini, A., Andalò, C., Brighigna, L., 2001. Ultrastructural aspects of the hypanthial epithelium of *Selenicereus grandiflorus* (L.) Britton and Rose (Cactaceae). Flora, 196(3), 194-203.

Stevens, P.F., 2001. Angiosperm Phylogeny Website. Version 14, July 2017 [and continuously updated since]." http://www.mobot.org/MOBOT/research/APweb/".

**FIGURE LEGENDS**

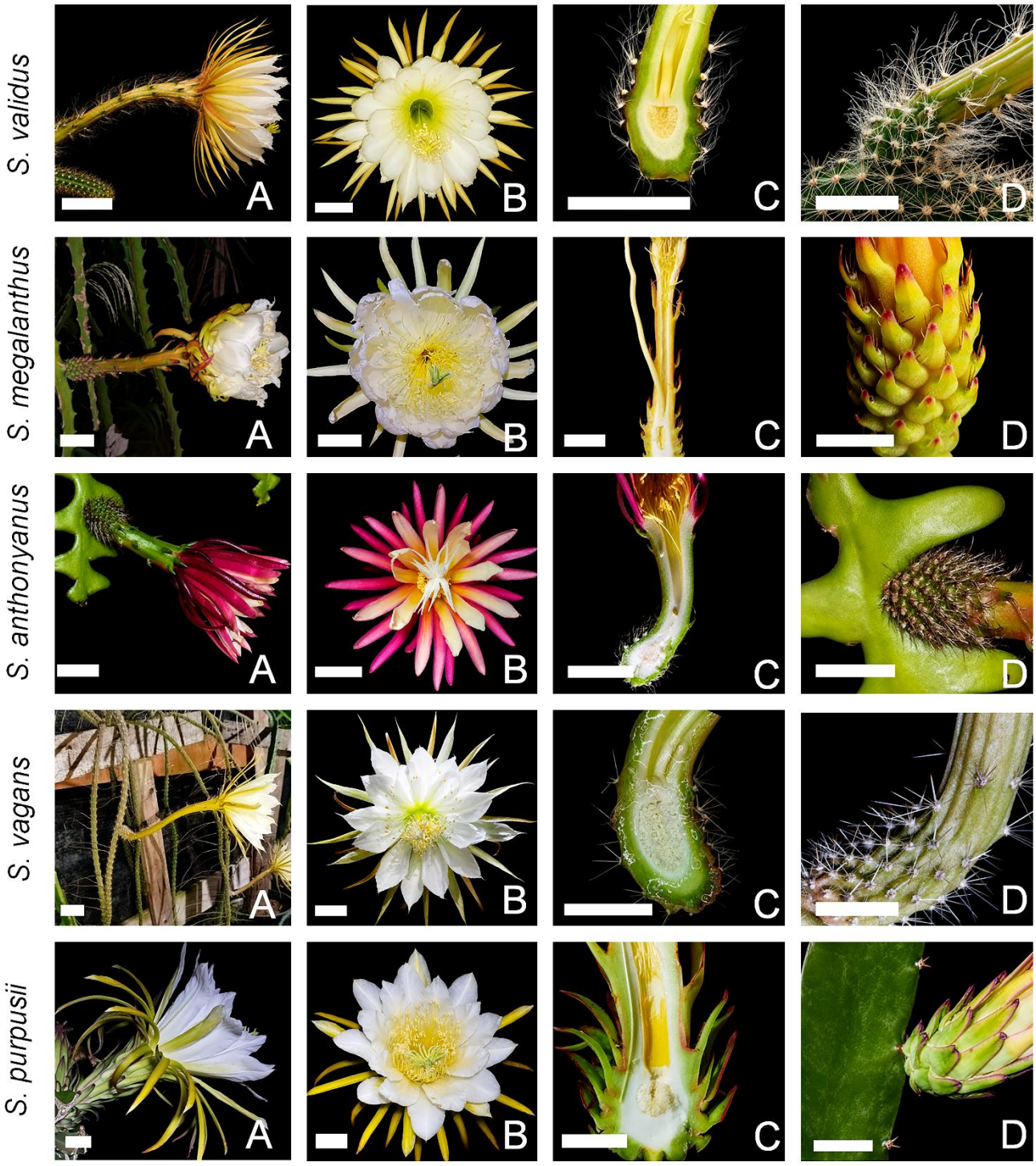



Figure 1. Floral morphology (photos) in selected hylocereoid clade representatives. A, B. Flower in lateral and frontal view. C. Flower in longitudinal section. D. Detail of the external pericarpel structure. Bars = 1cm (D); 2 cm (A); 2cm (B); 3cm (C).

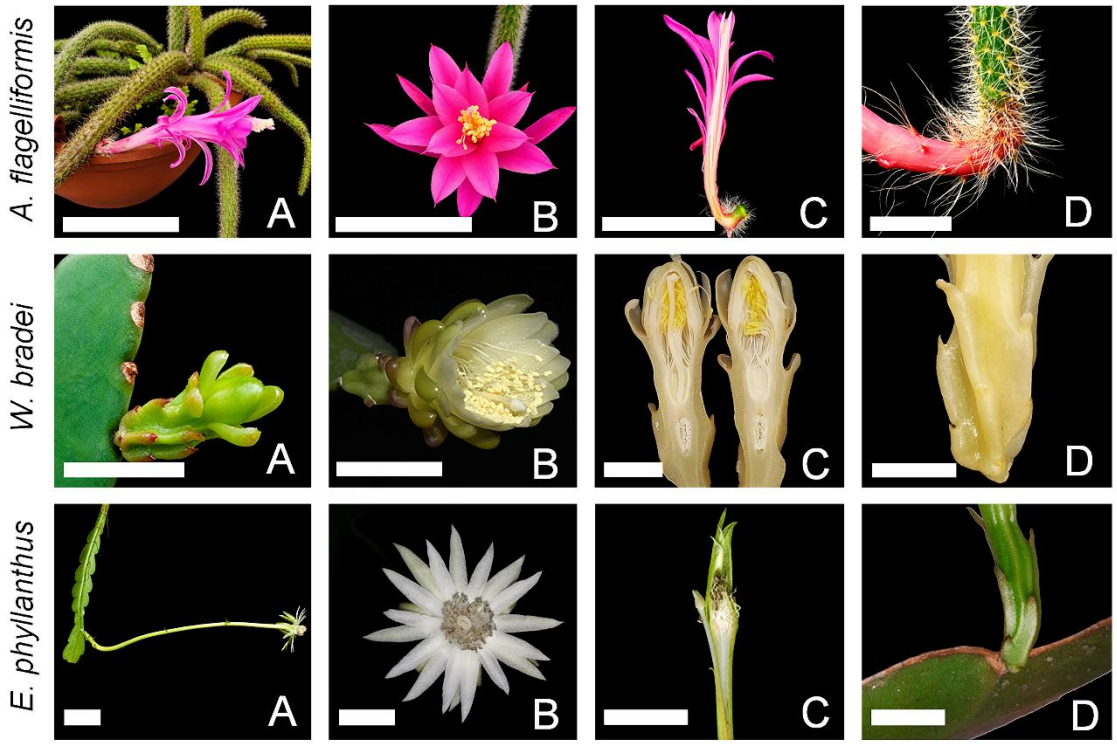



Figure 2. Floral morphology (photos) in selected hylocereoid clade representatives. A, B. Flower in lateral and frontal view. C. Flower in longitudinal section. D. Detail of the external pericarpel structure. Bars = 1cm (D); 2 cm (C); 3cm (B); 5cm (A).

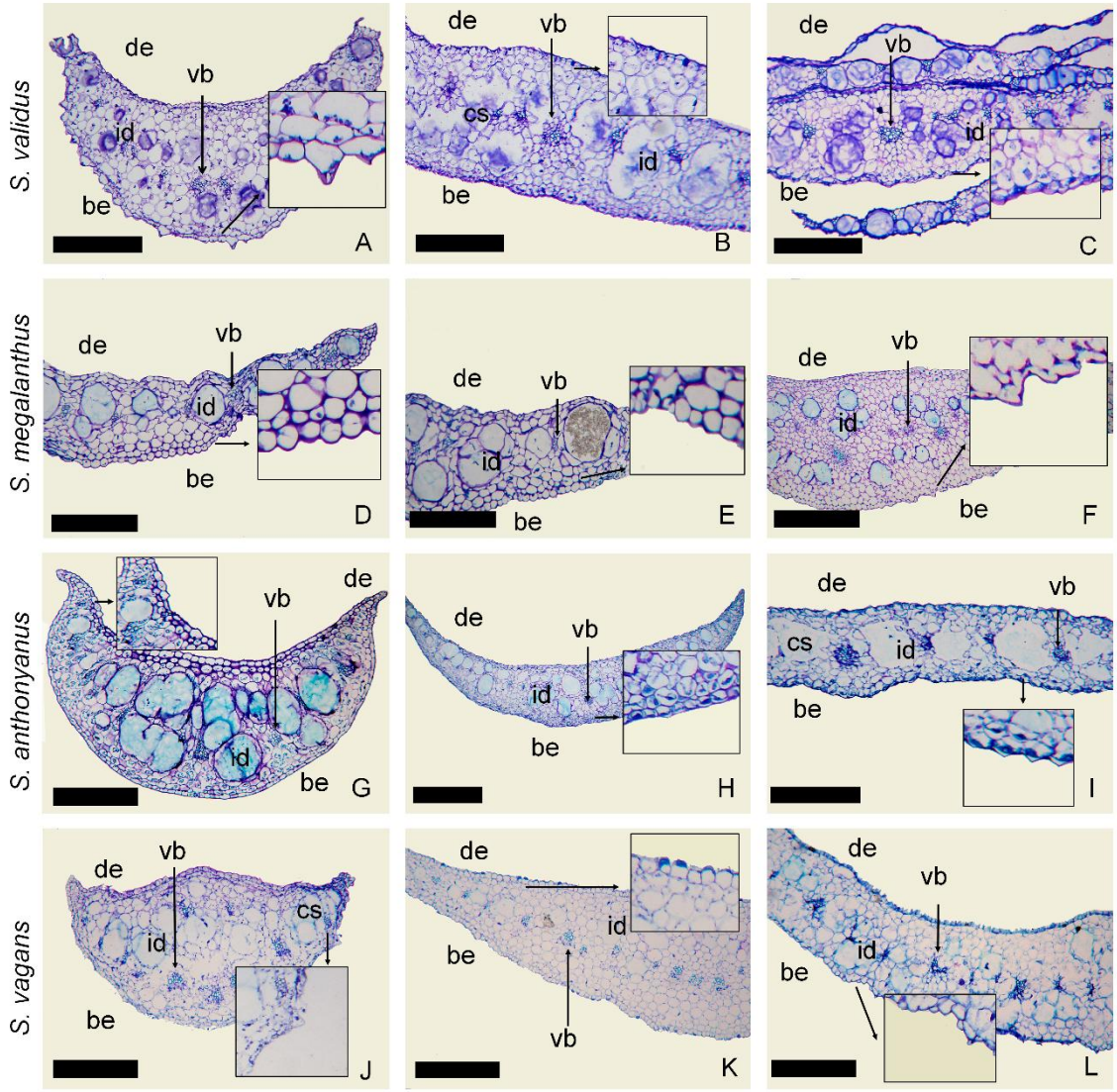



Figure 3. Perigone in transversal sections. A-C. *Selenicereus validus*, A. scale; B. outer tepal; C. internal tepal; D-F. *Selenicereus megalanthus*, D. scale; E. outer tepal; F. internal tepal; G-I. *Selenicereus anthonyanus*, G. scale. H. outer tepal; I. internal tepal; J-L. *Selenicereus vagans*, J. scale. K. outer tepal; L. internal tepal. Bars: 50µm = B; C 100µm =A; D; E; I-L; 200µm=F-H. Legends: be= adaxial apidermis; co= collenchimatous cells; de= abaxial epidermis; pa= papillae; id= idioblasts; vb= vascular bundles; cs= secretory canal.

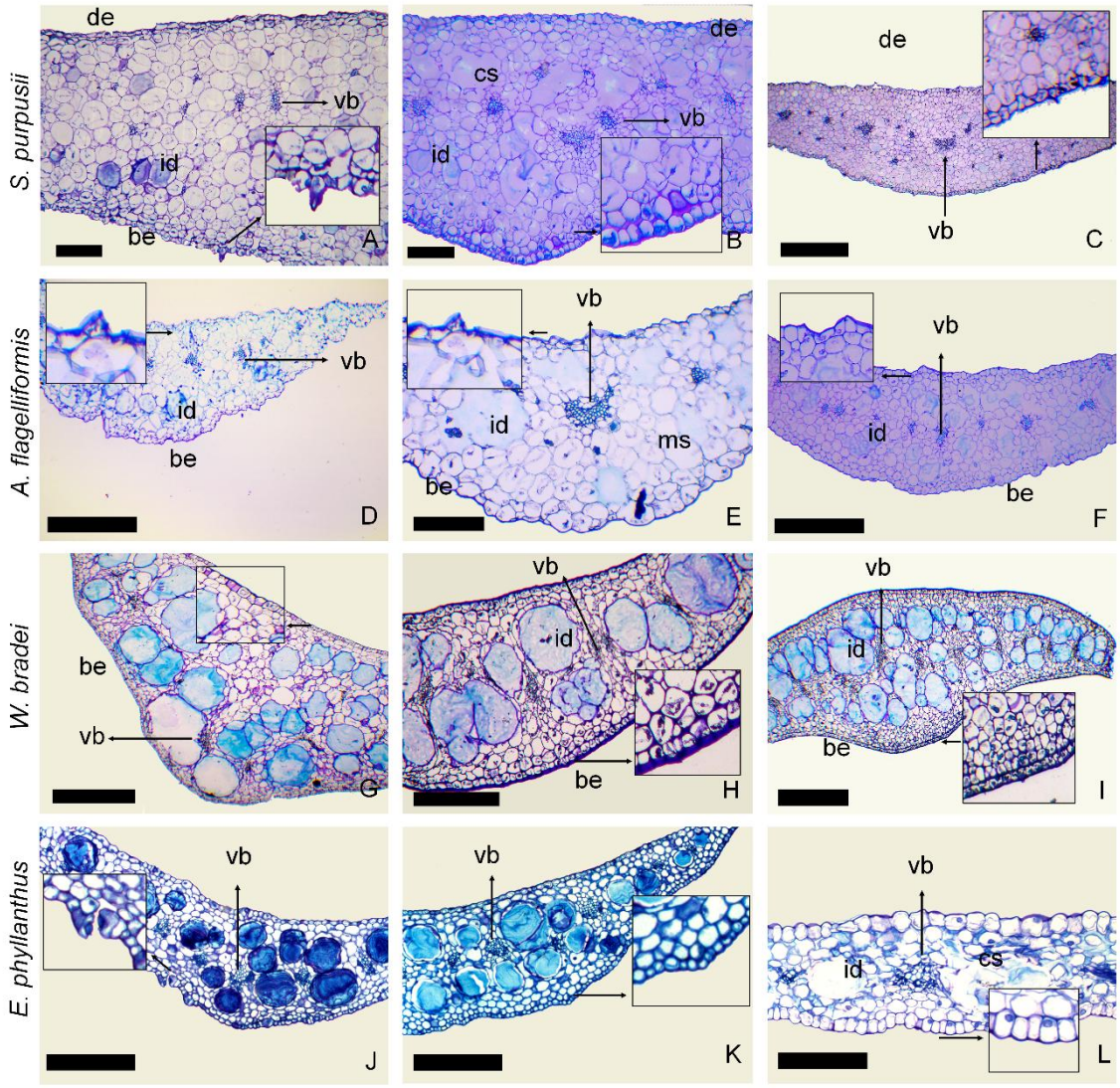



Figure 4. Perigone in transversal sections. A-C. *Selenicereus purpusii*, A. scale; B. outer tepal; C. internal tepal; D-F. *Aporocactus flagelliformis*, D. scale; E. outer tepal; F. internal tepal; G-I. *Weberocereus bradei,* G. scale. H. outer tepal; I. internal tepal; J-L. *Epiphyllum phyllanthus,* J. scale. K. outer tepal; L. internal tepal. Bars: 50µm = A; B; 100µm =D; F; H; J-L; 200µm=C; E; G; I. Legends: be= adaxial apidermis; co= collenchimatous cells; de= abaxial epidermis; pa= papillae; id= idioblasts; vb= vascular bundles; cs= secretory canal; ms= mesophyl.

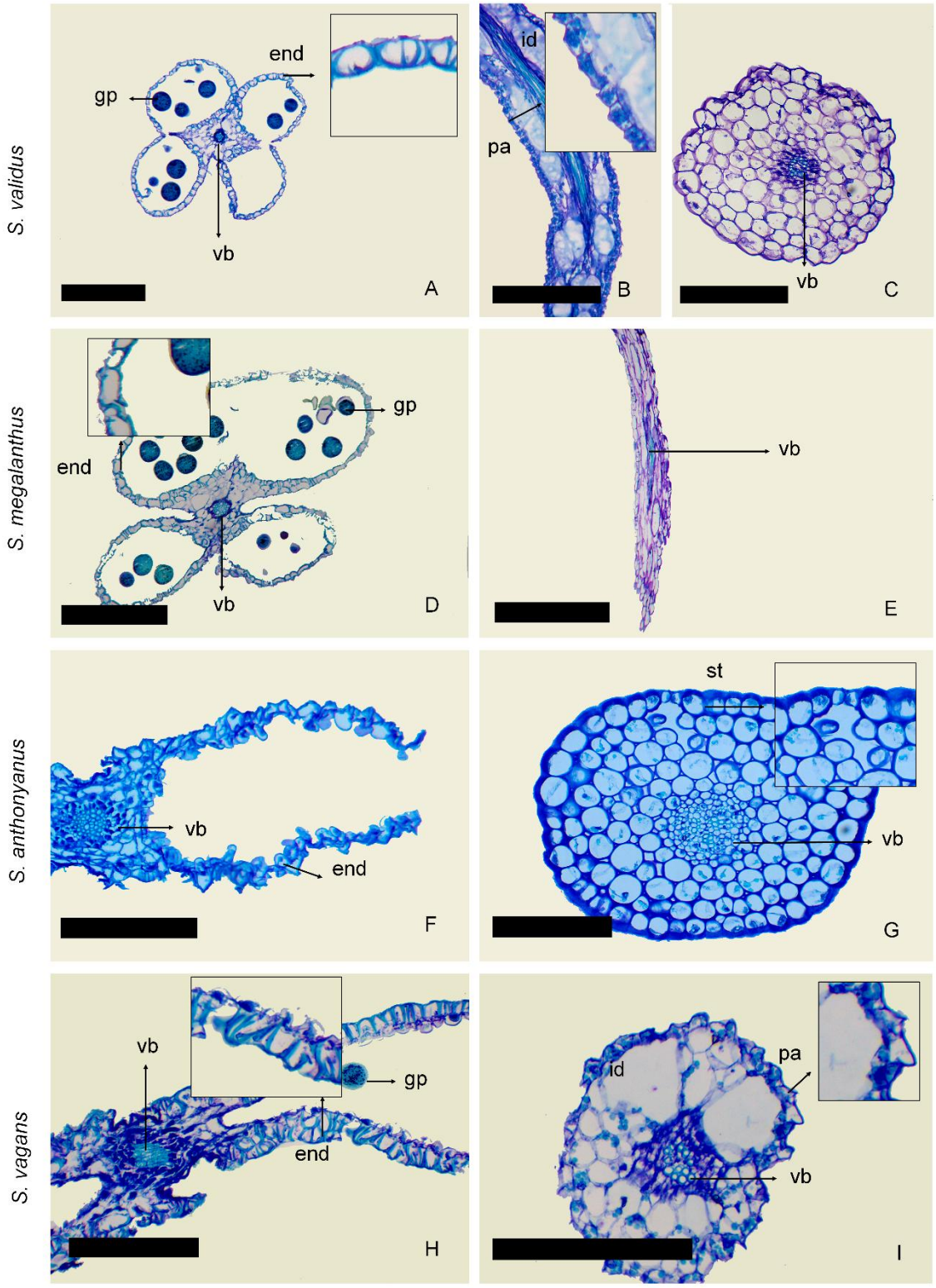



Figure 5. Androecium in transversal and longitudinal section. A-C. *S. validus,* A. anthers; B. filament in longitudinal section; C. filament in transversal section; D-E. *S. megalanthus*, D. anthers; E. filament in longitudinal section; F-G. *S. anthonyanus,* F. dehiscent anther. G. filament in transversal section; H-I. *S. vagans,* H. dehiscent anther. I. filament in transversal section. Bars = 50µm= C; G-I; 100µm= B;D;E 200µm= A Legends: (pa= papillae; vb= vascular bundles; gp= polen grain; end= endoecium; id= idioblast; st= stomata.

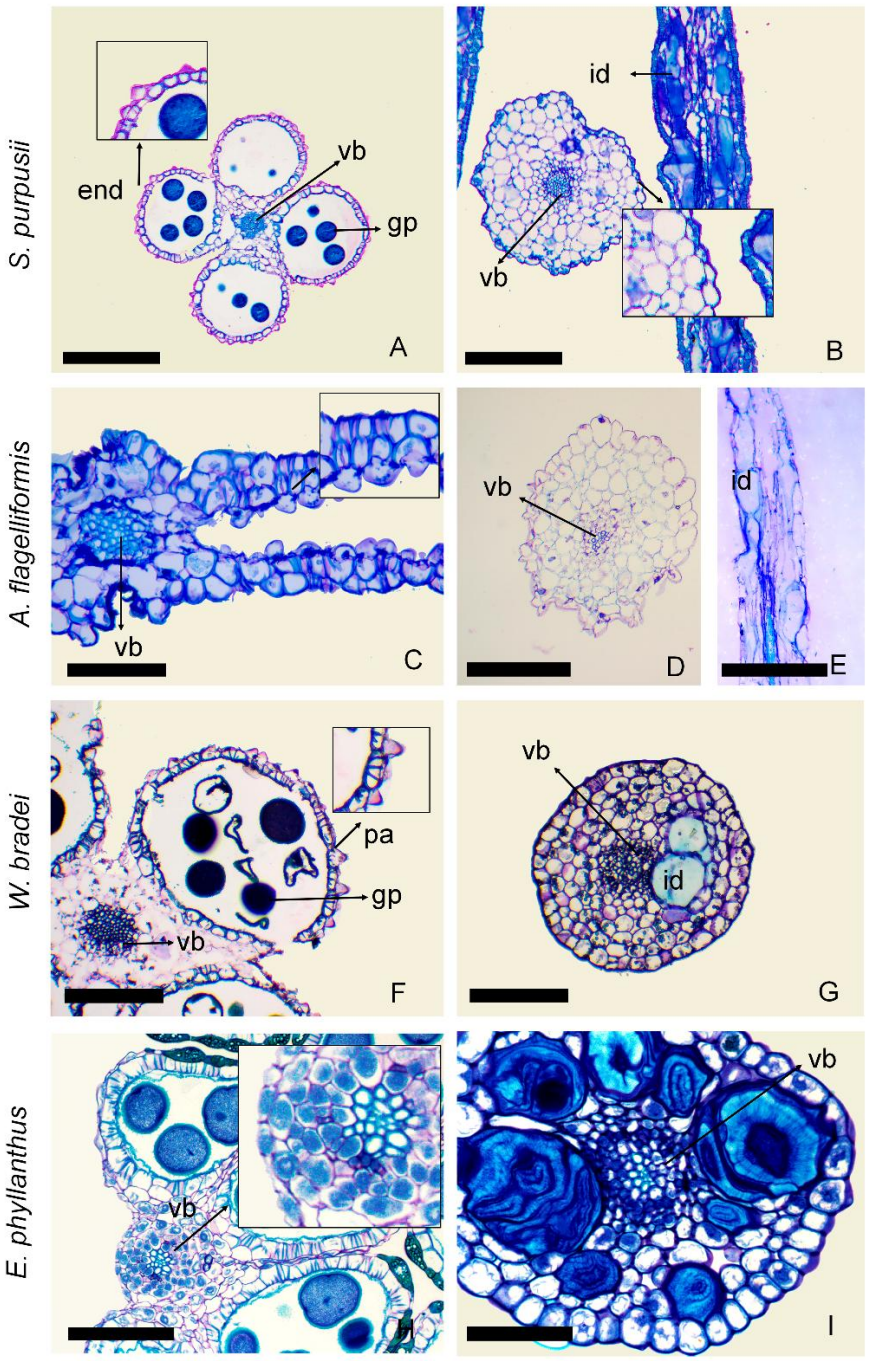



Figure 6. Androecium in transversal and longitudinal section. A-B. *S. purpusii,* A. anthers; B. filament in longitudinal and transversal sections; C-E. *A. flagelliformis*, C. anthers; D-E. filament in longitudinal and transversal sections; F-G. *W. bradei,* F. anther in transversal section. G. filament in transversal section; H-I. *E. phyllanthus,* H. anther in transversal section. I. filament in transversal section. Bars = 25µm= C;H-I; 50µm= D; F; G; 100µm= A-B; E. Legends: (pa= papillae; vb= vascular bundles; gp= polen grain; end= endoecium; id= idioblast; st= stomata.

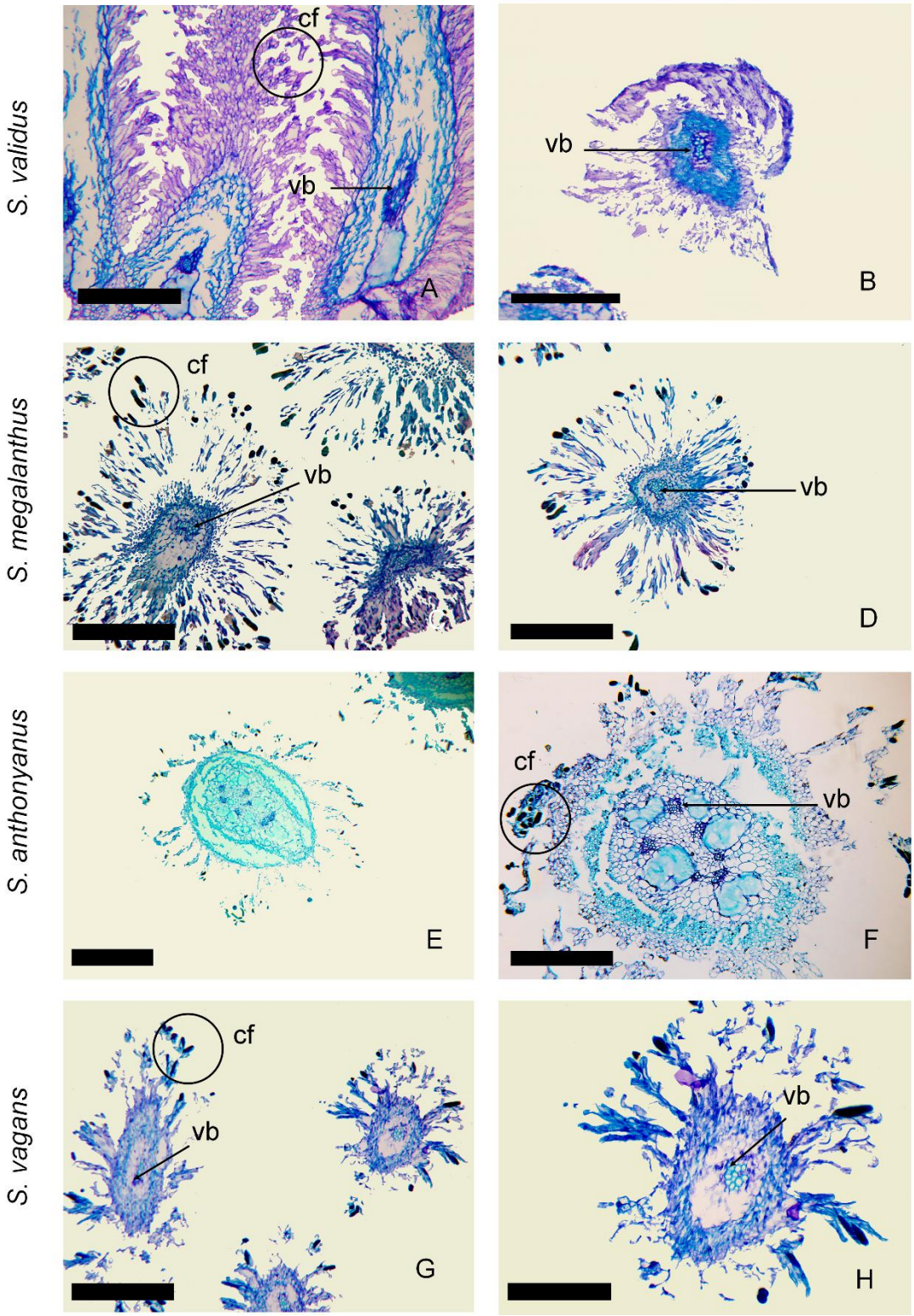



Figure 7. Gynoecium in transversal and longitudinal section. A-B. *S. validus,* A. lobe of style in longitudinal section; B. lobe of style in transversal section; C-D. *S. megalanthus*, C-D. lobe of style in transversal section; E-F. *S. anthonyanus,* E-F. lobe of style in transversal section; G-H. *S. vagans,* G-H. lobe of style in transversal section. Bars= 50 µm= (A; B; D; H); 100 µm = (C; F; G); 200µm= (E). Legends: cf= phenolic compound; vb= vascular bundle; id= idioblast.

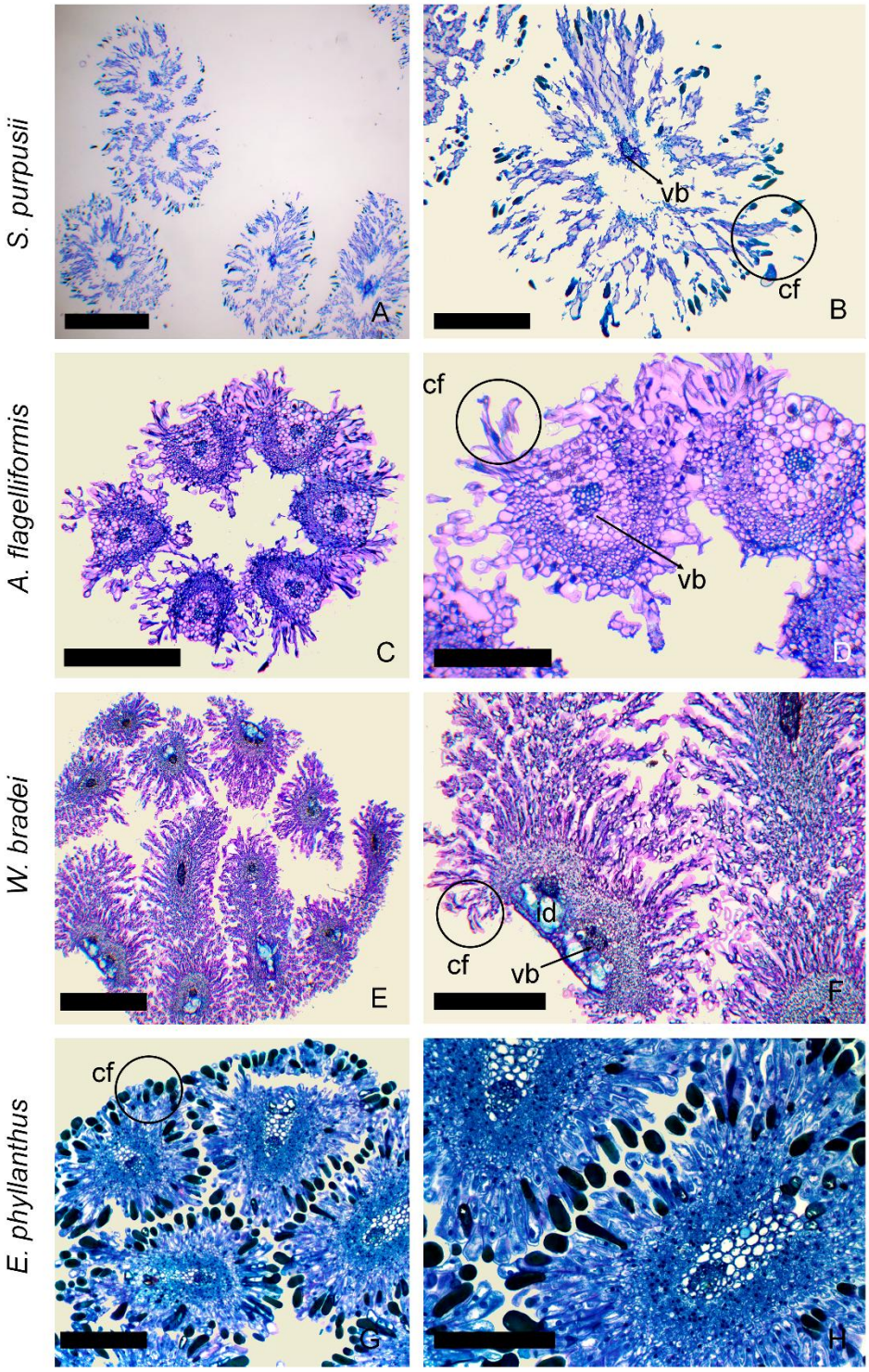



Figure 8. Gynoecium in transversal and longitudinal section. A-B. *S. purpusii,* A-B. lobe of style in transversal section; C-D. *A. flagelliformis*, C-D. lobe of style in transversal section; E-F. *W. bradei.* E-F. lobe of style in transversal and longitudinal section; G-H. *E. phyllanthus.* G-H. lobe of style in transversal section. Bars= 50 µm= (D); 100 µm =(C; G;H); 200µm= (A; B;E). Legends: cf= phenolic compound; vb= vascular bundle; id= idioblast.

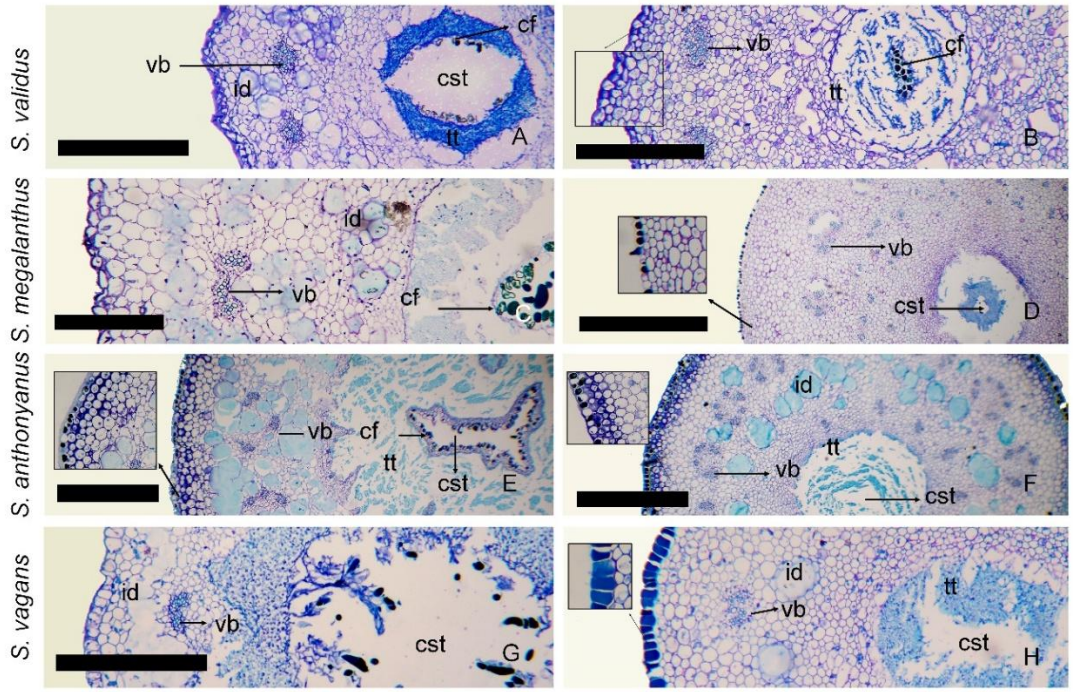



Figure 9. Style in transversal sections. A-B. *S. validus*, A. Apex of style; B. base of style; C-D. S. megalanthus, C. Apex of style; D. base of style; E-F. *S. anthonyanus*, E. Apex of style; F. base of style. G-H. *S. vagans*. G. apex of style. H. base of style. Bars=50µm (); 100µm (A; B; D -H). Legends: cf= phenolic compounds; vb= vascular bundles; id=idioblasts; st= stomata; tt= transmitting tissue; cst= stylar canal.

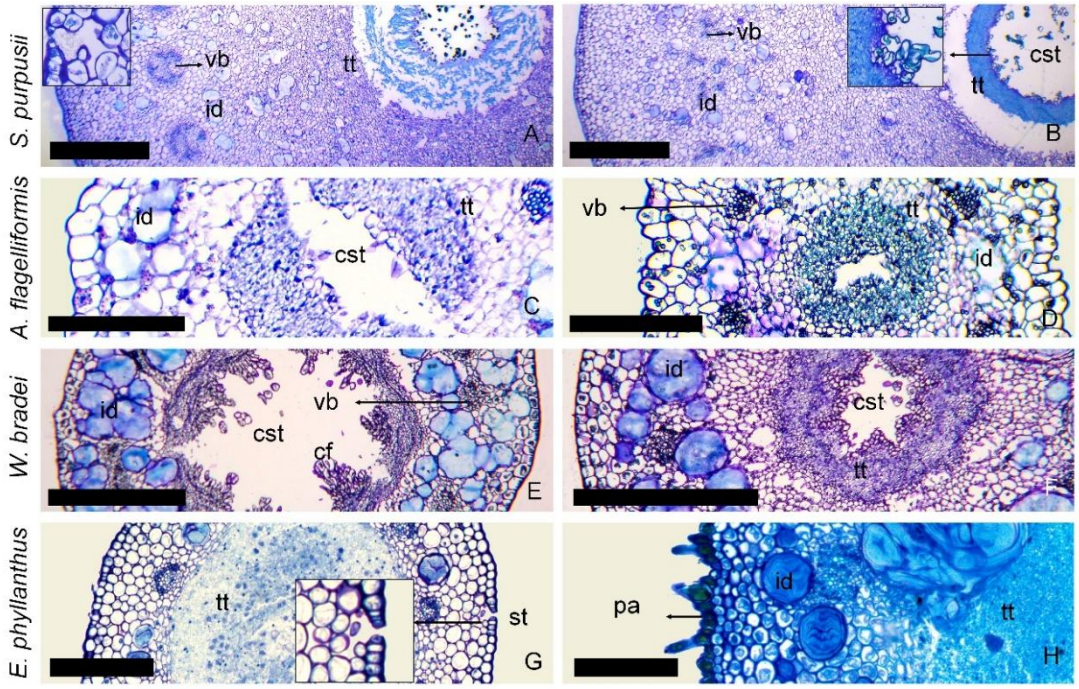



Figure 10. Style in transversal sections. A-B. *S. purpusii*, A. Apex of style; B. base of style; C-D. *A. flagelliformis*, C. Apex of style; D. base of style; E-F. *W. bradei.* E. Apex of style; F. base of style. G-H. *E. phyllanthus*. G. apex of style. H. base of style. Bars=50µm (C; D); 100µm (E;F); 200 µm = (A; B; G; H).

Legends: cf= phenolic compounds; vb= vascular bundles; id= idioblasts; st= stomata; tt= transmitting tissue; cst= stylar canal.

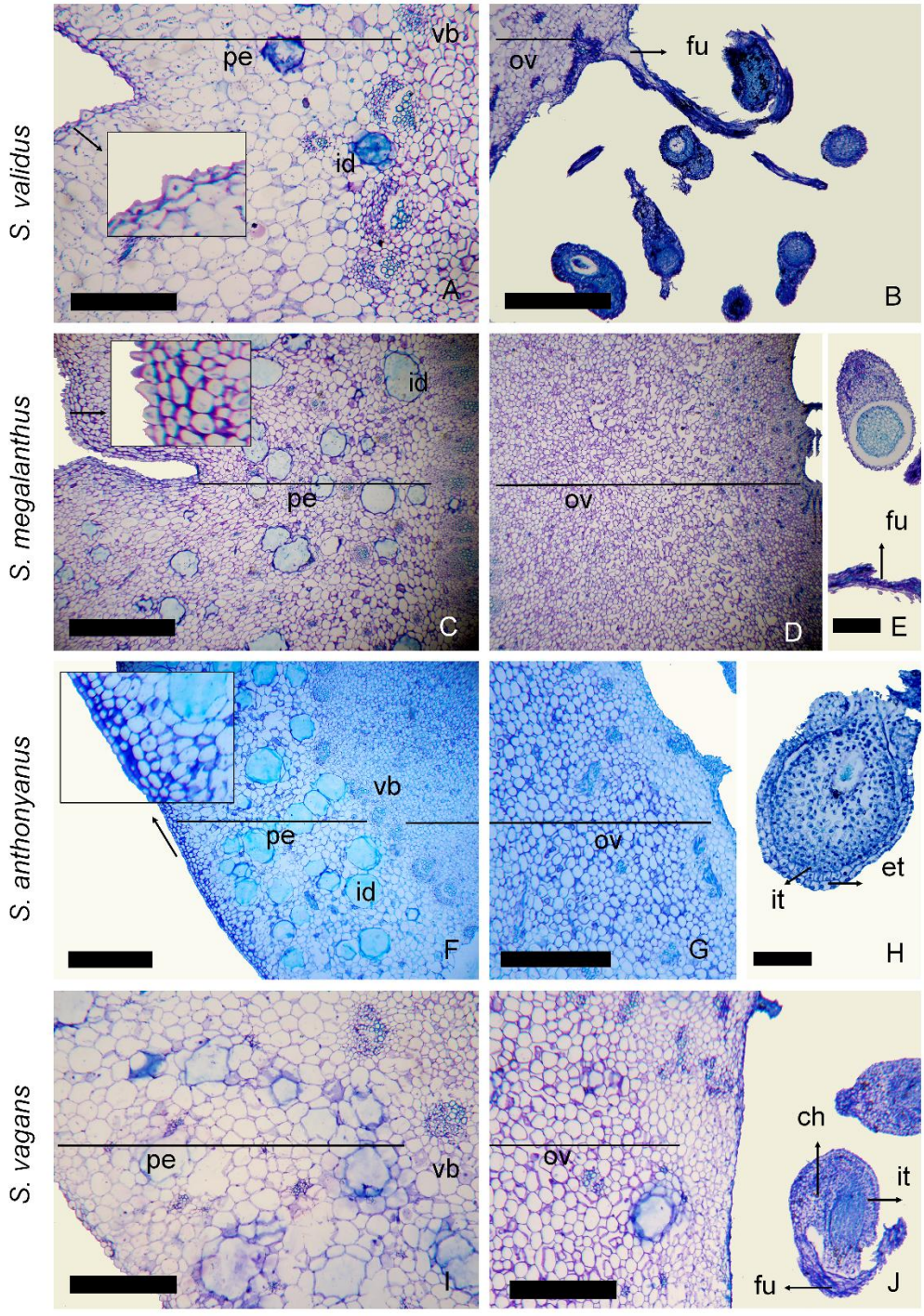



Figure 11. Pericarpel and ovary. A-B. *S. validus*, A. pericarpel; B. ovules; C-E. *S. megalanthus*, C; D. pericarpel and ovary; E. ovule; F-H. *S. anthonyanus*, F; G. pericarpel and ovary; H. ovule. I-J. *S. vagans*. I. pericarpel and ovary; J. ovule. Bars=25 µm (H) 100µm (G); 200µm (A-F). Legends: ch= chalaza; et= external tegument; vb= vascular bundle; fu= funicle; id= idioblast; it= internal tegument; pe= pericarpel; ov= ovary.

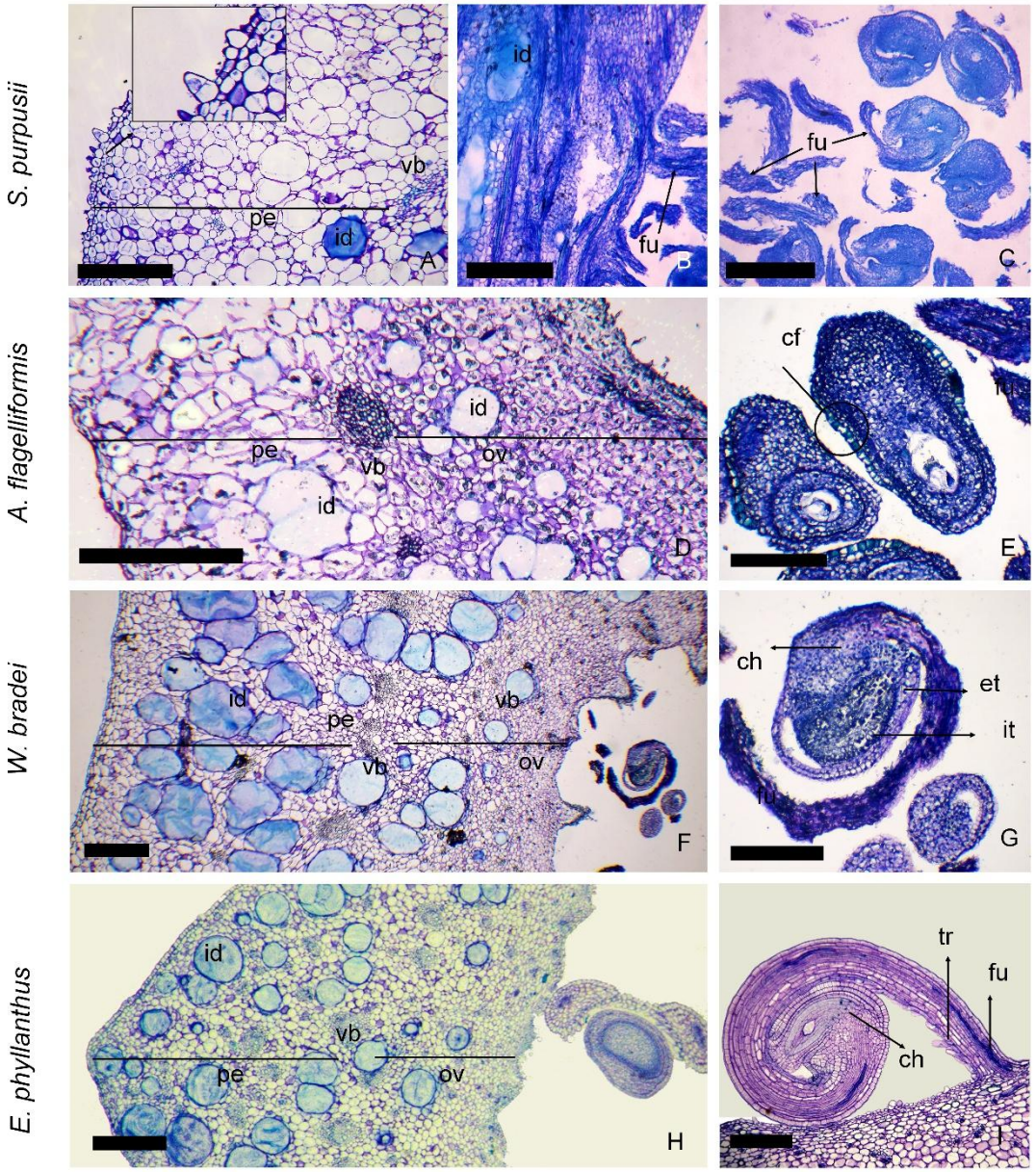



Figure 12. Pericarpel and ovary. A-C. *S. purpusii*, A. pericarpel; B. ovary; C. ovules. D; E. *A. flagelliformis*, D. pericarpel and ovary; E. ovule; F; G. *W. bradei*, F. pericarpel and ovary; G. ovule. H; I. *E. phyllanthus*. H. pericarpel and ovary; I. ovule. Bars=50 µm (A; E; G) 100µm (B; C; D; F; H); 200µm (I). Legends: ch= chalaza; et= external tegument; vb= vascular bundle; fu= funicle; id= idioblast; it= internal tegument; pe= pericarpel; ov= ovary. tr= trichomes; cf= phenolic compounds.

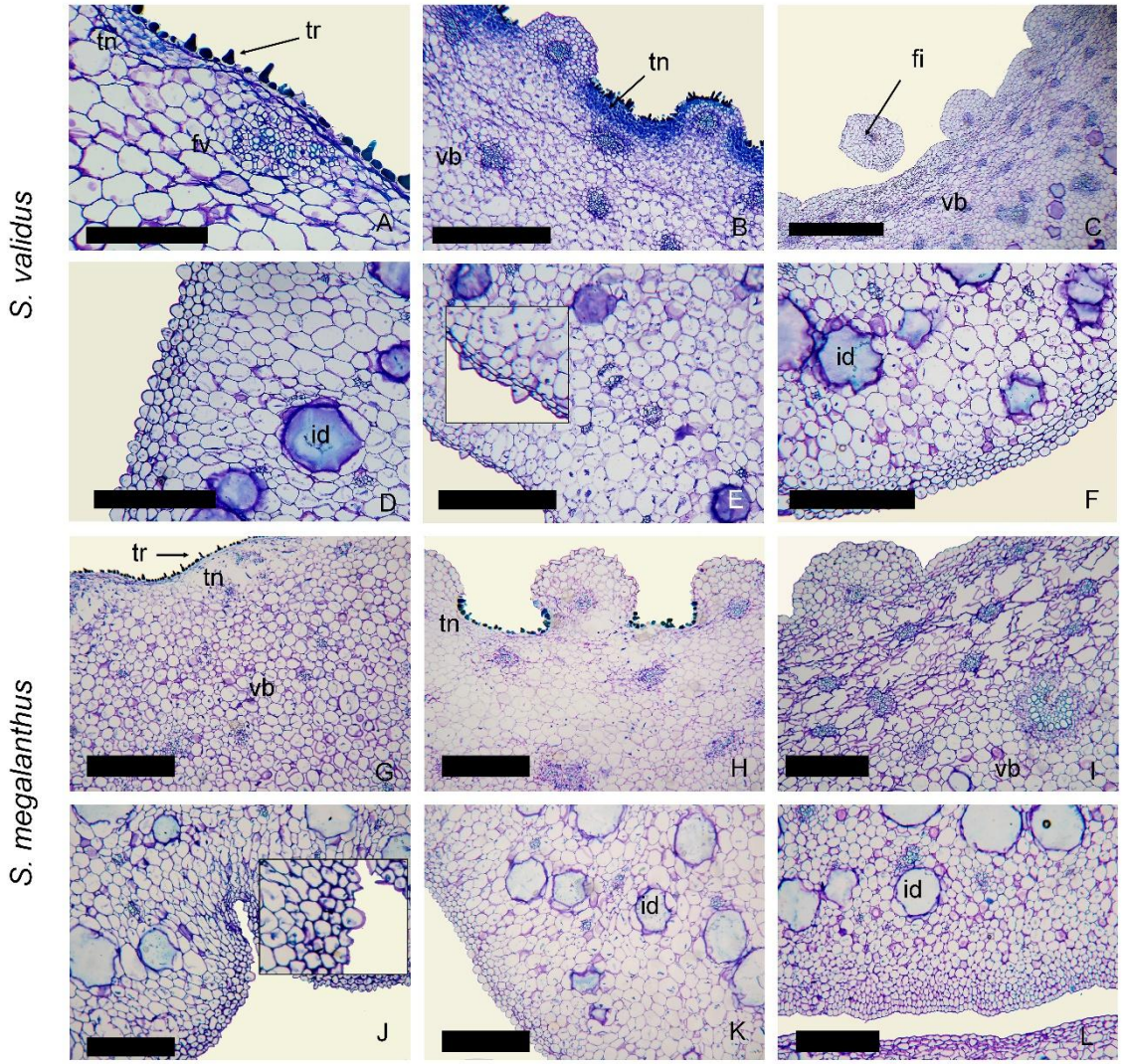



Figure 13. Floral tube. A-F. *S. validus*, A. base of the tube; B. median region; C. apex. D.base of the tube epidermis. E. median region epidermis. F. apex epidermis. G-L. S. *megalanthus*, G. base of the tube; H. median region; I. apex. J. base of the tube epidermis. K. median region epidermis. L. apex epidermis. Bars=50 µm (A; D) 100µm (B; E; F-L); 200µm (C). Legends: vb= vascular bundle; fi= filament; id= idioblast; tr= trichome; tn= nectar tissue.

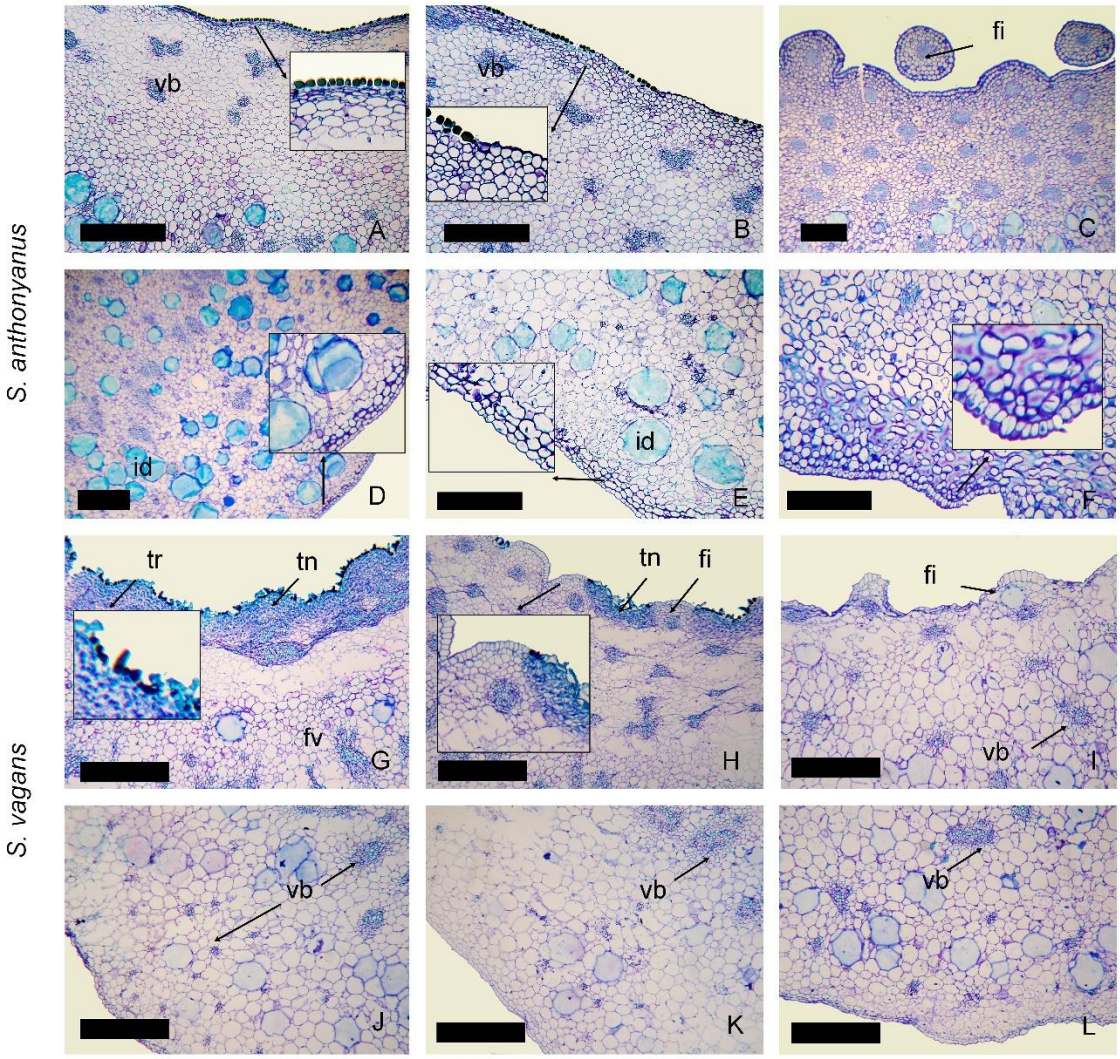



Figure 14. Floral tube. A-F. *S. anthonyanus*, A. base of the tube; B. median region; C. apex. D.base of the tube epidermis. E. median region epidermis. F. apex epidermis. G-L. *S. vagans*, G. base of the tube; H. median region; I. apex. J. base of the tube epidermis. K. median region epidermis. L. apex epidermis. Bars=100 µm (A-L). Legends: vb= vascular bundle; fi= filament; id= idioblast; tr= trichome; tn= nectar tissue.

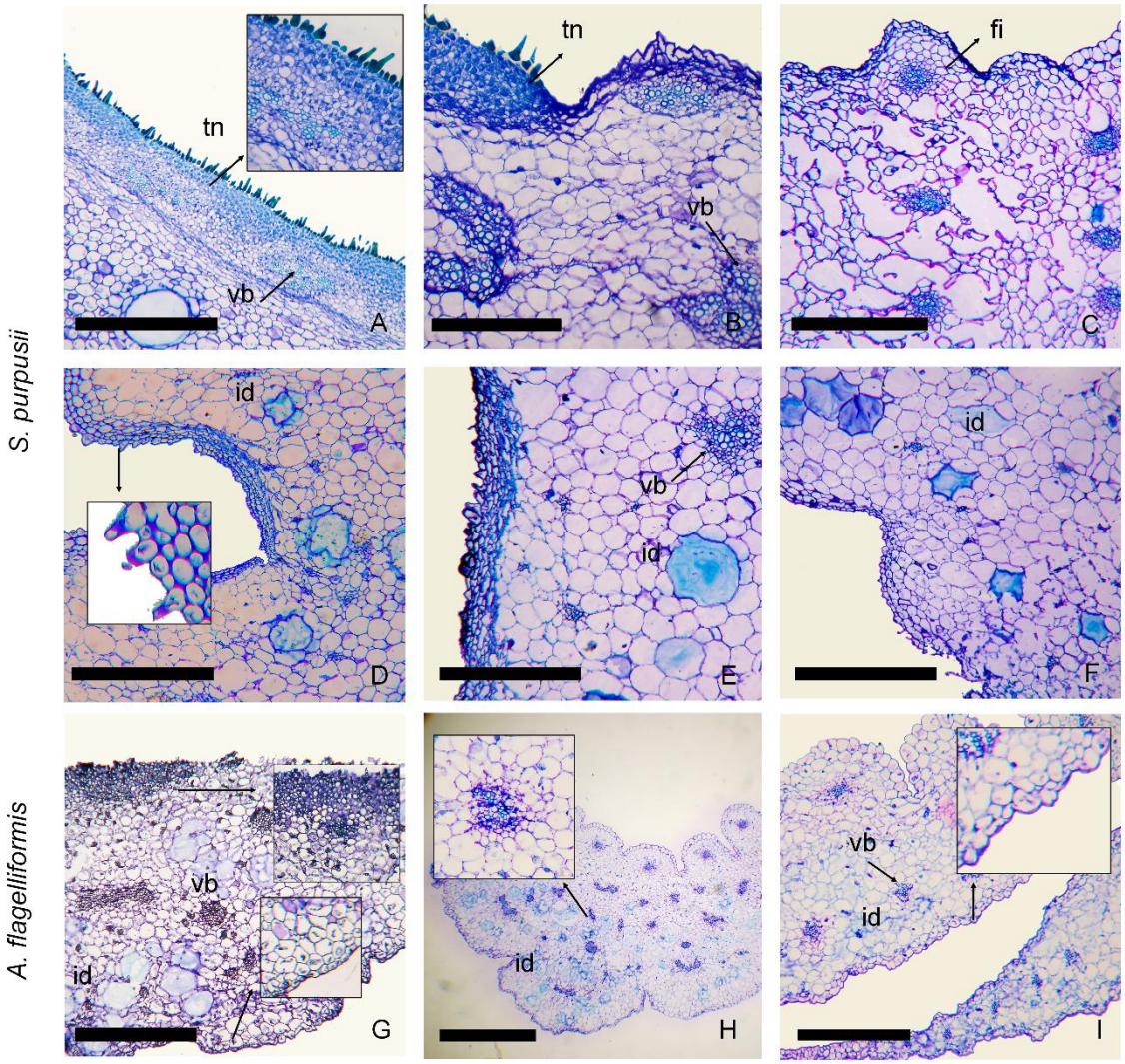



Figure 15. Floral tube. A-F. *S. purpusii*, A. base of the tube; B. median region; C. apex. D.base of the tube epidermis. E. median region epidermis. F. apex epidermis. G-I. *A. flagelliformis*, G. base of the tube; H. median region; I. apex. Bars=50µm (B); 100 µm (A; C-G; I), 200µm= (H). Legends: vb= vascular bundle; fi= filament; id= idioblast; tn= nectar tissue.

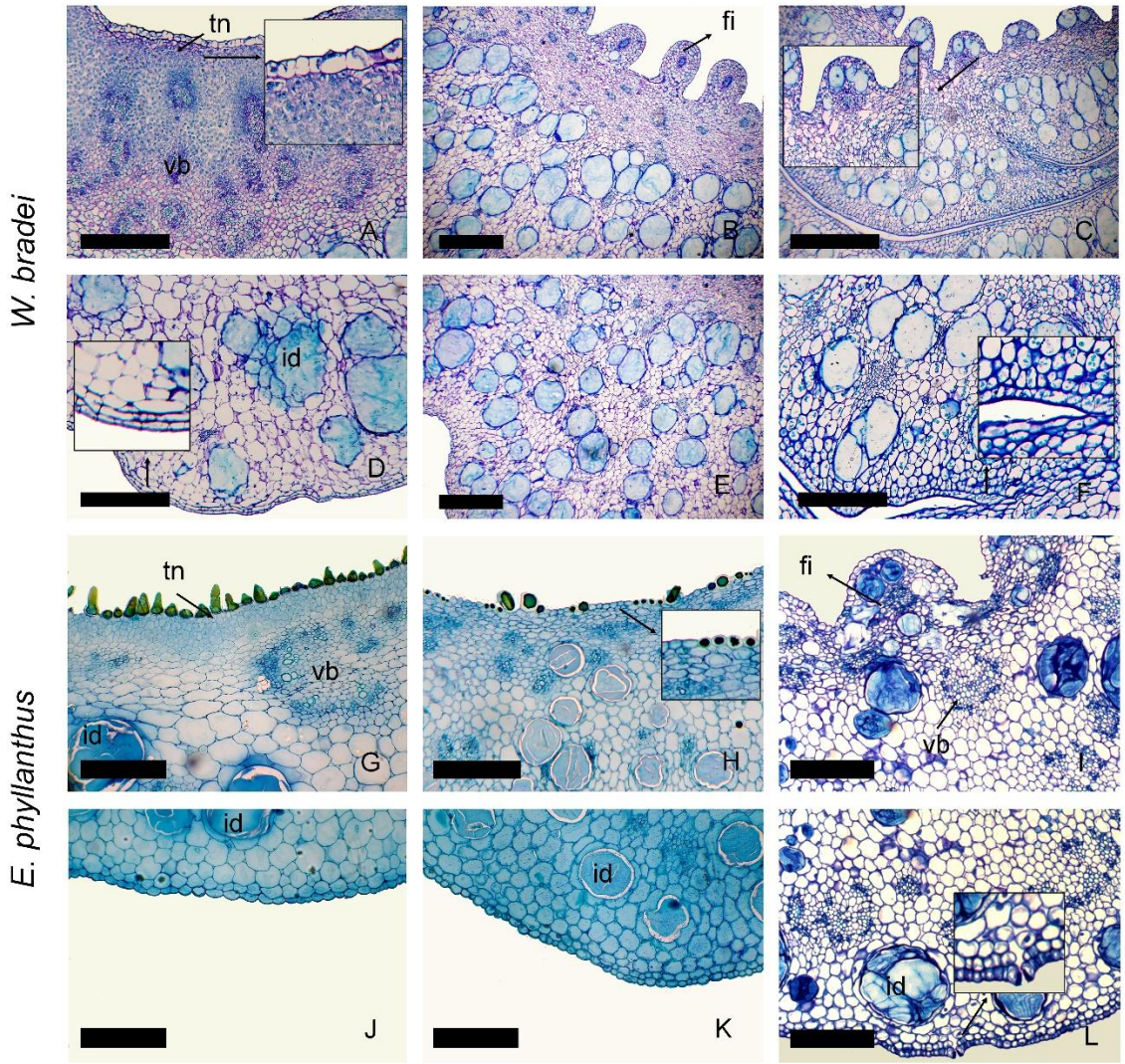



Figure 16. Floral tube. A-F. *W. bradei*, A. base of the tube; B. median region; C. apex. D.base of the tube epidermis. E. median region epidermis. F. apex epidermis. G-L. E. *phyllanthus*, G. base of the tube; H. median region; I. apex. J. base of the tube epidermis. K. median region epidermis. L. apex epidermis. I. apex. Bars=50µm (B); 100 µm (A; C-G; I), 200µm= (H). Legends: vb= vascular bundle; fi= filament; id= idioblast; tn= nectar tissue.

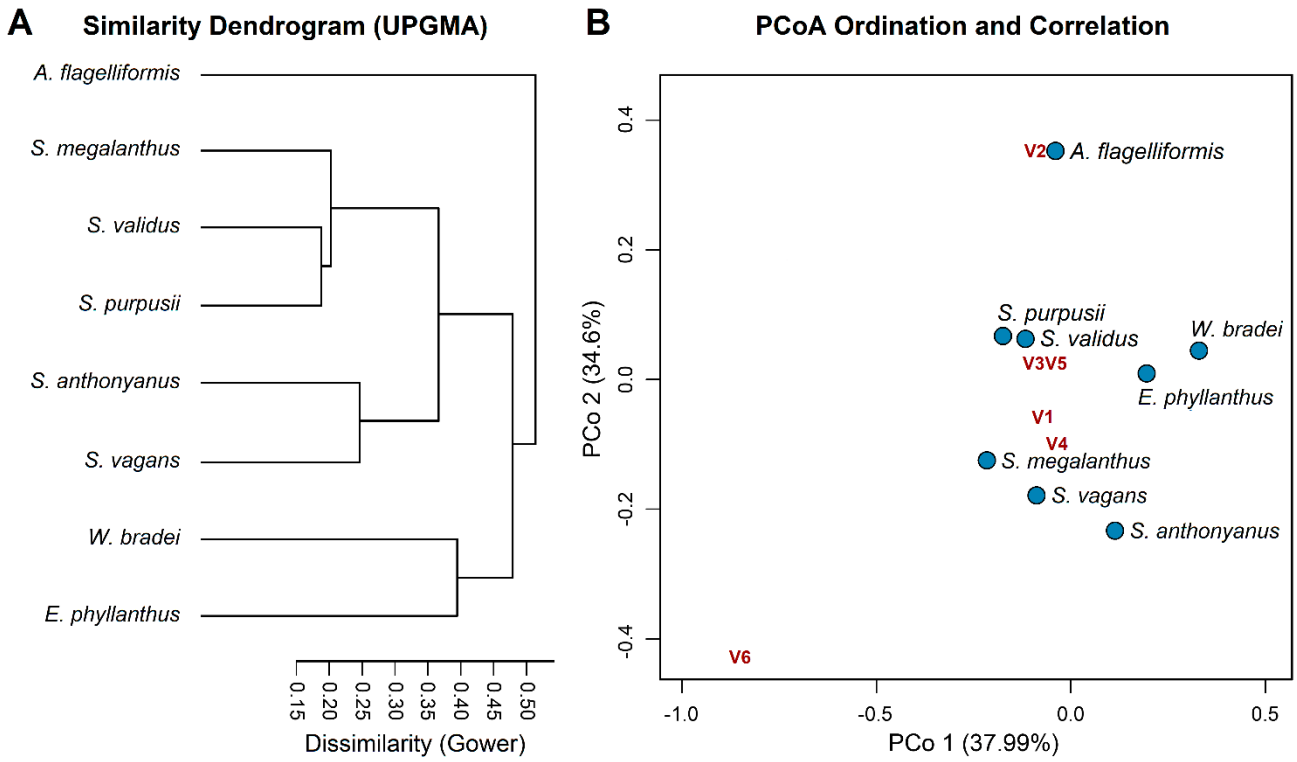



Figure 17. Morphological relationships among selected species of Hylocereeae based on qualitative floral characters. (**A**) UPGMA dendrogram generated from Gower dissimilarity. (**B**) Principal Coordinates Analysis (PCoA) based on the same similarity matrix. Legends: V1 (nocturnal anthesis), V2 (diurnal anthesis), V3 (normal scale epidermis), V4 (irregular external tepal epidermis), V5 (normal external tepal epidermis), V6 (number of stamens).

## SUPPLEMENTARY MATERIAL

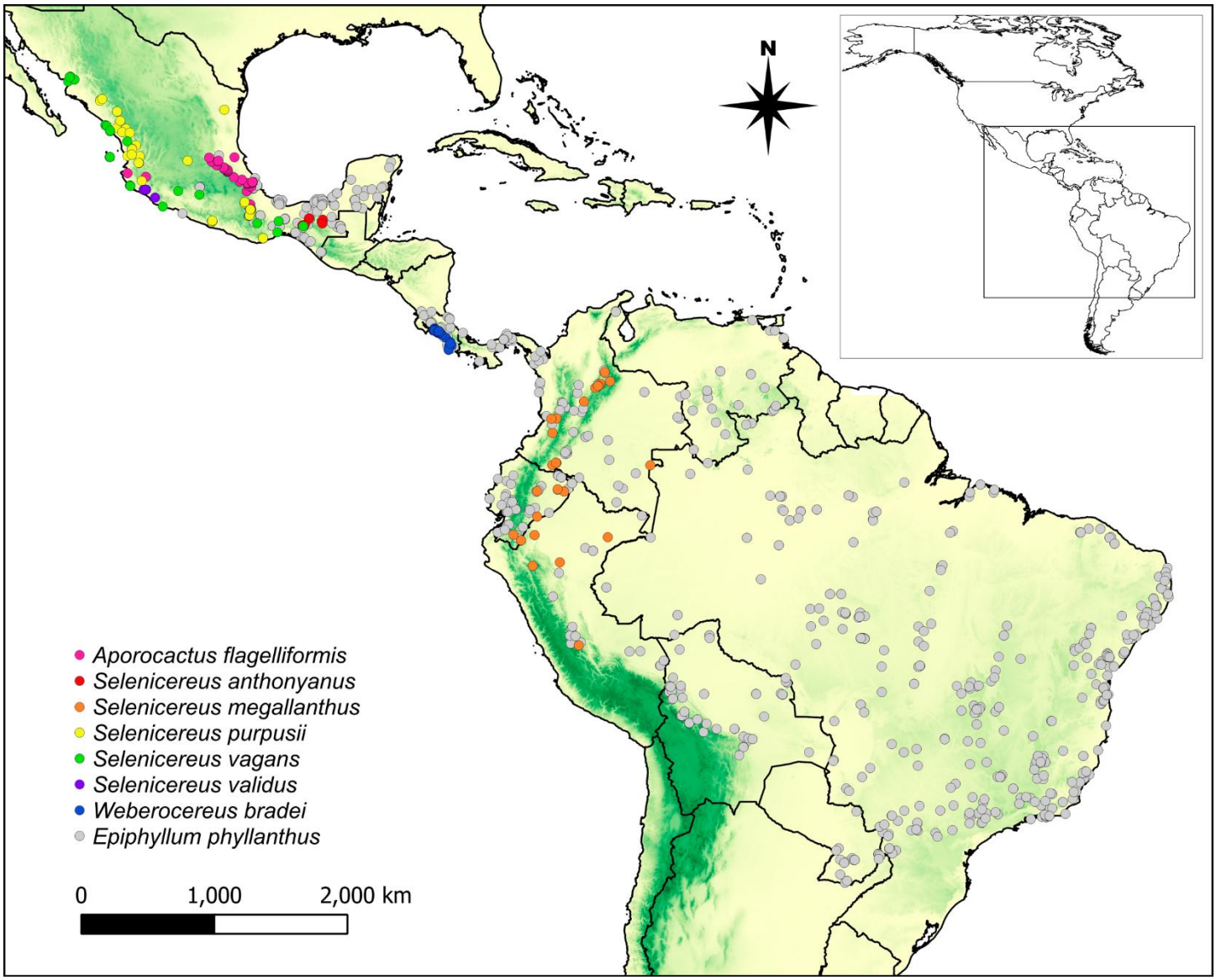



Figure S 1. Native geographic distribution of the species analyzed in the present study: *Aporocactus flagelliformis*, *Selenicereus anthonyanus*, *Selenicereus megalanthus*, *Selenicereus purpusii*, *Selenicereus vagans*, *Selenicereus validus*, *Weberocereus bradei*, and *Epiphyllum phyllanthus*. Colored points represent native occurrence records for each species across the Americas, as indicated in the legend. The inset map shows the location of the represented area within the American continent.

Table S 1. Floral morphoanatomy characters in selected hylocereoid clade representatives.

| **Morphological Flower details** | ***S. validus*** | ***S. megalanthus*** | ***S. anthonyanus*** | ***S. vagans*** | ***S. purpusii*** | ***A. flagelliformis*** | ***W. bradei*** | ***E. phyllantus*** |
|---|---|---|---|---|---|---|---|---|
| **Anthesis: nocturnal (n)/ diurnal (d)** | n | n | n | n | n | d | n | n |
| **flower (l) cm** | 16-22 | 39 | 15 | 23 | 25 | 4.26- 6.75 | 5.5-7 | 22-29 |
| **Color of perianth** | greenish white, golden outside | yellowish white, golden outside | yellowish white, whitenish pink and pinkish magenta outside | greenish white, yellowish green | yellowish white and purplish green outside | pale pink and magenta | greenish white, bownish green outside | white, greenish white outside |
| **scent** | present | present | present | present | present | absent | present | present |
| **Symmetry: actinomorphic (a) / ziggomorphic (z)** | a | a | a | a | a | z | a | a |
| **nectar chamber type,** | diffuse | diffuse | diffuse | diffuse | diffuse | diffuse | open chamber | open chamber |
| **(l) cm and sugar concentration** | 1.5 | 6-10 | 0.3-0.4 | 4.1-4.8 | 1.5-2 | 0.25-0.45 | 1.09 | 14 |
| **(%) BRIX** | - | 20 | - | 35 | 30 | 25 | - | 16.6 |
| **Number of stamens (±)** | 120 | 317 | 246 | 336 | 335 | 75 | 116 | 36 |
| **Stigma lobes. type** | 13-15 free | 23 free | 15-16 free | 11-13 free | 26-27 free | 6 merged | 12-13 merged | 9-10 merged |
| **Details of pericarpel** | scales/spines/bristles | scales/spines/wool | scales/spines/bristle/wool | spines/wool | scales | bristle/spines | scales | scales |
| **Anatomical Flower details** | ***S. validus*** | ***S. megalanthus*** | ***S. anthonyanus*** | ***S. vagans*** | ***S. purpusii*** | ***A. flagelliformis*** | ***W. bradei*** | ***E. phyllantus*** |
| **Scale epidermis** | papillose | irregular | irregular | irregular | papillose | papillose | normal | irregular |
| **Scale mesophyl** | compact | compact | not compact | not compact | compact | compact | not compact | compact |
| **External tepal mesophyl** | not compact | not compact | compact | compact | not compact | not compact | not compact | compact |
| **Internal tepal mesophyl** | not compact | compact | not compact | not compact | compact | not compact | not compact | not compact |
| **External tepal epidermis** | irregular | irregular | irregular | irregular | papillose | papillose | normal | irregular |

| | | | | | | | | |
|---|---|---|---|---|---|---|---|---|
| **Internal tepal epidermis** | irregular | irregular | irregular | irregular | irregular | irregular | normal | irregular |
| **Style Vascular bundle (n);** | 13 | 23 | 15 | 13 | 27 | 6 | 13 | 9 |
| **stylar canal; phenolic** | present | present | present | present | present | present | present | absent |
| **compounds at epidermis (a/b)** | - | b | a/b | b | b | - | - | b |
| **Pericarpel epidermis** | papillose | papillose | irregular | papillose | papillose | irregular | irregular | normal |
| **Floral tube epidermis** | papillose | papillose | irregular | papillose | papillose | irregular | normal | normal |

Table S 2. Qualitative and quantitative floral morphoanatomical characters in selected representatives of the hylocereoid clade, with corresponding $R^2$ (goodness-of-fit) and p -values.

| Variables | | $R^2$ | p-value |
|---|---|---|---|
| Quantitative | Flower length | 0.68 | 0.4 |
| | Nectar chamber length | 0.72 | 0.3 |
| | Brix (%) | 0.21 | 0.8 |
| | Stamens | 0.91 | 0.1 |
| | Stigma lobes (n) | 0.74 | 0.3 |
| | Stigma vascular bundles (n) | 0.61 | 0.4 |
| Qualitative | Phenolyc compounds in stigma apex | 0 | 1 |
| | Phenolyc compounds in stigma base | 0.48 | 0.2 |
| | Flower scent | 0.48 | 0.2 |
| | Pericarpel scale | 0.04 | 1 |
| | Pericarpel spines | 0.07 | 0.9 |
| | Pericarpel wool | 0.46 | 0.2 |
| | Pericarpel bristle | 0.48 | 0.2 |
| | Diurnal anthesys | 0.48 | 0.2 |
| | Nocturnal anthesys | 0.48 | 0.2 |
| | Actinomorphy symmetry | 0.48 | 0.2 |
| | Zygomorphy symmetry | 0.48 | 0.2 |
| | Open nectar chamber | 0.30 | 0.4 |
| | Diffuse nectar chamber | 0.30 | 0.4 |
| | Free stygma lobe (lobulate) | 0.53 | 0.1 |
| | Merged stygma lobe (not lobulate) | 0.53 | 0.1 |
| | Scale.pappilose epidermis | 0.46 | 0.2 |
| | Irregular scale epidermis | 0.46 | 0.2 |
| | Normal scale epidermis | 0 | 1 |
| | Compact scale mesophyll | 0.18 | 0.8 |
| | Loose scale mesophyll | 0.18 | 0.8 |
| | Compact external tepal mesophyll | 0.31 | 0.4 |
| | Loose external tepal mesophyll | 0.31 | 0.4 |
| | Compact internal tepal mesophyll | 0.24 | 0.5 |
| | Loose internal tepal mesophyll | 0.24 | 0.5 |
| | Ext.pappilose epidermis | 0.43 | 0.3 |
| | Ext.irregular epidermis | 0.43 | 0.3 |
| | Ext.normal epidermis | 0 | 1 |
| | Irregular internal tepal epidermis | 0 | 1 |
| | Normal internal tepal epidermis | 0 | 1 |
| | Stylar canal | 0.30 | 0.4 |
| | Pericarpel papillose epidermis | 0.30 | 0.4 |
| | Pericarpel irregular epidermis | 0 | 1 |
| | Pericarpel normal epidermis | 0.30 | 0.4 |
| | Pappilose floral tube epidermis | 0.53 | 0.1 |

| | | | |
|---|---|---|---|
| | Irregular floral tube epidermis | 0.48 | 0.2 |
| | Normal floral tube epidermis | 0.30 | 0.4 |

**CAPÍTULO 2: Palinologia de Hylocereeae, com foco em espécies do clado hylocereoide (Hylocereeae: Cactaceae)**

**Abstract**

Pollen morphology in Hylocereeae remains poorly explored despite its potential taxonomic relevance. This study characterized pollen diversity in seven species of *Aporocactus* (1), *Selenicereus* (5), and *Weberocereus* (1) using light microscopy and multivariate analyses. The species showed a relatively conserved pollen pattern, predominantly with isopolar monads, reticulate exine, spinules, and three colpi. Nevertheless, variation occurred in pollen size, shape, polar area, and aperture number. *Selenicereus megalanthus* showed the largest pollen grains and greatest dimensional variability, whereas *Weberocereus bradei* was distinguished by pantocolpate pollen with 12 short colpi. Spinule length ranged from 1.0 to 2.4 μm. The first two PCoA axes explained 64.3% of the morphological variation, and UPGMA clustering revealed substantial overlap among genera. Overall, the results support the stenopalynous nature of the hylocereoid clade while highlighting the taxonomic value of combined quantitative and qualitative pollen characters.

**Keywords:** palynology; pollen morphology; *Selenicereus*; stenopalynous.

## 1. INTRODUÇÃO

Hylocereeae é um dos grupos mais emblemáticos da família Cactaceae, distinguindo-se por sua notável diversidade de formas de vida e adaptações morfológicas. Atualmente, a tribo compreende oito gêneros: *Acanthocereus* (Engelm. ex A. Berger) Britton & Rose, *Aporocactus* Lemaire, *Disocactus* Lindley, *Epiphyllum* Haworth, *Kimnachia* S. Arias & N. Korotkova, *Pseudorhipsalis* (Britton & Rose), *Selenicereus* (incluindo *Hylocereus* e parte de *Weberocereus*) (A. Berger) Britton & Rose e *Weberocereus* (Britton & Rose). Sua circunscrição é sustentada principalmente por dados moleculares associadas a características morfológicas dos caules (Cruz *et al*., 2016; Korotkova *et al*., 2017; Martínez-Quezada *et al*., 2020). Entretanto, características florais, bem como informações detalhadas sobre a morfologia dos grãos de pólen, podem contribuir para uma melhor compreensão do perfil floral da tribo e corroborar sua circunscrição atual.

Com exceção de *Acanthocereus*, a maioria dos representantes da tribo é constituída por plantas epífitas, hemiepífitas ou trepadeiras nômades, refletindo elevado grau de plasticidade ecológica e estrutural (Nava-Bernabé *et al*., 2025; Martínez-Quezada, 2025). Observa-se grande diversidade, incluindo caules achatados e desprovidos de espinhos, bem como cladódios robustos com muitos espinhos, frequentemente dotados de numerosas costelas e raízes adventícias. Em razão disso, Hylocereeae é considerada uma tribo marcadamente heterogênea (Almeida, 2013; Cruz *et al*., 2016; Korotkova *et al*., 2017).

As flores também apresentam expressiva variação quanto ao tamanho, à simetria e ao período de antese. Em gêneros como *Aporocactus*, predominam flores diurnas de pequeno a médio porte, enquanto as espécies de *Selenicereus* geralmente apresentam flores noturnas grandes e vistosas. A simetria floral pode ser radial ou bilateral, e o tubo floral e o pericarpelo exibem ampla diversidade de formas e ornamentações. As aréolas do pericarpelo são frequentemente recobertas por escamas, tricomas lanosos (lã), cerdas ou espinhos, ressaltando a complexidade morfológica do grupo.

Muitos representantes de Hylocereeae são amplamente cultivados como plantas ornamentais, especialmente espécies de *Disocactus*, *Epiphyllum* e *Selenicereus*, valorizadas por suas flores, popularmente conhecidas como “rainhas da noite”. Além de sua importância ornamental, diversas espécies de *Selenicereus* (= *Hylocereus*) apresentam considerável valor econômico devido à produção de frutos comestíveis, conhecidos popularmente como pitaya ou fruta-do-dragão (Korotkova *et al*., 2017; Martínez-Quezada *et al*., 2020). Atualmente, essas espécies são cultivadas em regiões tropicais de todo o mundo, evidenciando a importância ecológica, ornamental e comercial da tribo (Anderson, 2001).

Estudos palinológicos voltados à identificação de caracteres informativos em Cactaceae incluindo a tribo Hylocereeae ainda são relativamente escassos quando comparados a outras abordagens morfológicas. Entre as contribuições mais relevantes, destacam-se os trabalhos de Ruiz-Domínguez *et al*., (2019), Majeed *et al*., (2020) e Gómez-Lizárraga *et al*., (2024), que ressaltaram o potencial da morfologia polínica como fonte complementar de evidências para a compreensão das relações sistemáticas dentro da família.

Na tribo Hylocereeae, os estudos disponíveis indicam que os grãos de pólen apresentam variação morfológica geral relativamente baixa, caracterizando o grupo como estenopolínico. Ainda assim, determinadas espécies exibem características polínicas

distintas, potencialmente relevantes do ponto de vista taxonômico, como demonstrado por Ruiz-Domínguez *et al*., (2019). Esses caracteres podem contribuir para a melhor compreensão atual de Hylocereeae, especialmente quando avaliados em conjunto com outras evidências morfológicas.

Nesse contexto, o presente estudo teve como objetivo ampliar o conhecimento atual sobre a diversidade polínica em Hylocereeae por meio de análises de microscopia óptica dos grãos de pólen de representantes selecionados de três gêneros da tribo, estes, compondo o clado hylocereoide.

## 2. MATERIAL E MÉTODOS

### 2.1. Análise palinológica

As espécies analisadas neste estudo são predominantemente táxons cultivados e ornamentais, muitos dos quais também possuem relevância comercial. Por esse motivo, parte do material botânico foi coletada na Fazenda Brasil Pitaia (Sítio Jatobá), localizada no município de Votuporanga, estado de São Paulo, Sudeste do Brasil (20°17′04,58″ S, 49°54′55,96″ W) (*S. megalanthus* e *S. purpusii*). Esse local foi selecionado por abrigar uma extensa área de cultivo que compreende múltiplas espécies emblemáticas de *Selenicereus*, e outra parte foi coletado de espécies cultivadas no Instituto de Biociências, campus do Litoral Paulista IBCLP/Unesp São Vicente/SP (*A. anthonyanus*, *S. vagans*, *S. validus*, *A. flagelliformis* e *W. bradei*).

Os grãos de pólen foram retirados de anteras de flores preferencialmente em pré-antese de cada espécie pertencente ao clado hylocereoide (Tabela 1). As flores foram coletadas em campo e preservadas em sílica gel. O material foi submetido a acetólise segundo o protocolo de Erdtman (1960). O tempo de acetólise para as amostras foi de 1 min 40 seg para todas as espécies, com exceção de *S. megalanthus* em que foi utilizado o tempo de 7 minutos, seguindo Muñoz Galíndez, (2012). Foram montadas quatro lâminas permanentes de cada amostra utilizando gelatina glicerinada e seladas com parafina. As lâminas foram analisadas sob microscópio óptico e fotografadas com celular Xiaomi Redminote 13 108Mpixels.

Foram analisados 20 grãos de pólen por amostra, dos quais foram obtidas as seguintes medidas: diâmetro equatorial em vista polar (DEVP), diâmetro equatorial em vista equatorial (DEVE), diâmetro polar em vista equatorial (DPVE) e apocolpia (AP). Para cada variável, foram calculadass a média e o desvio-padrão, bem como a razão entre

os diâmetros polar e equatorial (P/E = DPVE/DEVE) e o índice da área polar (IAP = AP/DEVP). Além disso, foi determinado o número de aberturas e analisada a ornamentação e espessura da exina. As mensurações foram realizadas utilizando o software ImageJ V1.54k em um período de sete dias após acetólise e montagem das lâminas. A descrição dos grãos de pólen seguiu a terminologia proposta por Erdtman (1952), Barth e Melhem (1988), Punt *et al.* (2007) e Halbritter *et al.* ( 2018).

Com a finalidade de ampliar a representatividade taxonômica e contextualizar os padrões morfológicos observados, foram incorporados dados palinológicos publicados por Ruiz-Domínguez *et al*., (2019), referentes a espécies adicionais do clado hylocereoide e a outros representantes da tribo.

### 2.2. Análise estatística

A similaridade morfológica entre as espécies foi avaliada utilizando uma abordagem estatística multivariada que integrou métodos de dissimilaridade, agrupamento hierárquico e ordenação. Caracteres quantitativos (Tabela 1) foram utilizados para calcular uma matriz de dissimilaridade empregando o coeficiente de Gower (Gower, 1971).

A análise de agrupamento hierárquico foi realizada utilizando o método UPGMA, Sokal e Michener, 1958), que representa as similaridades entre as espécies com base nas distâncias médias entre os grupos. Os resultados foram visualizados por meio de um dendrograma. Para explorar a variação morfológica em um espaço bidimensional contínuo, realizou-se uma Análise de Coordenadas Principais (PCoA) com base na matriz de dissimilaridade. Todas as análises foram realizadas no software R v. 4.5.1 (R Core Team, 2025) utilizando os pacotes *tidyverse* v. 2.0 (Wickham, 2023), *clusters* v. 2.1.8.2 (Maechler *et al*., 2026) e *ggdendro* v. 0.2 (de Vries & Ripley, 2025).

## 3. RESULTADOS

### 3.1. Palinologia do clado hylocereoide

Os grãos de pólen das espécies selecionadas do clado hylocereoide variam de tamanho grandes a gigantes (Figura 1, Tabela 1), com formato oblato-esferoidal, prolato-esferoidal ou subprolato. Todas as espécies analisadas apresentam grãos 3-zonocolpados, exceto *Weberocereus bradei* que apresenta grãos de pólen pantocolpados (Tabela 2).

### 3.1.1. *Aporocactus flagelliformis*

Grãos de pólen em mônades, isopolares, prolato-esferoidais, de tamanho grande (75–91 × 71–87 μm), âmbito elíptico, área polar pequena a média, 3-zonocolpados. A exina é reticulada, fina (3,3 μm) e apresenta espínulas (2,4 μm) (Fig. 1, Tabelas 1, 2).

### 3.1.2. *Selenicereus anthonyanus*

Grãos de pólen em mônades, isopolares, prolato-esferoidais, de tamanho grande (62–79 × 67–82 μm), âmbito elíptico, área polar grande, 3-zonocolpados. A exina é reticulada, fina (4,3 μm) e apresenta espínulas (1 μm), (Fig. 1, Tabelas 1, 2).

### 3.1.3. *Selenicereus megalanthus*

Grãos de pólen em mônades, isopolares, oblato-esferoidais, de tamanho grande (97–142 × 70–148 μm), âmbito circular, área polar muito pequena, 3-zonocolpados. A exina é reticulada, fina (3 μm) e apresenta espínulas (1,3 μm), (Fig. 1, Tabelas 1, 2).

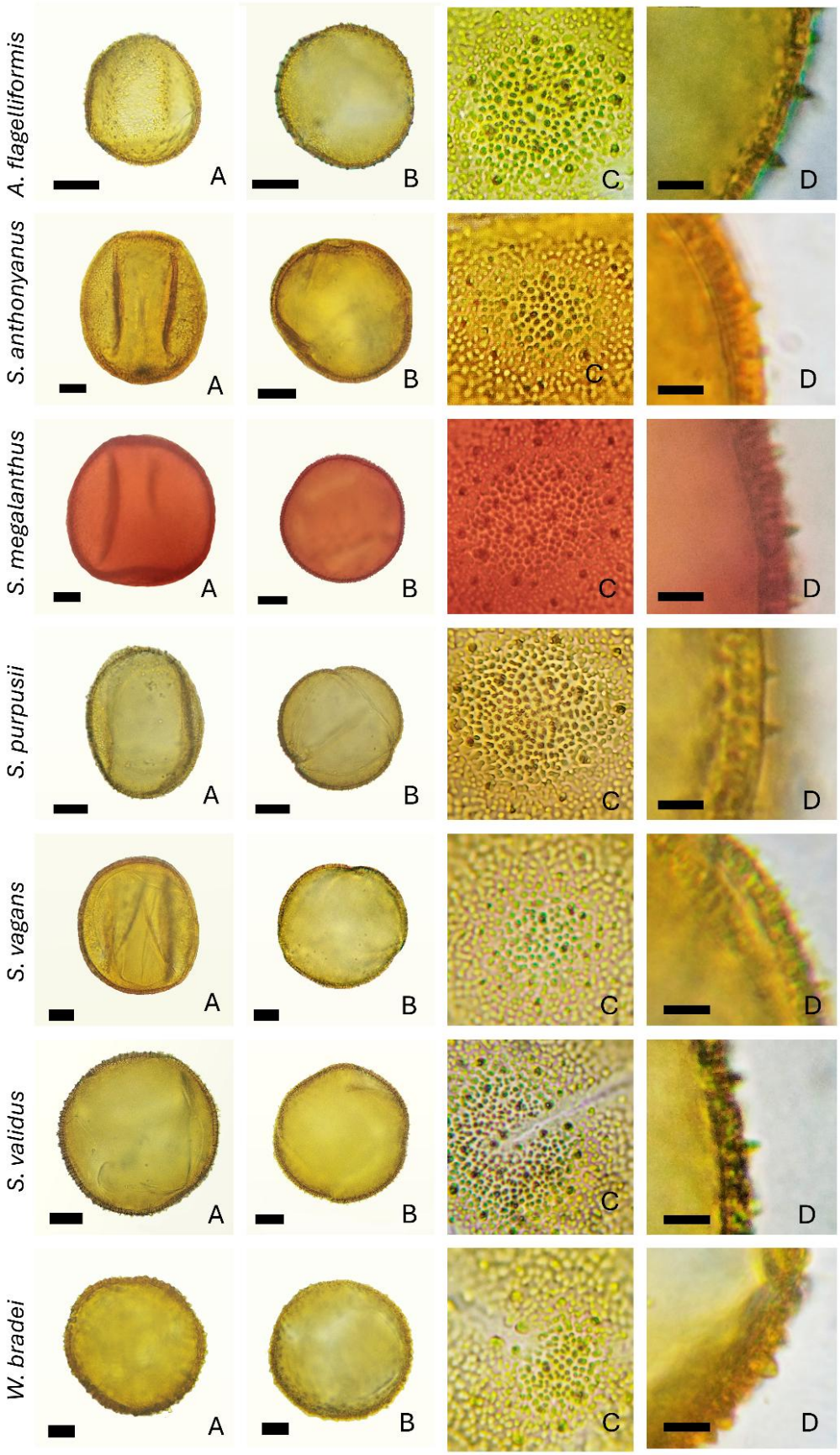



Figura 1. Fotomicrografias obtidas por microscopia óptica de grãos de pólen de espécies selecionadas do clado hylocereoide. A. Vista equatorial; B. Vista polar; C. Ornamentação do grão; D. Espessura da exina e espínulas. Barras = 10 $\mu m$.

### 3.1.4. *Selenicereus purpusii*

Grãos de pólen em mônades, isopolares, prolato-esferoidais, tamanho grande (85–103 × 74–102 μm), âmbito elíptico, área polar pequena a média, 3-zonocolpados. A exina é reticulada, fina (4,8 μm) com espínulas (1,8 μm), (Fig. 1, Tabelas 1, 2).

### 3.1.5. *Selenicereus vagans*

Grãos de pólen em mônades, isopolares, subprolatos, de tamanho grande (77–88 × 64–76 μm), âmbito circular, área polar pequena a média, 3-zonocolpados. A exina é reticulada, fina (4,1 μm) e apresenta espínulas (1,3 μm), (Fig. 1, Tabelas 1, 2).

### 3.1.6. *Selenicereus validus*

Grãos de pólen em mônades, isopolares, prolato-esferoidais, tamanho grande (98–117 × 95–110 μm), âmbito circular, área polar muito pequena, 3-zonocolpados. A exina é reticulada, fina (3,3 μm) com espínulas (1,7 μm), (Fig. 1, Tabelas 1, 2).

### 3.1.7. *Weberocereus bradei*

Grãos de pólen em mônades, isopolares, prolato-esferoidais, de tamanho grande (82–101 × 81–97 μm), âmbito circular, área polar muito pequena, 12-pantocolpados. A exina é reticulada, fina (4 μm) e apresenta espínulas (2 μm), (Fig. 1, Tabelas 1, 2).

Tabela 1. Dados quantitativos dos grãos de pólen de espécies selecionadas do clado hylocereoide ($n$ = 20).

| Espécie | Diâmetro Equatorial em vista Equatorial (DEVE) | | | | | Diâmetro Polar em vista Equatorial (DPVE) | | | | |
|---|---|---|---|---|---|---|---|---|---|---|
| | ***R* (µm)** | **$x \pm s_x$ (µm)** | ***s* (µm)** | **V (%)** | **IC (µm)** | ***R* (µm)** | **$x \pm s_x$ (µm)** | **s *(*µm)** | **V (%)** | **IC (µm)** |
| *A. flagelliformis* | 71–87 | 79,6 ± 1,32 | 5,92 | 7,44 | 76,82–82,37 | 75–91 | 85,5 ± 0,96 | 4,33 | 5,06 | 83,47–87,52 |
| *S. anthonyanus* | 70–80 | 73 ± 1,05 | 4,7 | 6,44 | 70,79–75,20 | 80–90 | 83,5 ± 1,09 | 4,89 | 5,86 | 81,20–85,79 |
| *S. megalanthus* | 70–150 | 121 ± 7,39 | 33,07 | 27,33 | 105,52–136,47 | 100–140 | 114 ± 3,58 | 16,02 | 14,05 | 106,49–121,50 |
| *S. purpusii* | 70–100 | 89,5 ± 1,53 | 6,86 | 7,66 | 86,28–92-71 | 82–100 | 97,05 ± 0,96 | 4,31 | 4,44 | 95,03–99,06 |
| *S. vagans* | 60–80 | 70 ± 0,72 | 3,24 | 4,63 | 68,48–71,51 | 60–80 | 74 ± 1,52 | 6,8 | 9,19 | 70,81–77,18 |
| *S. validus* | 100–110 | 104,5 ± 5,1 | 5,1 | 4,88 | 102,11–106,88 | 100–120 | 103,5 ± 1,31 | 5,87 | 5,67 | 100,75–106,24 |
| *W. bradei* | 81–97 | 88,4 ± 4,79 | 4,79 | 5,42 | 86,15–90,64 | 90–100 | 94,5 ± 1,14 | 5,1 | 5,4 | 92,11–96,88 |

$R$ = Intervalo (range); $x$ = Média; $s_x$ = Desvio padrão, $s$ = Erro padrão da média, V = Coeficiente de variação; IC = Intervalo de confiança.

Tabela 1. Caracterização morfológica de grãos de pólen de espécies selecionadas do clado hylocereoide.

| Espécie | P/E | Formato | IAP | Área Polar | Ab. | Or. | NAb. |
|---|---|---|---|---|---|---|---|
| *A. flagelliformis* | 1,07 | prolato-esferoidal | 0,42 | pequena a média | Co | R | 3 |
| *S. anthonyanus* | 1,02 | prolato-esferoidal | 0,55 | Grande | Co | R | 3 |
| *S. megalanthus* | 0,97 | oblato-esferoidal | 0,22 | muito pequena | Co | R | 3 |
| *S. purpusii* | 1,03 | prolato-esferoidal | 0,32 | pequena a média | Co | R | 3 |
| *S. vagans* | 1,19 | subprolato | 0,34 | pequena a média | Co | R | 3 |
| *S. validus* | 1,01 | prolato-esferoidal | 0,20 | muito pequena | Co | R | 3 |
| *W. bradei* | 1,1 | prolato-esferoidal | 0,20 | muito pequena | Co | R | 12 |

P/E = Razão entre os diâmetros polar e equatorial (PDEV/EDEV); IAP = Índice de área polar; Ab. = Aberturas; NAb. = número de aberturas; Or. = Ornamentação; Co = Colpado; R = Reticulada.

3.2. Análises estatísticas

As espécies analisadas apresentaram variações nas medidas de diâmetro polar e equatorial. O eixo polar médio variou de 74 µm, em *S. anthonyanus*, a 114 µm, em *S. megalanthus*, enquanto o diâmetro equatorial médio variou de 69 µm, em *S. vagans*, a 118,00 µm, em *S. megalanthus*. *Selenicereus megalanthus* apresentou também os intervalos de confiança mais amplos para ambas as medidas, evidenciando maior variabilidade nas dimensões dos grãos (Fig. 2, Tabela 1). No diâmetro equatorial, observou-se sobreposição dos

intervalos de confiança entre *Weberocereus bradei* e *S. purpusii*, bem como entre *S. validus* e *S. megalanthus* (Fig. 2).

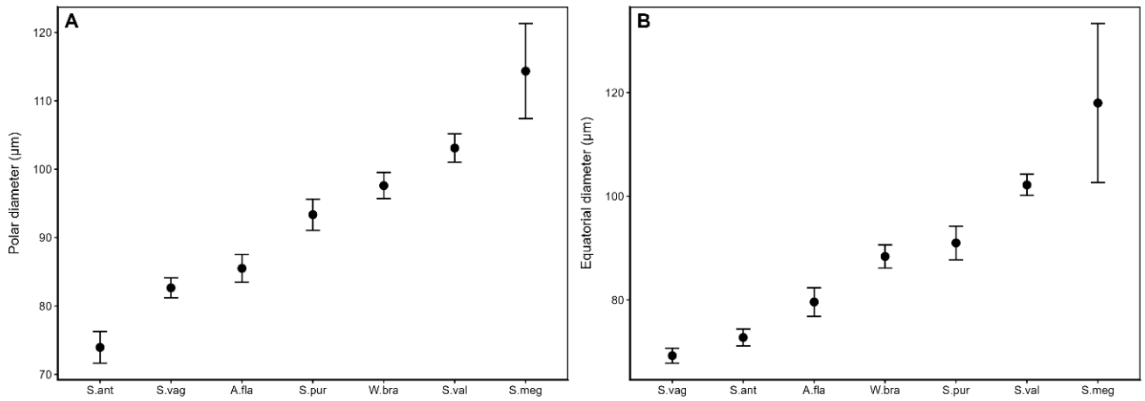



Figura 2. Média e intervalo de confiança (95%) dos diâmetros polar e equatorial dos grãos de pólen das espécies selecionadas do clado hylocereoide. A. Diâmetro polar; B. Diâmetro equatorial.

A análise de agrupamento UPGMA em conjunto com outras espécies da tribo Hylocereeae, analisadas por Ruiz-Domínguez *et al*., (2019), não mostrou o agrupamento das espécies de acordo com a circunscrição genêrica atual. Entre os pares com menor dissimilaridade destacaram-se *Selenicereus monacanthus–S. vagans*, *S. polyrhizus–S. guatemalensis*, *S. purpusii–A. flagelliformis*, *S. undatus–S. hamatus*, *S. validus–S. megalanthus* e *Weberocereus tunilla–S. glaber*. Também foram observadas associações entre *S. ocamponis* e *Disocactus ackermannii*, *S. setaceus* e *D. speciosus*, e *S. triangularis* e *Epiphyllum thomasianum*. *Weberocereus bradei* associou-se ao agrupamento formado por *S. validus* e *S. megalanthus*, mas não se agrupou diretamente com *W. tunilla*. *Kimnachia ramulosa* apresentou a maior dissimilaridade em relação aos demais táxons, (Fig. 3).

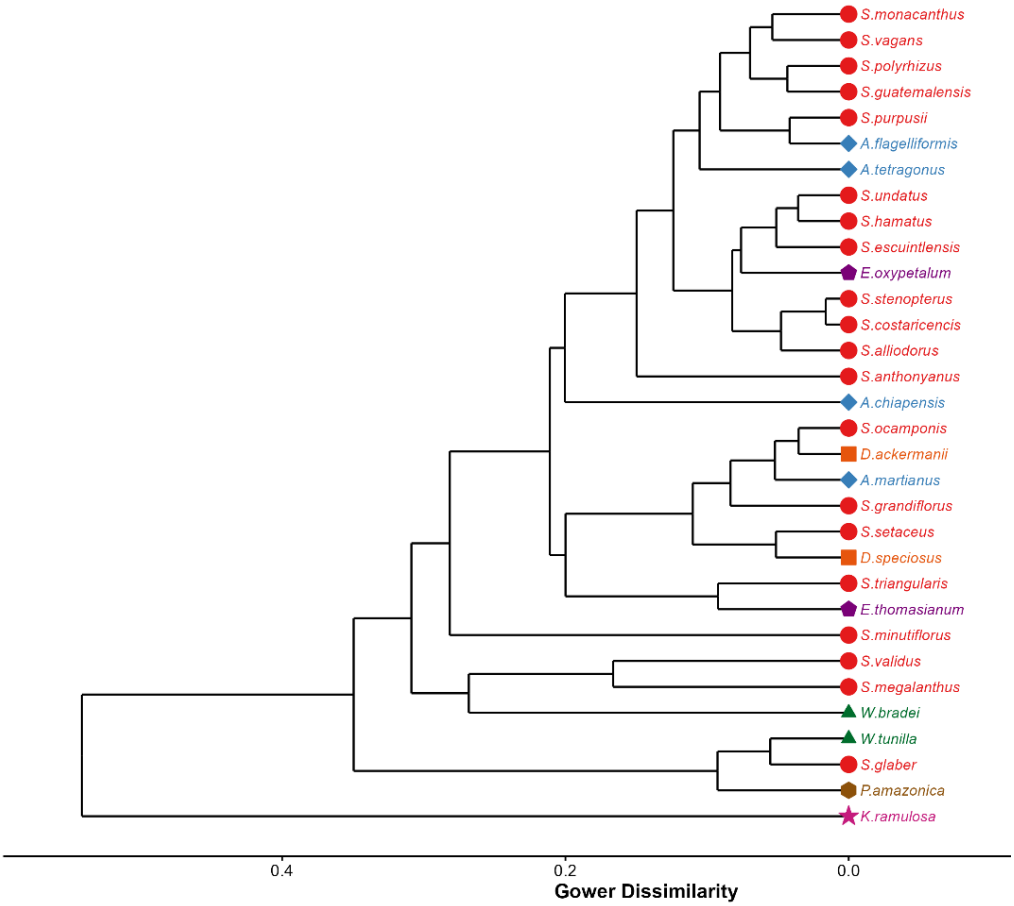



Figura 3. Dendrograma de similaridade morfológica entre os táxons de Hylocereeae, obtidos pelo método UPGMA e coeficiente de Gower. Dados complementares obtidos de Ruiz-Domínguez *et al*. (2019).

Na Análise de Coordenadas Principais, os dois primeiros eixos explicaram conjuntamente 64,3% da variação dos dados, sendo 39,1% representados pela PCo1 e 25,2% pela PCo2 (Figure 4). A maioria dos táxons concentrou-se próxima à região central da ordenação, indicando elevada sobreposição em seus caracteres quantitativos. *Kimnachia ramulosa* apresentou a posição mais isolada, com elevado valor positivo na PCo1. *Selenicereus glaber*, *W. tunilla* e *Pseudorhipsalis amazonica* foram separados dos demais principalmente ao longo da PCo2 positiva, enquanto *S. validus* e *S. megalanthus* ocuparam posições próximas na região negativa desse eixo. *S. triangularis* e *E. thomasianum* também permaneceram próximas na ordenação. *Weberocereus bradei* apresentou deslocamento positivo na PCo1 e não se associou diretamente a *W. tunilla*. De modo geral, a PCoA corroborou as principais associações e a diferenciação dos táxons observadas no dendrograma (Fig. 2). Entretanto, nenhuma das

características polínicas avaliadas apresentou associação estatisticamente significativa com a distribuição dos táxons nos eixos da ordenação, indicando que o padrão observado resulta provavelmente da contribuição conjunta de múltiplos caracteres, e não da influência isolada de uma única variável.

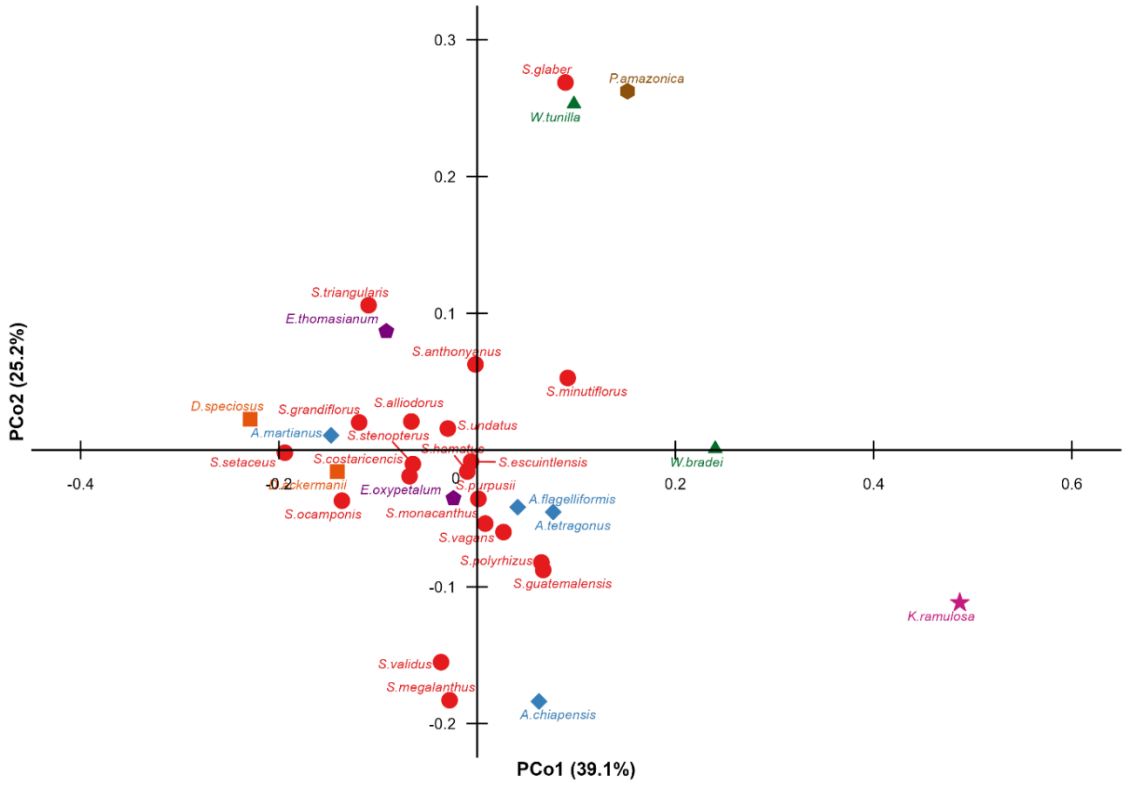



Figura 4. Análise de Coordenadas Principais (PCoA) dos táxons de Hylocereeae, baseada na matriz de dissimilaridade de Gower calculada a partir dos caracteres polínicos quantitativos.

## 4. DISCUSSÃO

Os grãos de pólen das espécies analisadas do clado hylocereoide apresentaram um padrão morfológico relativamente homogêneo. Sob microscopia óptica, caracterizaram-se em mônades, isopolares, sendo predominantemente zonocolpados e 3-colpados. A condição 3-colpada é amplamente registrada em diferentes gêneros de Cactaceae, especialmente entre representantes de Cactoideae (Lattar & Cuadrado, 2010; Cancelli *et al*., 2017; Gonzaga *et al*., 2019). Esse padrão também foi observado por Ruiz-Domínguez *et al*. (2019), que analisaram 27 táxons pertencentes a oito gêneros da tribo Hylocereeae e verificaram o predomínio de grãos tricolpados, com exceção de representantes de *Kimnachia*, *Pseudorhipsalis* e *Weberocereus*,

nos quais foram registrados grãos pantocolpados. No presente trabalho, *S. megalanthus* apresentou área polar muito pequena, com índice de 0,22, diferente Ruiz-Domínguez *et al*. (2019) que registraram valor de 0,40, correspondente a uma área polar média. Essa diferença pode estar relacionada à variação intraespecífica da espécie, visto que foi a espécie que apresentou maiores intervalos de variabilidade nas dimensões dos grãos (Fig. 2), ou a diferenças nos procedimentos de preparação do material. *S. megalanthus* apresentou conteúdo interno particularmente resistente ao processamento acetolítico, exigindo sucessivos ajustes no tempo de exposição, entre 1 minuto e 30 segundos e 7 minutos (Erdtman, 1952; Muñoz Galíndez, 2012), para permitir a remoção adequada do conteúdo celular e a obtenção de imagens sem comprometer a integridade da exina. Muñoz Galíndez (2012) também destacou a necessidade de padronização específica da acetólise para essa espécie, demonstrando que o tempo, a temperatura e a concentração da mistura interferem na qualidade de preservação e visualização dos grãos.

*Weberocereus bradei* diferenciou-se das demais espécies pela presença de grãos pantocolpados, com 12 colpos curtos. Além disso, apresentou grãos prolato-esferoidais, com razão P/E de 1,10, e área polar muito pequena, com índice de 0,20. Ruiz-Domínguez *et al*. (2019) observaram em *W. tunilla* grãos igualmente pantocolpados e prolato-esferoidais, com 12–15 colpos curtos, mas com área polar grande. A relação quanto ao número elevado e ao comprimento reduzido dos colpos reforça a ocorrência desse padrão em *Weberocereus*, enquanto a diferença no índice da área polar demonstra que esse caráter não é uniforme entre as espécies do gênero. A pantocolpia, entretanto, não deve ser interpretada como caráter exclusivo de *Weberocereus*, pois grãos com 12 colpos ou mais também foram registrados em *K. ramulosa*, *P. amazonica* e *S. glaber*, espécie anteriormente incluída em *Weberocereus* (Korotkova *et al*., 2017). Portanto, a condição pantocolpada constitui um caráter diagnóstico de *W. bradei* em relação às demais espécies da presente amostragem, mas não representa uma autapomorfia da espécie nem sustenta, isoladamente, uma sinapomorfia exclusiva de *Weberocereus*.

Todas as espécies aqui analisadas apresentaram exina com ornamentação reticulada com espínulas e de espessura fina desde 3 µm em *S. megalanthus* até 4,8 µm em *S. purpusii*. Entretanto, Ruiz-Domínguez *et al*. (2019) registraram ausência de espínulas em *S. minutiflorus* e *S. stenopterus*, enquanto as demais espécies do gênero apresentaram esses elementos. Esse contraste evidencia um padrão heterogêneo na ornamentação da exina em *Selenicereus*, particularmente quanto à presença ou ausência de espínulas, e demonstra o potencial taxonômico desse caráter para a diferenciação de determinados táxons. O comprimento das

espínulas variou de 1,0 µm, em *S. anthonyanus*, a 2,4 µm, em *A. flagelliformis*. Entre as espécies de *Selenicereus*, os valores oscilaram de 1,0 a 1,8 µm, enquanto *W. bradei* apresentou espínulas relativamente longas, com 2,0 µm. A variação no desenvolvimento das espínulas reforça o caráter heterogêneo da micromorfologia da exina no clado hylocereoide e demonstra que esse atributo deve ser analisado quantitativamente e em conjunto com os demais caracteres polínicos.

De modo geral, os resultados sustentam a existência de um plano morfológico polínico conservado no clado hylocereoide, sobretudo quanto à unidade, à polaridade, seu âmbito e ao padrão predominante das aberturas e da exina. Entretanto, a variação na forma, no tamanho dos grãos, na razão P/E, no índice da área polar e, principalmente, no número e no comprimento dos colpos demonstra que o padrão estenopolínico do grupo não implica ausência de informação taxonômica. A combinação de caracteres qualitativos e quantitativos apresenta, portanto, maior potencial para a diferenciação das espécies do que a utilização isolada de qualquer atributo polínico.

## 5. CONCLUSÃO

Em Hylocereeae a exina possui normalmente espínulas de 1-3 µm de altura (Leuenberger 1976; Ruiz-Domínguez *et al*. 2019) sendo que as únicas espécies que não apresentaram espínulas foram *S. minutiflorus* e *S. stenopterus*, o que sugere que dados de palinologia sejam também considerados em analises filogenéticas para a taxonomia da tribo, além de dados moleculares e morfológicos; visto que *Selenicereus* foi o táxon com maior variação nos atributos polínicos em 27 espécies analisadas na tribo Hylocereeae (Ruiz Domínguez *et al*. 2019).

Nossos resultados em conjunto com os fornecidos por (Ruiz-Domínguez *et al*. 2019) sustentam a natureza estenopolínica do clado hylocereoide e da tribo Hylocereeae, mas não indicam ausência de informação taxonômica. Em grupos com morfologia polínica conservada, a diferenciação depende principalmente da análise conjunta de caracteres quantitativos e qualitativos, incluindo dimensões dos grãos, razão P/E, índice da área polar, número e comprimento dos colpos e atributos micromorfológicos da exina.

## 6. REFERÊNCIAS

Almeida, O. J. G. (2013). Órgãos reprodutivos em Hylocereeae e Rhipsalideae (Cactaceae): morfologia floral e desenvolvimento estrutural do fruto e da semente. Tese (Doutorado em Biologia Vegetal) – Universidade Estadual Paulista, Rio Claro, São Paulo.

Anderson, E. F. (2001). The cactus family. Timber Press, Inc. Oregon.

Barth, O. M., Melhem, T. S. (1988). Glossário ilustrado de palinologia. Unicamp.
Cancelli, R. R., Menezes, I. C., & Souza, P. A. (2017). Morfologia polínica de espécies epífitas de Cactaceae Juss. do Rio Grande do Sul, Brasil. Iheringia, Série Botânica., 72(2), 181-189.

Collins, T. J. (2007). ImageJ for microscopy. Biotechniques, 43(sup1), S25-S30.

Cruz, M. A., Arias, S. and Terrazas, T., 2016. Molecular phylogeny and taxonomy of the genus *Disocactus* (Cactaceae), based on the DNA sequences of six chloroplast markers. Willdenowia 46: 145–164. https://doi.org/10.3372/wi.46.46112

Erdtman, G. (1960).The acetolysis method, a revised description. Sv. Bot. Tidskr., [s.l.], 54, 561–564.

Gómez-Lizárraga, L. E., Ramírez-Arriaga, E., Mendoza-Garfias, M. B., Prámparo, M. B., & Valiente-Banuet, A. (2024). Pollen morphology of columnar cacti from Tehuacán-Cuicatlán Valley, Mexico. Palynology, 48(1). https://doi.org/10.1080/01916122.2023.2251560

Gonzaga, D. R., de Souza, M. A., Neto, L. M., Peixoto, A. L., Mendonça, C. B. F., & Goncalves-Esteves, V. (2019). The systematic value of pollen morphology in *Arthrocereus* A. Berger (Cactaceae, Cactoideae). Review of Palaeobotany and Palynology, 269, 33-41.

Gower, J. C. (1971). A general coefficient of similarity and some of its properties. Biometrics, 857-871.

Halbritter, H., Ulrich, S., Grímsson, F., Weber, M., Zetter, R., Hesse, M., Buchner, R., Svojtka, M. & Frosch-Radivo, A. (2018). Illustrated pollen terminology. Springer. https://doi.org/10.1007/978-3-319-71365-6.

Korotkova, N., Borsch, T., and Arias, S. (2017). A phylogenetic framework for the Hylocereeae (Cactaceae) and implications for the circumscription of the genera. Phytotaxa, 327(1), 1. https://doi.org/10.11646/phytotaxa.327.1.1

Lattar, E., & Cuadrado, G. (2010). Estudios palinológicos de especies argentinas de los géneros *Cereus*, *Cleistocactus*, *Denmoza*, *Echinopsis* y *Monvillea* (Cactaceae, Cactoideae). Boletín de la Sociedad Argentina de Botánica, 45(1-2), 93-107.

Leuenberger, B. E. (1976). Pollen morphology of the Cactaceae. The Cactus and Succulent Journal of Great Britain, 38(4), 79–94.

Maechler, M., Rousseeuw, P., Struyf, A., Hubert, M., & Hornik, K. (2026). cluster: Cluster Analysis Basics and Extensions. R package version 2.1.8.2. https://CRAN.R-project.org/package=cluster

Majeed, S., Zafar, M., Ahmad, M., Kilic, O., Sultana, S., Raza, J., & Jabeen, M. (2020). Pollen morphological investigations of family Cactaceae and its taxonomic implication by light microscopy and scanning electron microscopy. Microscopy research and technique, 83(7), 767-777.

Martínez-Quezada, D. M., Arias, S., Korotkova, N., & Terrazas, T. (2025). From the ground up: the evolution of structurally dependent plants in Hylocereeae (Cactaceae). Brazilian Journal of Botany, 48(1), 31.

Martínez-Quezada, D.M., Arias, S., Korotkova, N., Terrazas, T. (2020). The phylogenetic significance of the stem morpho-anatomy in the Hylocereeae (Cactoideae, Cactaceae). Plant Systematics and Evolution, 306(1). https://doi.org/10.1007/s00606-020-01639-x

Muñoz Galíndez, E. (2012). Caracterización polínica de *Selenicereus megalanthus* (K. Schum. Ex Vaupel) Moran (pitahaya amarilla) mediante microscopia óptica y electrónica de barrido y transmisión. Dissertação De Mestrado- Universidad Nacional De Colombia Sede Palmira, Facultad De Ciencias Agropecuarias.

Nava-Bernabé, P. H., Valencia-Diaz, S., Toledo-Hernández, V. H., & Flores-Palacios, A. (2025). Does germination and early survival in different substrates filter the growing habit among terrestrial, nomadic vine, and epiphytic cacti? A field experiment. Plant Ecology, 226(6), 633-644. https://doi.org/10.1007/s11258-025-01519-9

Punt, W.; Blackmore, S.; Nilsson, S. & Le Thomas, A. (2007). Glossary of pollen and spore terminology. Review of Paleobotany and Palynology 143: 1-81.

R Core Team. 2025. R: A language and environment for statistical computing. R Foundation for Statistical Computing. Vienna, Austria. https://www.r-project.org

Ruiz-Domínguez, C., Vovides, A. P., & Sosa, V. (2019). Systematic relevance of pollen morphology in tribe Hylocereeae (Cactaceae). PhytoKeys, 128, 121.

Sokal, R. R., & Michener, C. D. (1958). A statistical method for evaluating systematic relationships.

Vries, A., & Ripley, B. D. (2025). ggdendro: Create Dendrograms and Tree Diagrams Using 'ggplot2'. R package version 0.2.0. https://andrie.github.io/ggdendro/

Wickham, H. (2023). tidyverse: Easily Install and Load the 'Tidyverse'. R package version 2.0.0. https://CRAN.R-project.org/package=tidyverse

## CONSIDERAÇÕES FINAIS

Os resultados obtidos nesta pesquisa sugerem que o clado hylocereoide apresenta um padrão floral misto, refletido na diversidade de seus gêneros, que incluem flores diurnas e noturnas, com comprimentos que variam de 6 a 40 cm, e simetrias tanto bilaterais quanto radiais. Observa-se, ainda, a ocorrência de padrões mistos de polinização, indicando uma grande plasticidade adaptativa em relação aos polinizadores.

Apesar dessas evidências, a compreensão detalhada do padrão floral do clado ainda é limitada, uma vez que dados de algumas espécies permanecem indisponíveis. A inclusão dessas espécies será essencial para refinar o padrão observável e avaliar com maior precisão a diversidade morfológica e funcional do clado.

Em contraste com a elevada diversidade floral, os dados palinológicos revelaram um padrão geral relativamente conservado. Os grãos de pólen foram mônades, isopolares e predominantemente 3-zonocolpados, sustentando a natureza estenopolínica atribuída a Hylocereeae. Apesar dessa uniformidade, foram identificadas variações na forma e no tamanho dos grãos, na razão P/E, no índice da área polar, no número e posição dos colpos e nas dimensões das espínulas da exina. Esses resultados demonstram que a estenopolinia do grupo não implica ausência de informação taxonômica, uma vez que combinações específicas de caracteres permitiram diferenciar determinados táxons.

Em síntese, os dados obtidos apontam para uma elevada variabilidade floral dentro do da tribo Hylocereeae e do clado hylocereoide, mas os resultados ainda são parciais. Estudos complementares, incluindo espécies não analisadas, como por exemplo, novos táxons de *Weberocereus* e dados palinológicos dessas espécies, serão fundamentais para consolidar um entendimento mais robusto da evolução floral e das relações filogenéticas dentro do clado.